An International Standard Formulation for the Thermodynamic Properties of 1,1,1,2-Tetrafluoroethane (HFC-134a) for Temperatures From 170 K to 455 K and Pressures up to 70 MPa

Reiner Tillner-Roth and Hans Dieter Baehr

Institut fuer Thermodynamik, Universitaet Hannover, Callinstrasse 36, 30167 Hannover, Germany

Received March 7, 1994; revised manuscript received August 3, 1994

A fundamental equation of state for the Helmholtz free energy of R 134a (1,1,1,2-tetrafluoroethane) is presented which is valid for temperatures between 170 K and 455 K and pressures up to 70 MPa. It is based on the most accurate measurements of pressure-density-temperature (p,ρ,T), speed of sound, heat capacity, and vapor pressure which are currently available. A linear regression analysis and a non-linear least squares fitting technique, based on the selected measurements, were used to determine the structure of the fundamental equation of state and the values of its 21 coefficients. The equation represents nearly all selected experimental data within their estimated accuracy with the exception of heat capacities and speed of sound in the region close to the critical point. Typical accuracies are ±0.05% for density, ±0.02% for the vapor pressure or ±0.5 and ±1% for the heat capacity. This equation of state has been compared to equations established by other research groups by Annex 18 of the International Energy Agency (IEA) and has been selected as an international standard formulation for the thermodynamic properties of R 134a by this group.

Key words: data analysis; fundamental equation of state; Helmholtz-free energy correlation; R 134a; 1,1,1,2-tetrafluoroethane; thermodynamic properties.

Contents

List of Tables

List of Figures

1. Introduction

1.1. Background

HFC-134a (1,1,1,2-tetrafluoroethane, CF_3CH_2F) is an environmentally acceptable refrigerant which has replaced the ozone-depleting CFC-12 (dichloro-difluoro-methane) in a wide range of applications especially in automotive air-conditioners and domestic refrigeration. Because of its current and future importance, accurate knowledge of its thermodynamic properties is essential in order to design economic refrigeration cycles. In particular, a common standard for the thermodynamic properties of HFC-134a is desirable for the refrigeration industry.

This task has been taken on by a group working under the auspices of the Heat Pump Programme of the International Energy Agency (IEA). This program was established in 1978 and is currently supported by fifteen countries. It offers opportunities of international collaboration in research, development, demonstration, and promotion of heat pumping and related technologies. The aim is to accelerate the knowledge, acceptance, and implementation of this energy saving and environmentally important technology. Eight member countries (Austria, Canada, Germany, Japan, Norway, Sweden, the United Kingdom, and the United States) have joined together to form Annex 18 – Thermophysical Properties of the Environmentally Acceptable Refrigerants. One of the goals of this Annex is to provide property formulations that will become de facto international standards for the most important alternative refrigerants.

It was proposed at the meeting of Annex 18 in Heidelberg, Germany, in Novermber 1990 and agreed at the meeting held

in Boulder, Colorado, USA in June 1991, that comparisons should be made of existing equations of state for the refrigerants HFC-134a and HCFC-123. These two fluids have the most immediate industrial applications, since they are proposed as replacements for CFC-12 and CFC-11, respectively. For both of these fluids, a large amount of experimental results exists and more than one equation of state has been correlated for each.

Two independent groups were asked to carry out these comparisons, namely the Center for Applied Thermodynamic Studies (CATS) at the University of Idaho, Moscow, Idaho, USA and the International Union of Pure and Applied Chemistry (IUPAC), Thermodynamic Tables Project Centre, Imperial College, London, UK. These two groups prepared independent preliminary reports for the meeting held in July 1992 at Purdue University, West Lafayette, Indiana, USA. The IUPAC report comprised comparisons of three equations of state for HFC-134a with the ideal gas, saturation and single phase *PVT*-properties while the CATS report gave comparisons of four equations of state for HFC-134a and of three equations of state for HCFC-123 with all available data. At that meeting several suggestions were made for modification of the final report. It was decided that draft final reports should be distributed one month before the next Annex meeting on April 30, 1993, and with that aim in view, all new experinemtal results and new equations of state were to be submitted to both participating groups by 1st December 1992.

At the meeting of the Annex 18 in Maastricht, The Netherlands, in April 1993 both groups presented their results of the equation of state comparisons for HFC-134a and for HCFC-123. After discussion of the advantages and disadvantages of each equation of state it was decided to recommend the equation presented in this paper as an international standard for thermodynamic properties of HFC-134a.

1.2. Other Equations of State for HFC-134a

Three other equations of state (EOS) for HFC-134a were reviewed as part of the Annex 18 work. They differ in structure and also in the ranges of validity. Huber and McLinden established a 32-term EOS[22] (referred to as HM-EOS) the structure of which corresponds to the modified BWR-type originally developed for nitrogen by Jacobsen and Stewart[25]. It is valid in about the same ranges of temperature pressure as our own equation of state, namely from the triple point temperature to 455 K for pressures up to 70 MPa. Huber and Ely[21] used a 32-term equation of state for the Helmholtz free energy (referred to as HE-EOS) which was originally developed for oxygen by Schmidt and Wagner[48]. It is valid between 170 K and 453 K for pressures up to 70 MPa. The equation of Piao, Noguchi, Sato, and Watanabe[44] (referred to as PNSW-EOS) is a modified BWR-equation with 18 coefficients. The range of validity is for temperatures from 180 K to 450 K and pressures up to 70 MPa.

Furthermore, a cross-over model was developed by Tang *et al.*[53] describing thermodynamic properties in the critical region. This model has been extended into regions beyond the critical, but does not predict these properties accurately. It will, therefore, only be used for comparisons in the critical region.

1.3. Organization of the Paper

In Sec. 2, a survey of experimental data for the thermodynamic properties of HFC-134a is summarized. The experimental results which were used to establish the fundamental equation of state are identified.

Section 3 is concerned with the development of the fundamental equation of state. Briefly, the optimization process is described, especially the application of different strategies during different steps of optimization. Furthermore, structure and coefficients of the fundamental equation of state together with relations between thermodynamic properties and the Helmholtz free energy are given.

In Sec. 4, the equation of state is compared with experimental data and the equations of state mentioned in Sec. 1.2. Tables of thermodynamic properties are also included in this paper. More detailed tables will be published separately in a properties bulletin by the International Institute of Refrigeration (IIR).

All experimental data, available up to January 1993 are discussed. All temperatures for the new equation are based on the ITS–90. For simplification our own equation of state will be referred to as EOS or fundamental EOS.

2. Experimental Results

2.1. Survey of Available Measurements

2.1.1. Triple Point

Only one experimental value of the triple point temperature has been reported which is by Magee[33]. They found

$$T_{tr} = (169.85 \pm 0.01)\text{K}.$$

Their measurements were performed with a sample of 99.999% purity; therefore, their value is regarded as highly reliable. Density and pressure at the triple point have not been measured. Calculation from the fundamental EOS yields

$$p_{tr} = 391 \text{ Pa} \qquad \text{and} \qquad \rho'_{tr} = 1591.1 \text{ kg/m}^3.$$

2.1.2. Critical Point

Experimental values of the critical parameters are summarized in Table 1. All values are in close agreement. The measured critical temperatures differ by only 0.18 K, the pressure p_c by less than 0.4%, and the critical density by less than 1.6%. Critical parameters were only used to define the dimensionless variables $\tau := T^*/T$ and $\delta := \rho/\rho^*$. For this purpose we selected

$$T^* = 374.18 \text{ K} \qquad \text{and} \qquad \rho^* = 508 \text{ kg/m}^3.$$

We did not constrain the equation of state to any of these measurements because this would unnecessarily restrict the

optimization. Another approach to consider the behaviour in the critical region is described in Sec. 3.2.2.

2.1.3. Single-Phase Properties

Extensive measurements of various thermodynamic properties in the single-phase have been carried out for HFC-134a. The sources are listed in Table 2. 18 data sets of (p,ρ,T)-properties are reported comprising 2611 data points within 180 K and 453 K at pressures up to 70 MPa. Numerous caloric properties, namely speed of sound, isochoric and isobaric heat capacity and Joule-Thomson coefficients, were measured in the vapor and liquid regions as well.

Second virial coefficients were reported by six sources listed in Table 2. These values were derived from other measurements such as speed of sound or (p,ρ,T)-measure-ments, covering the range from 233 K to 453 K.

2.1.4. Saturation Properties

The majority of available saturation property measurements are for vapor pressure and saturated liquid density. For the saturated vapor density, six data sets are available for temperatures above 293 K. 160 isochoric heat capacities in the two-phase region have been measured by Magee[33] which are very useful to check an equation of state with respect to its representation of the whole (p,ρ,T)-surface. Available saturation property measurements are listed in Table 3.

2.2. The Data Set for the Formulation of the Fundamental Equation of State

In this section, the results of the data analysis are outlined briefly. The selection of single-phase measurements is mainly based on tests of consistency as described in Sec. 2.2.1 for the liquid phase. Further criteria, which apply to the assessment of all data sets, are the uncertainties claimed by the authors, the scatter of a set of data when compared to an equation of state, or systematic deviations between different sets of data. The reasons for selecting or rejecting a certain set of measurements are given in detail in Sec. 4 where experimental data are compared with the fundamental equation of state.

Figure 1 shows the distribution of experimental values in the single-phase region which were used to establish the fundamental equation of state. The values cover the range between 180 K and 453 K for pressures up to 70 MPa. From the large amount of available (p,ρ,T)-data only those measured by Tillner-Roth and Baehr[54,55] and of Dressner and Bier[12] were selected because they agree extremely well and cover an extended range of pressure and temperature. (p,ρ,T)-measurements of other authors were not used because they generally overlap the selected data or show systematic deviations. In the liquid and in the vapor phase, speed of sound values of Goodwin and Moldover[18] and Guedes and Zollweg[19], isobaric heat capacities of Gürtner and Ernst[20] and of Wirbser[59] are included in the data set. Furthermore, measurements of isochoric heat capacity by Magee[33] were selected and found to be consistent with the selected data so were included during the formulation of the fundamental equation of state.

From available saturation properties four sets of measured vapor pressures by Goodwin *et al.*[7] Baehr and Tillner-Roth[3], Weber[58], and Magee and Howley[34] were selected which agree extraordinary well with each other, cf. Fig. 26. They cover nearly the whole vapor pressure curve between 180 K and the critical point. We refrained from using measurements of saturation densities because the single-phase regions adjacent to the saturation boundary are well-defined by (p,ρ,T)-data. Additionally, isochoric heat capacities in the two-phase region by Magee[33] below 190 K were included. Those measured at higher temperatures were not used because they contain about the same information of state as the single-phase heat capacities reported from the same source and already selected.

2.2.1. Consistency Tests Between Thermal and Caloric Properties

In this section, a test of consistency between thermal and caloric properties in the liquid phase is described which was carried out prior to the formulation of the fundamental equation of state. This test was performed to find out the best combination of thermal and caloric data which obey the laws of thermodynamics. Furthermore, it has been necessary to find an explanation for the systematic difference between the liquid density values reported by Tillner-Roth and Baehr[55] and those measured by Hou *et al.*[23].

The consistency test is based on the following thermodynamic equations relating caloric properties with the thermal equation of state $p=p(v,T)$. The speed of sound w is written as

$$w=v\sqrt{\frac{T}{c_v}\left(\frac{\partial p}{\partial T}\right)_v^2-\left(\frac{\partial p}{\partial v}\right)_T}, \tag{1}$$

the isobaric heat capacity c_p as

$$c_p=c_v-T\left(\frac{\partial p}{\partial T}\right)_v^2\left(\frac{\partial p}{\partial v}\right)_T^{-1}, \tag{2}$$

and the Joule-Thomson coefficient is given by

$$\mu=\frac{v\left(\frac{\partial p}{\partial v}\right)_T+T\left(\frac{\partial p}{\partial T}\right)_v}{T\left(\frac{\partial p}{\partial T}\right)_v^2-c_v\left(\frac{\partial p}{\partial v}\right)_T}. \tag{3}$$

Using these equations, a value of the isochoric heat capacity can be transformed into any other desired caloric property when the thermal equation of state is known. Alternatively, any other kind of transformation between caloric properties is possible, for example speed of sound can be calculated from a value of the isobaric heat capacity using Eqs. (2) and (1). For this purpose, the thermal equation of state must be consistent with the caloric information otherwise a transformation would produce results which disagree with reliable measurements. Thus, consistency between sets of thermal and caloric measurements can be checked by setting up thermal equations of state based on different sets of denisty measurements, transforming different caloric measurements into a unique prop-

erty, and comparing the results with measured values of that property. Results which agree would indicate consistency between the thermal and caloric values while disagreement indicates inconsistency.

For liquid HFC-134a, two equations of state were established. The first one was based exclusively on the densities of Tillner-Roth and Baehr[55] for temperatures between 243 K and 413 K, for densities $\rho>750$ kg/m^3, and for pressures up to 20 MPa. The second one was fitted to the densities of Hou *et al.*[23] in the same ranges of temperatures and pressure. The equations of state in the liquid had the form:

$$\frac{p}{p_0} = \delta^3\left(g_1\tau^{-1} + g_2\delta^3 + g_3 + g_4\tau^4\delta^3\right) + g_5\tau\delta^6 \exp(-\delta) + \delta^3 \exp(-\delta^2)\left(g_6\tau^5\delta + g_7\tau^{-1} + g_8\tau\delta^3 + g_9\tau^4\delta + g_{10}\tau^{-1}\delta\right) \quad (4)$$

with $\tau = T^*/T$, $\delta = \rho/\rho^*$, $p_0 = 1$ MPa, T^* 374.18 K, and $\rho^* = 508$ kg/m^3. The coefficients and exponents are given in Table 4. For both data sets the same structure of Eq. (4) was used. Therefore, only the coefficients are different.

The choice was made to transform all available caloric measurements into speed of sound values because there exists a correlation function $w=w(p,T)$ reported by Guedes and Zollweg[19] for the region of interest by which transformed and originally measured values can be compared. The results are plotted in Fig. 2. In the upper plots, Fig. 2a, density deviations from Eq. (4) are shown using the respective set of coefficients. The densities of Tillner-Roth and Baehr[55] are represented within ±0.05% while the densities of Hou *et al.*[23] are predicted within ±0.12% due to their greater uncertainty. On the average both equations represent well the (p,ρ,T)-behaviour incorporated in the respective input values.

The second row of plots, Fig. 2b, shows deviations of measured speed of sound reported by Guedes and Zollweg[19] and by Takagi[52] from the correlation function reported by the first mentioned authors. The values of Guedes and Zollweg[19] are represented within ±0.3% while the results of Takagi[52] are about 0.7% lower.

The last three rows of plots, Figs. 2c-2e, present deviations of speed-of-sound values obtained from transformation of isobaric and isochoric heat capacities and of Joule-Thomson coefficients using the correlation function of Guedes and Zollweg[8]. The plots on the left-hand side show the values transformed with Eq. (4) using the set of coefficients obtained for the data of Tillner-Roth and Baehr[55]. The plots on the right-hand side represent values transformed using the coefficients obtained using the density data of Hou *et al.*[23]. Generally, transformation leads to smaller deviations when using the densities of Tillner-Roth and Baehr[55] to establish the thermal equation of state. Using the information of the densities of Hou *et al.*[23] leads to higher systematic deviations. The maximum deviations in the latter case are 4% for transformed c_p-values, 1.5% for transformed c_v-values, and −8% to 8% for the Joule-Thomson coefficients, while the respective deviations are only 1.5%, 0.4% and −2% to 8% when using the densities of Tillner-Roth and Baehr[55].

Based on this result, we concluded that the densities of Hou *et al.*[23] are not very much consistent with the available caloric properties and, therefore, should not be used to develop a fundamental equation of state with high accuracy. Therefore, our equation of state is based on the densities of Tillner-Roth and Baehr[55] although they do not extend to very low temperatures. This decision is confirmed by the density measurements by Klomfar *et al.*[28] which were published after the work on the equation of state was finished. The densities of Klomfar *et al.*[28] agree with the EOS within ±0.05% at temperatures below 243 K, cf. Fig. 6, that is for temperatures for which no (p,ρ,T)-measurements were selected by us.

From the available caloric measurements the w-values measured by Guedes and Zollweg[19], c_v-values of Magee[23], and c_p-values reported by Wirbser[59] were used as input data. We did not include the c_p-values of Nakagawa *et al.*[39] and of Saitoh *et al.*[46] in the data set because they overlap those of Wirbser[59]. Furthermore, the large scatter of the transformed Joule-Thomson coefficients gave us reason also to exclude these data in order to prevent convergence problems during the optimization process.

3. The Fundamental Equation of State

The equation of state for HFC-134a presented here is a fundamental equation of state for the dimensionless Helmholtz free energy

$$\Phi(\tau,\delta): = \frac{A_m}{R_m T} = \frac{A}{RT} = \Phi^\circ(\tau,\delta) + \Phi^r(\tau,\delta) \quad (5)$$

where R_m=8.314471 J/(mol K) is the universal gas constant according to Moldover *et al.*[37], $R=R_m/M$ the gas constant of HFC-134a with the molar mass M=0.102032 kg/mol. A_m is the molar free energy, A the specific free energy, $\tau=T^*/T$ the inverse reduced temperature, and $\delta=\rho/\rho^*$ the reduced density. For reduction of temperature and density the critical parameters $T^*=T_c$=374.18 K[36] and $\rho^*=\rho_c$=508 kg/m^3 [26] were used. The dimensionless form Φ of the fundamental equation of state is split into an ideal part Φ° describing ideal gas properties and into a residual part Φ^r taking into account the behaviour of the real fluid.

3.1. The Free Energy for the Ideal Gas

The ideal part Φ° of the fundamental equation of state is analytically derived from the ideal gas law and an equation for the isobaric heat capacity c_p° of the ideal gas. Starting from the Helmholtz free energy of the ideal gas

$$A^\circ(\rho,T) = u^\circ(T) - T\,s^\circ(\rho,T) = h^\circ(T) - RT - T\,s^\circ(\rho,T) \quad (6)$$

and introducing the c_p°-equation leads to

$$A^\circ(\rho,T) = \int_{T_n}^{T} c_p^\circ\,dT + h_n - RT - T\int_{T_n}^{T}\frac{c_p^\circ - R}{T}\,dT - RT\ln(\rho/\rho_n) - Ts_n \quad (7)$$

where $\rho_n=p_n/(RT_n)$ is a reference density. Equation (7) requires reference values for the temperature T_n, the pressure p_n, the entropy s_n, and the enthalpy h_n. For HFC-134a, we chose to set a reference entropy s_n=1 kJ/(kg K) and a reference enthalpy h_n=200 kJ/kg at the state of saturated liquid at T_n=273.15 K and $p_n=p_s(T_n)$. Since the residual part Φ^r of the fundamental equation of state is needed to calculate the saturation properties at the reference state, the normalization of the equation of state is carried out after the residual part Φ^r had been established.

Ideal gas heat capacities have been derived by Beckermann and Kohler[6], Goodwin and Moldover[18], Chen *et al.*[9], and Gürtner and Ernst[20] either from speed of sound measurements, extrapolation of heat capacities to zero pressure, or from frequency spectra by the relations of statistical thermodynamics. HFC-134a is a derivative of ethane where rotation occurs with respect to the C—C-axis. The frequency of this energy level is very difficult to resolve, thus determination of c_p°-values from frequency spectra becomes quite uncertain. Therefore, we excluded the c_p°-values of Chen *et al.*[9] during the formulation of the c_p°-equation which is written as

$$\frac{c_p^\circ}{R} = c_1^\circ + c_2^\circ\tau^{-1/2} + c_3^\circ\tau^{-3/4} \tag{8}$$

with $\tau=T^*/T$ according to Sec. 3. Preliminary values of the coefficients were obtained from fitting Eq. (8) to values reported by Goodwin and Moldover[18] and by Gürtner and Ernst[20] in the temperature range between 230 K and 420 K. In subsequent steps the coefficients were improved by fitting the c_p°-equation together with the residual part Φ^r to caloric measurements of the real fluid which are available in a more extended temperature range. Because each caloric property of the real fluid is related to the ideal gas heat capacity c_p°, additional information is introduced into the c_p°-equation, thus extending its range of validity from 172 K to 473 K. The final coefficient values are c_1° =−0.629789, c_2° = 7.292937, and c_3° = 5.154411.

Figure 3 shows deviations of experimental heat capacities c_p° from those calculated with equation (8). The results obtained by Goodwin and Moldover[18] derived from speed of sound measurements and those of Gürtner and Ernst[20] extrapolated from c_p-measurements are represented within ±0.5%. c_p°-equations used for the HM-EOS, HE-EOS, and PNSW-EOS agree well in the intermediate temperature range, while at higher temperatures deviations exceed 1%. There, deviations are attributed to the fact that the real gas caloric properties were not taken into account by the other authors during the formulation of the c_p°-equation. The equation established by Basu and Wilson[5] is based exclusively on c_p°-values derived from spectral data and shows deviations up to +2.5% similar to the data reported by Chen *et al.*[9].

The dimensionless form $\Phi^\circ=A^\circ/(RT)$ is finally obtained from Eq. (7) using the c_p°-Eq. (8), yielding:

$$\Phi^\circ(\tau,\delta) = a_1^\circ + a_2^\circ\tau + a_3^\circ \ln\tau + \ln\delta + a_4^\circ\tau^{-1/2} + a_5^\circ\tau^{-3/4} \tag{9}$$

where a_1°=−1.019535, a_2°=9.047135, a_3°=−1.629789, a_4°=−9.723916, and a_5°=−3.927170. The coefficients a_3°, a_4°, and a_5° are derived from the coefficients of the c_p°-equation. The values of the coefficients a_1° and a_2° were calculated from enthalpy h_n and entropy s_n at the reference state chosen above.

3.2. The Formulation of the Residual Part Φ^r

In contrast to the simplicity of establishing the ideal part Φ°, it is much more difficult to find a mathematical expression for the residual part $\Phi^r(\tau,\delta)$ of the Helmholtz free energy. Since the laws of thermodynamics do not provide general relationships about the shape of the residual part, such a function must be established by fitting an appropriate equation to experimental values with the lowest standard deviation possible. Because the Helmholtz free energy cannot be measured directly, the information about it must be obtained from other thermodynamic properties accessible to measurement and related to the free energy by the equations given in Table 5. All measureable thermodynamic properties are appropriate to form the data set for the optimization process. Fitting an equation of state to different thermodynamic property data is often called a *multiproperty fit*.

The goal of any optimzation procedure is to minimize a sum of squares. For the formulation of the residual part Φ^r we used a weighted form of the least squares sum:

$$S = \sum_{i=1}^{n} (z_{exp,i} - z_{calc}(x_{exp,i}, y_{exp,i}, \phi^r, \vec{a}))^2 \, \sigma_i^{-2} \rightarrow \text{Min.} \tag{10}$$

$z=z(x,y,\phi^r,\vec{a})$ denotes a relationship between any thermodynamic property (such as p, c_p, c_v, ...), the residual part Φ^r of the free energy, the parameter vector $\vec{a}$ to be optimized and the independent variables x and y, which are in our case τ and δ. The relationships given in Table 5 allow us to include residuals for experimental values $z_{exp}(x_{exp},y_{exp})$ of different thermodynamic properties.

The residual quantity $\Delta z = z_{exp} - z_{calc}$ is divided by the total uncertainty σ obtained from the Gaussian error propagation law according to

$$\sigma^2 = \left(\frac{\partial(\Delta z)}{\partial z}\right)^2 \sigma_z^2 + \left(\frac{\partial(\Delta z)}{\partial x}\right)^2 \sigma_x^2 + \left(\frac{\partial(\Delta z)}{\partial y}\right)^2 \sigma_y^2. \tag{11}$$

σ_x, σ_y, σ_z denote the uncertainties of the variables x, y, and z, respectively which are obtained from estimated experimental uncertainties. The partial derivatives may be calculated from ancillary equations given in Sec. 3.2.3 or from a preliminary fundamental equation of state when available during the optimization process. However, changing the total uncertainty by recalculation has negligible influence on the result of the optimization.

Two optimization strategies have been employed to establish the fundamental equation of state for HFC-134a. The first one is the regression analysis developed by Wagner[57]. Based on statistical significance this algorithm selects from a so-called *bank of terms* those terms which form an equation giving the best fit to a given data set. Since it is a linear method, only those experimental data can be used which linearly depend on the independent variables δ and τ. Such *linear* experimental values are (p,ρ,T)-values, isochoric heat

capacities or virial coefficients. Linear properties are marked in Table 5. Beside these, any other linear relationship may be included during optimization (see Sec. 3.2.1). However, since the form of the equation of state is unknown at the beginning of the optimization process, only measured linear property data can be used at a first step.

The bank of terms which we used contained 615 terms. It may be written in the following form:

$$\Phi^r_{BOT}=\sum_{i=1}^{N_0} a_i \delta^{d_i}\tau^{t_i} + \sum_{k=1}^{5}\left(\exp(-\delta^k)\cdot\sum_{i=N_{k-1}+1}^{N_k} a_i\delta^{d_i}\tau^{t_i}\right). \quad (12)$$

A detailed description of exponents is given in Table 6. A similar bank of terms has already successfully been employed by different correlators to establish various fundamental equations of state (Setzmann and Wagner[51], Saul and Wagner[47], Marx *et al.*[35]). The bank of terms does not include the two-dimensional Gaussian terms which have been used by Wagner his co-workers to improve the representation in the critical region. For HFC-134a too few experimental data exist in the immediate vicinity of the critical point to justify the use of such terms.

A large initial bank of terms causes a significant increase of computing time. Therefore, the regression analysis is based on a subset of about 100 terms. During regression analysis, this subset is continuously modified. Useful terms were kept in the *working bank of terms* while unused terms are exchanged with terms from the *mother bank of terms*. By this pre-optimization of the working bank of terms computing time could be decreased to about 5%. A detailed description of this procedure is given by Tillner-Roth[56].

Once a preliminary structure of the residual part has been determined it is transferred to a non-linear optimization routine. For this purpose, we used the Gauss-Newton-method described by Dennis *et al.*[10]. The *non-linear* optimization allows us to consider also non-linear experimental data, such as speed of sound, isobaric heat capacities or vapor pressure, according to the direct method proposed by Ahrendts and Baehr[1]. The least squares sum is given according to Eq. (10). The result is a very much improved equation of state which is used to linearize non-linear data to be considered additionally in a subsequent step of the regression analysis. Therefore, the whole optimization process is a cycle, Fig. 4, switching continuously between regression analysis (improving the structure) and non-linear optimization. Whenever an improved equation of state was obtained from the non-linear regression the linearized non-linear data have been recalculated to always provide the actual information of thermodynamic behaviour to the regression analysis.

3.2.1. Linearization of Non-linear Relationships

The most important relationships to be linearized are those for the saturation properties, namely the combination of vapor pressure, saturated liquid and saturated vapor density. These properties are calculated by iteration for a given temperature from the following set of equations written in the free energy form

$$p_s = RT\rho'(1+\delta'\Phi^r_\delta)(\tau,\delta') \quad (13)$$

and

$$p_s = RT\rho''(1+\delta''\Phi^r_\delta)(\tau,\delta''), \quad (14)$$

$$\frac{p_s}{RT}\left(\frac{1}{\rho''}-\frac{1}{\rho'}\right) - \ln\frac{\rho'}{\rho''} = \Phi^r(\tau,\delta')-\Phi^r(\tau,\delta''). \quad (15)$$

Each of these equations is linear with respect to the coefficients of Φ^r when all three saturation properties p_s, ρ', ρ'' are given at a unique temperature (cf. Bender[7]). However, measured properties which fulfill this requirement are rarely found. Therefore, the saturation properties have been pre-correlated by separate equations for the vapor pressure (19), saturated liquid density (20), and saturated vapor density (21) thus enabling *artificial* measurements to be generated at unique temperatures. The equations for vapor pressure and saturation densities are given in Sec. 3.2.3. For HFC-134a, 130 artificial quadruples (p_s,ρ',ρ'',T) were generated between 180 K and the critical temperature every 2 K. At temperatures close to the critical point the intervals were decreased down to 0.2 K.

Further linearization of non-linear data was carried out after a preliminary equation of state had been established. This linearization is applied to caloric data that are non-linear, namely the isobaric heat capacity and speed of sound. It is based on Eqs. (1) and (2) which connect an isochoric heat capacity with derivatives of pressure with respect to density and temperature. Each of these components is linear itself and the information contents of such a caloric property can be linearized by calculating values for

$$\frac{\partial p}{\partial T} = R\,\rho\,(1+\delta\Phi^r_\delta - \delta\tau\Phi^r_{\delta\tau}) \text{ and } \frac{\partial p}{\partial \rho} = RT(1+2\delta\Phi^r_\delta+\delta^2\Phi^r_{\delta\delta}) \quad (16)$$

from the preliminary equation of state. These are used to transform speed of sound or isobaric heat capacity into a value of the isochoric heat capacity which linearly depends on the fundamental equation and, therefore can be used during regression analysis. Additionally, the derivatives according to Eq. (16) were used as input values. By this linearization c_p- or w-values can be considered during the optimization of the structure. The artificial linearized data must be recalculated at every iteration, if an improved equation of state has been found after non-linear optimization.

3.2.2. Restrictions in the Critical Area

To obtain a physically correct shape of the isotherms in the immediate vicinity of the critical point a special restriction in the critical region has been introduced during non-linear optimization. It is based on the condition of stability which is written as

$$(\partial p/\partial\rho)_T \geq 0, \quad (17)$$

that must be fulfilled at every single-phase state. From this condition the residual

$$R_i = \frac{\partial p}{\partial\rho} - \sqrt{\left(\frac{\partial p}{\partial\rho}\right)^2} \quad (18)$$

has been derived which is considered in the sum of least squares at predefined points (T,ρ) immediately above the highest measured critical temperature. Those points have been chosen on two isotherms at 374.30 K 374.60 K for densities between 450 kg/m^3 and 560 kg/m^3. Outside of this range there are enough experimental data to ensure a correct fit of the equation of state. These residuals force the optimization process to act in the following way:

When thermodynamic stability is met the derivative $(\partial p/\partial \rho)$ is positive and therefore the residual quantity of Eq. (18) will be zero. When the derivative becomes negative the stability condition is not fulfilled. This results in a comparatively large residual quantity, thus forcing the optimization to correct the shape of the (p,ρ,T)-surface. The advantage of this strategy is the smoothness of this restriction compared to a strategy of constraining the equation of state to a measured critical point. The optimization process is only influenced, when the equation of state does not obey the stability condition (17), while there is maximum flexibility for optimization in other parts of the (p,ρ,T)-surface when the stability condition is fulfilled.

3.2.3. Ancillary Equations

This section describes three equations which were used to linearize saturation properties to be included during the regression analysis. These are namely a vapor pressure equation and equations for the densities of saturated liquid and saturated vapor. All equations were established by employing the regression analysis of Wagner[57].

The vapor pressure is represented by

$$\vartheta \ln \frac{p_s}{p_c} = -7.686556\,\theta + 2.311791\,\theta^{3/2} - 2.039554\,\theta^2 - 3.583758\,\theta^4 \quad (19)$$

where $\vartheta = T/374.18$ K, $\theta = 1 - \vartheta$ and $p_c = 4.05629$ MPa. It is based on the same vapor pressure measurements as used to establish the fundamental equation of state covering temperatures between 180 K and 374.15 K. The data are represented within ± 20 Pa or $\pm 0.03\%$ whichever is greater. The critical pressure used in Eq. (19) was determined by fitting it, simultaneously with the coefficients, to the input data.

The equation for the saturated liquid density is based on a selection of available data. It is valid between 180 K 374 K although its uncertainty increases in the vicinity of the critical temperature. It is written as

$$\frac{\rho'}{\mathrm{kg/m^3}} = 518.20 + 884.13\,\theta^{1/3} + 485.84\,\theta^{2/3} + 193.29\,\theta^{10/3} \quad (20)$$

with the same definitions used in Eq. (19). It represents the selected input values within 0.2% except those for temperatures above 370 K where deviations increase up to 1%.

The equation for the saturated vapor density is written as

$$\ln \frac{\rho''}{\rho_0} = -2.837294\,\theta^{1/3} - 7.875988\,\theta^{2/3} + 4.478586\,\theta^{1/2} - 14.140125\,\theta^{9/4} - 52.361297\,\theta^{11/2} \quad (21)$$

where $\rho_0 = 516.86$ kg/m^3 was determined during the formulation of that equation. The definitions of variables correspond to those used in Eq. (19). Equation (21) has been fitted to experimental values above 293 K and to artificial values which were calculated down to 180 K from the function for the second virial coefficient reported by Goodwin and Moldover[18]. It represents the artificial and originally measured input data within 0.6% except for temperatures above 368 K where deviations increase up to 2%.

3.2.4. The Residual Part Φ^r for HFC-134a

The function of the residual part for HFC-134a resulting from the optimization process described is written as

$$\Phi^r = \sum_{i=1}^{8} a_i \tau^{t_i} \delta^{d_i} + \exp(-\delta) \sum_{i=9}^{11} a_i \tau^{t_i} \delta^{d_i} + \exp(-\delta^2) \sum_{i=12}^{17} a_i \tau^{t_i} \delta^{d_i} + \exp(-\delta^3) \sum_{i=18}^{20} a_i \tau^{t_i} \delta^{d_i} + a_{21} \exp(-\delta^4) \tau^{t_{21}} \delta^{d_{21}}. \quad (22)$$

Coefficients exponents are given in Table 7. The definitions of variables are chosen according to the description given in Sec. 3.

Derivatives of the fundamental EOS are required to evaluate thermodynamic properties. They are given in the following equations corresponding to the most general form of the EOS given by Eqs. (9) and (12). The first derivatives are calculated according to

$$\Phi^o_\delta = 1/\delta \quad (23)$$

$$\Phi^o_\tau = a_2^o + \frac{a_3^o}{\tau} + \sum_{j=4}^{N^o} a_j^o t_j^o \tau^{t_j^o - 1} \quad (24)$$

$$\Phi^r_\delta = \sum_{i=1}^{N_0} a_i\, d_i \delta^{d_i - 1} \tau^{t_i} + \sum_{k=1}^{4} \left(\exp(-\delta^k) \sum_{i=N_{k-1}+1}^{N_k} a_i\, (d_i - k\delta^k)\, \delta^{d_i - 1} \tau^{t_i} \right) \quad (25)$$

$$\Phi^r_\tau = \sum_{i=1}^{N_0} a_i t_i \delta^{d_i} \tau^{t_i - 1} + \sum_{k=1}^{4} \left(\exp(-\delta^k) \sum_{i=N_{k-1}+1}^{N_k} a_i t_i \delta^{d_i} \tau^{t_i - 1} \right) \quad (26)$$

The second derivatives are obtained from

$$\Phi^o_{\delta\delta} = -1/\delta^2 \quad (27)$$

$$\Phi^o_{\tau\tau} = -\frac{a_3^o}{\tau^2} + \sum_{j=4}^{N^o} a_j^o t_j^o (t_j^o - 1) \tau^{t_j^o - 2} \quad (28)$$

$$\Phi^o_{\tau\delta} = 0 \quad (29)$$

$$\Phi^r_{\delta\delta} = \sum_{i=1}^{N_0} a_i d_i (d_i - 1)\, \delta^{d_i - 2} \tau^{t_i} + \sum_{k=1}^{4} \left(\exp(-\delta^k) \sum_{i=N_{k-1}+1}^{N_k} a_i \left[d_i^2 - d_i - k\delta^k (2d_i + k - 1 + k\delta^k) \right] \delta^{d_i - 2} \tau^{t_i} \right) \quad (30)$$

$$\Phi^r_{\tau\tau} = \sum_{i=1}^{N_0} a_i t_i (t_i - 1)\delta^{d_i}\tau^{t_i-2} + \sum_{k=1}^{4}\left(\exp(-\delta^k)\sum_{i=N_{k-1}+1}^{N_k} a_i t_i (t_i-1)\delta^{d_i}\tau^{t_i-2}\right) \quad (31)$$

$$\Phi^r_{\tau\delta} = \sum_{i=1}^{N_0} a_i d_i t_i \delta^{d_i-1}\tau^{t_i-1} + \sum_{k=1}^{4}\left(\exp(-\delta^k)\sum_{i=N_{k-1}+1}^{N_k} a_i t_i (d_i - k\delta^k)\delta^{d_i-1}\tau^{t_i-1}\right) \quad (32)$$

The counters N_k are N_0=8, N_1=11, N_2=17, N_3=20, N_4=21.

4. Comparisons with Experimental Data

In the following section comparisons are given between experimental values, our own EOS, and the equations of state mentioned in Sec. 1.2. Generally, deviations shown in the figures are based on our own EOS. Where comparisons with the other equations of state are made, those equations were evaluated for temperatures or pressures lying in the middle of the interval of the specific plot. If a deviation plot is concerned with a certain isotherm or isochore the equations were evaluated at the temperature or density values indicated in the respective plot.

4.1. Single-Phase Properties

4.1.1. (p,ρ,T)-Data

Because of the large number of measurements the (p,ρ,T)-surface is divided into four sections for appropriate discussion:

- vapor region ($\rho<0.8\rho_c$, T<385 K),
- liquid region ($\rho>1.3\rho_c$, T<385 K),
- near-critical region ($0.8\rho_c<\rho<1.3\rho_c$, 370 K <T<385 K),
- supercritical region T>385 K.

Pressure deviations between values calculated from our own EOS and experimental results in the gaseous phase are shown in Fig. 5. The data of Dressner and Bier[12] and of Tillner-Roth and Baehr[54] are generally represented within ±0.05%. Deviations are slightly larger for the two lowest Burnett-isotherms of Tillner-Roth and Baehr[54] reaching +0.08%. This is due to the larger uncertainties of the relatively short Burnett-isotherms. Good agreement is also observed for the values measured by Qian *et al.*[45] and those of Weber[58] at densities below 100 kg/m^3 with deviations mostly below ±0.05%. At higher densities, Weber's results show deviations up to +0.12% increasing with density. The other three equations of state had also been fitted to the values of Tillner-Roth and Baehr[54] and predict about the same behaviour in the gaseous phase. Differences in representation are observed near the saturation boundary and for densities approaching the critical value, where deviations of the HE-EOS and the PNSW-EOS from our own EOS increase up to ±0.3% which is higher than the estimated uncertainties of the measurements.

In the liquid, Fig. 6, our own EOS represents the densities of Tillner-Roth and Baehr[55] generally within ±0.06% without considerable systematic deviations. These measurements are in slight contradiction to the extensive series of Hou *et al.*[23] whose densities deviate from them by almost 0.2%. Approaching the critical temperature, the deviations between both series increase up to 1%. The decision to prefer the data of Tillner-Roth and Baehr[55] was based on a consistency test between liquid densities and caloric measurements in the liquid phase described in Sec. 2.2.1. This test indicates that the densities of Hou *et al.*[23] are not consistent with the measured caloric properties in the liquid. Another indicator for the accuracy of the liquid densities of Tillner-Roth and Baehr[55] is the HM-EOS, originally fitted to the densities of Hou *et al.*[23]. The HM-EOS predicts density values about 0.2% lower than our own EOS at low temperatures but agreement with the densities of Tillner-Roth and Baehr[55] improves with rising temperature. Obviously, the influence of the slightly inconsistent densities of Hou *et al.*[23] is superseded by the influence of caloric input data in the liquid phase forcing the HM-EOS to tend more to the consistent densities of Tillner-Roth and Baehr[55], although they had not been used for establishing the HM-EOS. Very recently, a new set of liquid densities was published by Klomfar *et al.*[28]. Their measurements confirm the densities of Tillner-Roth and Baehr[55] within ±0.08%. The HE-EOS and the PNSW-EOS show density deviations from our own correlation of about 0.2% at low temperatures but they increase when approaching the saturation boundary at higher temperatures.

Deviations of pressure and density in the near-critical and supercritical region are shown in Fig. 7. The fundamental EOS represents the pressures of Tillner-Roth and Baehr[54,55] and Dressner and Bier[12] within ±0.2% even as close as 1 K to the critical temperature. For higher supercritical temperatures density deviations are within ±0.2% for these two sets of data. Good agreement is also observed for the (p,ρ,T)-data of Piao *et al.*[43] in the vicinity of the critical point. The HM-EOS, HE-EOS, and the PNSW-EOS show relatively large deviations from the experimental data up to 0.5% of pressure in the near-critical region. For higher supercritical temperatures, density deviations of these three equations of state from our own EOS are particularly large for high pressures, exceeding ±0.5%. Deviations of (p,ρ,T)-properties calculated from the extended cross-over model developed by Tang *et al.*[53] are included in Fig. 7. The range of validity of Tang's model is from 200 kg/m^3 to 800 kg/m^3 for temperatures up to 450 K. Differences in pressure are within ±0.5% in the near-critical region and deviations in density are below ±0.5% in the supercritical region except for the highest isotherm evaluated at 447.5 K which is rather close to the upper limit of validity of Tang's model. The agreement between our own EOS and Tang's model is best for densities and temperatures close to the critical point where deviations are below ±0.2% of pressure. Generally, deviations of Tang's model increase for high and low density values.

In the following paragraphs the results of data analysis for all available (p,ρ,T)-measurements are referred to seperately for each source listed in Table 2.

1. (p,ρ,T)-values of Baroncini *et al.*[4] (Fig. 8)
   These values comprise a temperature range from260 K to 360 K in the vapor phase and overlap with the

selected values of Tillner-Roth and Baehr[54]. As shown in Fig. 8, these values show large scatter from −0.5% to +1.2% of density and were not selected.

2. (p,ρ,T)-values of Basu and Wilson[5] (Fig. 9)
These were among the first experimental (p,ρ,T)-values reported for HFC-134a. On the average, these data agree with the selected densities. Because of their large scatter ranging from −1% to +1%, indicating their larger uncertainty, the measurements of Basu and Wilson[5] were not used as input values.
3. (p,ρ,T)-values of Dressner and Bier[12] (Figs. 5, 7)
Dressner and Bier[12] performed Burnett-measurements on 4 isotherms between 333 K and 423 K which agree to within ±0.06% with the Burnett-values of Tillner-Roth and Baehr[54] in the whole range of temperature and pressure. Although these data overlap with the other selected (p,ρ,T)-data in the vapor phase, they were used as input values due to their exceptional accuracy.
4. (p,ρ,T)-values of Döring[11] (Fig. 10)
The investigations of Döring[11] were carried out in the gaseous phase for temperatures between 260 K and 400 K at medium densities overlapping the values of Tillner-Roth and Baehr[54]. The densities show large systematic deviations up to +2% and do not supply accurate information.
5. (p,ρ,T)-values of Fukushima *et al.*[15] (Fig. 11)
This series has been rejected due to its scatter of about ±1% of density and because it overlaps the selected more accurate data. On the average the values agree with the selected measurements.
6. (p,ρ,T)-values of Hou *et al.*[23] (Fig. 6)
This extensive experimental study comprises 429 liquid densities between 180 K and 380 K and pressures up to 70 MPa. The values are about 0.2% lower than the densities obtained by Tillner-Roth and Baehr[55] used in the selected data set. The consistency test presented in Sec. 2.2.1 proves that the values of Hou *et al.*[23] are inconsistent with the available caloric measurements in the liquid phase, and thus were not used to develop the EOS.
7. (p,ρ,T)-values of Kesselman *et al.*[27] (Fig. 12)
Most of the liquid densities of Kesselman *et al.*[27] agree with the selected values within 0.3% but some data points show deviations up to 1% of density especially in the vicinity of the saturation boundary and at very high pressures. Since they also overlap the selected liquid densities they were not included.
8. (p,ρ,T)-values of Maezawa *et al.*[32] (Fig. 13)
Ten densities in the liquid phase were measured by Maezawa *et al.*[32] overlapping other measurements. They agree well with the measurements of Hou *et al.*[23] and are, therefore, about 0.2% lower than the measurements of Tillner-Roth and Baehr[55] thus being not selected.
9. (p,ρ,T)-values of Magee[33] (Fig. 14)
150 liquid densities were reported by Magee[33] obtained during his isochoric heat capacity measurements. His results are located between those of the series of Hou *et al.*[23] and of Tillner-Roth and Baehr[55] showing deviations of about −0.1% on the average. Furthermore, deviations on isochores increase with increasing temperatures. Due to these deviations and due to the result of the consistency test, Sec. 2.2.1, we decided not to select the (p,ρ,T)-data of Magee[33].
10. (p,ρ,T)-values of Morrison and Ward[38] (Figs. 15a,b)
These measurements were performed with a vibrating tube densimeter in the liquid phase between 280 K and 365 K and pressures up to 5.5 MPa completely overlapping the results of Tillner-Roth and Baehr[55]. Although deviations from the fundamental EOS are within ±0.1% for temperatures below 340 K the scatter is about two times larger than that of the selected densities of Tillner-Roth and Baehr[55]. Deviations at temperatures above 340 K occasionally reach 0.4%. The densities of Morrison and Ward[38] were not used due to these deviations and due to overlapping the selected measurements.
11. (p,ρ,T)-values of Piao *et al.*[43] (Figs. 16a,b)
The results of Piao *et al.*[43] cover both the vapor and the liquid region and agree within ±0.5% with the selected input values. They have not been used as input data because they completely overlap the selected data and because their uncertainty is about three times larger compared to the input values in the region of interest.
12. (p,ρ,T)-values of Park[42] (Fig. 17)
Large systematic deviations exceeding −3% of density are observed between the Burnett-measurements of Park[42] and our own EOS at higher pressures. Therefore, these measurements were not selected.
13. (p,ρ,T)-values of Qian *et al.*[45] (Fig. 5)
All 21 Burnett-values reported by Qian *et al.*[45] agree within 0.1% with the Burnett-values of Tillner-Roth and Baehr[54]. They completely overlap with the selected measurements and, therefore, can be neglected without loss of experimental information.
14. (p,ρ,T)-values of Tillner-Roth and Baehr[54] (Figs. 5, 7)
This set of measurements comprises 411 values for temperatures between 293 K and 453 K at pressures from 0.1 MPa to 16 MPa. Comparisons between these values and measurements of Qian *et al.*[45] and Dressner and Bier[12] show excellent agreement. Furthermore, comparisons between derived second virial coefficients and results reported by other sources[18,12,58] confirm the accuracy of these measurements. 393 of these (p,ρ,T)-data were used as input values for thecorrelation process except for the first one or two values of the supercritical Burnett-isotherms at the highest pressures, which are generally of lower accuracy than the remaining points of a Burnett series.
15. (p,ρ,T)-values of Tillner-Roth and Baehr[55] (Figs. 6, 7)
432 (p,ρ,T)-values in the liquid and supercritical region at high densities between 243 K and 413 K at pressures up to 16 MPa are reported from this source measured with a vibrating tube densimeter. From these data, 413 values were selected but those at low densities in the supercritical region at pressures below

4 MPa were excluded because their accuracy was significantly lower.

16. (p,ρ,T)-values of Weber[58] (Figs. 5, 7, 18)
The isochoric measurements performed by Weber[58] are based upon a Burnett expansion series performed at 368.15 K to which the densities of the isochoric measurements are related. His results agree within ±0.05% of pressure with the Burnett measurements of Tillner-Roth and Baehr[54] at low densities but show deviations up to +0.12% at pressures above 2 MPa (cf. Figs. 5, 7). A more detailed comparison between the (p,ρ,T)-data of Tillner-Roth and Baehr[54], Dressner and Bier[12], and Weber[58] is given in Fig. 18. It shows deviations of pressure between 360 K and 400 K for pressures between 1 MPa and 5 MPa. The results of Tillner-Roth and Baehr[54] and of Dressner and Bier[12], which were both selected, agree within 0.05% which is smaller than the combined limit of uncertainty estimated to be about ±0.08% for these sets of measurements. The pressures reported by Weber[58] are systematically higher than those of Tillner-Roth and Baehr and also than those of Dressner and Bier for densities around 200 kg/m³. Deviations occasionally exceed the combined limits of uncertainty. Due to these systematic deviations, we decided not to select the measurements of Weber[58].
17. (p,ρ,T)-values of Zhu *et al.*[63] (Fig. 19)
The results of Zhu *et al.*[63] are located in the gaseous phase and show systematic deviations of density from −1% to +0.7% compared to other reliable values.

4.1.2. Second Virial Coefficient

Values of the second virial coefficient were reported by six authors (see Table 2). They were mostly derived from (p,ρ,T) or speed of sound measurements. We preferred not to include virial coefficients during the correlation process because they are derived properties and, therefore, their accuracy may be affected by deficiencies of the models used to derive them. However, the experimental information of the second virial coefficient is still considered because speed of sound and (p,ρ,T)-properties from which they were derived are included during the optimization process.

Deviations of B-values from the fundamental EOS are plotted in Fig. 20. Above 290 K, the virial coefficients of Tillner-Roth and Baehr[54], Dressner and Bier[12], and Goodwin and Moldover[18] are represented by our own EOS within ±1%. At temperatures below 290 K the results of Goodwin and Moldover[18] are represented within 1.5% because their speed of sound values had been included during the formulation of the equation of state. Another set of second virial coefficients by Beckermann and Kohler[6] was also derived from speed of sound measurements showing deviations of about +1%. The values reported by Schramm *et al.*[49,50] show deviations up to 3%.

The HM-EOS and the HE-EOS agree well with the own equation within ±2%. The PNSW-EOS shows deviations up to 4% at the upper and lower temperature limits of Fig. 20.

4.1.3. Isochoric Heat Capacity

150 isochoric heat capacities were measured by Magee[33] in the liquid region. A detailed sample of the deviations from the EOS is given in Fig. 21. Most of these experimental data are represented within ±1% which corresponds to twice the uncertainty given by Magee[33]. The highest deviations occur for the isochores in the high temperature range while at lower temperatures deviations are generally less than ±0.6%. Although deviations are comparatively low, it seems that there are sometimes deviations on an isochore being systematic with respect to temperature. These effects may be related to the deviations observed for Magee's (p,ρ,T)-values discussed in Fig. 14.

There are small differences of data representation between our own EOS and the other three equations of state being largest at temperatures above 300 K where they reach ±1%.

4.1.4. Isobaric Heat Capacity

Measurements of the isobaric heat capacity c_p are reported by Gürtner and Ernst[20] in the gaseous phase, and by Wirbser[59], Saitoh *et al.*[46], and Nakagawa *et al.*[39] in the liquid phase. Only those by Gürtner and Ernst[20] and 117 of those measured by Wirbser[59] were used as input data during the optimization process. The values of Saitoh *et al.*[46] and of Nakagawa *et al.*[39] overlap those of Wirbser[59] and, therefore, were not selected.

Deviations of isobaric heat capacities from the fundamental EOS are plotted for several isobars in Fig. 22. The c_p-values of Wirbser[59], Nakagawa *et al.*[39], and of Saitoh *et al.*[46] are generally represented within ±1%. Exceptions are the critical region where deviations increase up to 60% and the supercritical region above 500 K where deviations are up to 2%. In the critical region there are only a few c_p-measurements available. Therefore, caloric properties are not represented well near the critical point by the analytical equation of state presented here. Thus, calculation of heat capacities and speed of sound should be avoided for densities within 400 kg/m³ to 600 kg/m³ at temperatures between 370 K and 380 K. This exclusion does not apply to (p,ρ,T)-properties; they are represented within ±0.15% of pressure as shown in Fig. 7. For temperatures above 480 K, HFC-134a is supposed to decompose[31]. This might explain slightly larger deviations above 500 K.

The three other equations of state show good agreement with our own EOS in the liquid phase, especially at low temperatures. In the gas, when approaching the state of saturated vapor, the three other equations of state all exhibit a downturn in heat capacity of about 3% compared to our own EOS and available measurements. This effect is particularly large for the PNSW-EOS and for the HE-EOS while the amount of deviation between the HM-EOS and our own correlation is generally below 2%. These differences between the equations are attributed to the small number of available experimental c_p-data in the immediate vicinity of the saturation line, thus allowing too much flexibility during the optimization of any equation of state. At higher temperatures, deviations increase particularly for the HM-EOS and the HE-EOS exhibiting values up to ±5%. The PNSW-EOS agrees better

with our own EOS. Large differences between all four equations of state occur in the critical area also for the cross-over model developed by Tang *et al.*[53]. c_p-values calculated from their model show large systematic deviations from the measurements located outside the limits of the diagrams of Fig. 22.

4.1.5. Speed of Sound

Four sets of speed of sound measurements are reported in the literature which are listed in Table 2. In the gaseous phase, the speed of sound was measured by Goodwin and Moldover[18] and by Beckermann and Kohler[6] for temperatures between 233 K and 410 K at pressures up to 0.6 MPa. In the liquid phase, speed of sound measurements are reported by Guedes and Zollweg[19] and by Takagi[52] for temperatures between 180 K and 380 K at pressures up to 70 MPa. Deviations between values calculated from the fundamental EOS and the measurements are plotted in Fig. 23 for the gaseous phase and in Fig. 24 for the liquid phase.

In the gaseous phase, our equation has been fitted to the values of Goodwin and Moldover[18] which are represented within ±0.03%. The measurements of Beckermann and Kohler[6] generally agree with the values of Goodwin and Moldover[18] within the limits of uncertainty but on some isotherms they reveal systematic deviations up to ±0.07%. Therefore, the values of Beckermann and Kohler[6] have not been used as input data. The HM-EOS predicts about the same values as our own correlation but deviations increase up to ±0.06% when approaching the saturated vapor state. This effect corresponds to the respective c_p-deviations shown in Fig. 22 attributed to the absence of caloric measurements in the immediate vicinity of the saturation boundary.

Furthermore, an offset of about 0.02% between our own equation of state and the equations of the other authors is observed at higher temperatures for diminishing pressure due to a slightly different representation of the ideal gas heat capacity c_p° at high temperatures (cf. Fig. 3) corresponding to the c_p°-deviation of about 0.5%.

In the liquid, our equation is based on the speed of sound values of Guedes and Zollweg[19] which are predicted within ±0.3% except for some values in the critical region. The values of Takagi[52] are up to 0.7% lower than those of Guedes and Zollweg[19] and, therefore, were not used to establish our EOS. Comparisons with the HE-EOS and the HM-EOS reveal small systematic deviations although these equations still predict the speed of sound measurements within ±0.3%. The PNSW-EOS shows large systematic errors especially at low temperatures and low pressures.

4.1.6. Joule-Thomson Coefficient

108 Joule-Thomson coefficients measured by Wirbser[59] cover the range of temperature between 333 K and 423 K at pressures up to 20 MPa. Deviations are plotted in Fig. 25. In the gaseous phase, the measurements are represented within ±3% compared to our own equation of state. In the liquid phase at increasing pressures the value of the Joule-Thomson coefficient decreases exhibiting negative values at temperatures below 375 K. These data are represented with deviations up to 10% due to their small values. Absolute deviations in the liquid phase are always less than 0.1 K/MPa. In the whole range of measurements, all equations of state predict about the same Joule-Thomson coefficients as indicated in Fig. 25.

4.2. Saturation Properties

4.2.1. Vapor Pressure

Four sets of measured vapor pressures fulfil the requirements of being highly accurate data and were selected for the formulation of the EOS. These are namely the measurements of Goodwin *et al.*[17], Weber[58], Tillner-Roth and Baehr[3], and the six lowest pressures measured by Magee and Howley[34]. Deviations between these values and the fundamental EOS are shown in Fig. 26. The values are represented within ±0.05 % at temperatures above 220 K and within ±20 Pa at lower temperatures. The offset of about 0.1% observed for the values of Goodwin *et al.*[17] at 265 K results from changing the apparatus. At temperatures above 310 K the series of Tillner-Roth and Baehr[3] and of Weber[58] agree remarkably well, within ±0.01%. Both series are represented by the EOS within about the same limits of uncertainty. The representation of vapor pressure by the HM-EOS is about the same in the whole temperature range. The HE-EOS and the PNSW-EOS show larger systematic deviations up to +0.4% in the vicinity of the critical temperature.

The 12 remaining series listed in Table 3 were not used as input values. These data either show larger scatter or systematic deviations from the above mentioned measurements as shown in Fig. 27.

4.2.2. Saturated Liquid Density

Available measurements of the saturated liquid density are listed in Table 3 and are plotted as deviations from the EOS in Fig. 28. The equation of state has not been fitted to any saturated liquid densities. These were mostly derived from compressed liquid densities of which numerous values were used as input data.

Four data sets agree well within ±0.15% and are represented by our EOS within the same narrow limits. These are namely the measurements performed by Yokoyama and Takahashi[61], Kruse[29], Niesen *et al.*[40], and Tillner-Roth and Baehr[55]. At lower temperatures, the fundamental EOS shows deviations from the measurements of Hou *et al.*[23] and Maezawa *et al.*[32] similar to their compressed liquid densities (see also Fig. 6). At temperatures approaching the critical point, the values reported by Fukushima *et al.*[16] are smaller while the densities reported by Kabata *et al.*[26] are larger than the ρ'-values predicted by the EOS.

From the other equations of state, the HM-EOS agrees best with our own equation although at low temperatures, systematic deviations are observed which accord with the results for the compressed liquid density. The HE-EOS and the PNSW-

EOS show their largest deviations when approaching the critical temperature.

4.2.3. Saturated Vapor Density

There are six sets of measurements for the saturated vapor density which are listed in Table 3. Comparisons of them to our own EOS are shown in Fig. 29. The results obtained by Weber[58], Fukushima[14,16], and Niesen *et al.*[40] agree with our own equation within ±2% which is in most cases within the estimated uncertainty. The deviations for the values reported by Morrison and Ward[38] are considerably large, reaching values up to 18%. In the vicinity of the critical region the equation agrees best with the data of Fukushima[14] while the values of Kabata *et al.*[26] show large negative deviations. The prediction of the saturated vapor density by the other three equations of state is similar to our own EOS at high temperatures. At lower temperatures, deviations are up to ±2% due to the different prediction of the second virial coefficient.

4.2.4. Isochoric Heat Capacity in the Two-phase Region

160 values of the isochoric heat capacity $c_v^{(2)}$ in the two-phase region were measured by Magee[33]. This kind of property is very complex. In Fig. 30, the shape of a c_v-isotherm is qualitatively plotted versus volume. A value for the two-phase heat capacity $c_v^{(2)}$ is obtained from the two-phase heat capacities at saturated liquid and saturated vapor $\bar{c}_v'$ and $\bar{c}_v''$ according to

$$c_v^{(2)} = \bar{c}_v' + \frac{v-v'}{v''-v'}(\bar{c}_v''-\bar{c}_v'). \tag{33}$$

The jumps $\Delta\bar{c}_v'$ and $\Delta\bar{c}_v''$ of the isochoric heat capacity on the saturation boundaries are calculated from

$$\Delta c_v'^{-} = \bar{c}_v' - c_v(v',T) = -T\left[\frac{dp_s}{dT} - \left(\frac{\partial p}{\partial T}\right)_{v'}\right]^2 \left(\frac{\partial p}{\partial v}\right)_{v'}^{-1} \tag{34}$$

and

$$\Delta\bar{c}_v'' = \bar{c}_v'' - c_v(v'',T) = -T\left[\frac{dp_s}{dT} - \left(\frac{\partial p}{\partial T}\right)_{v''}\right]^2 \left(\frac{\partial p}{\partial v}\right)_{v''}^{-1}. \tag{35}$$

The single phase isochoric heat capacities and the derivatives $(\partial p/\partial v)$ and $(\partial p/\partial T)$ are obtained from the fundamental equation of state according to the relations given in Table 5. The first derivative of the vapor pressure is calculated from the law of Clausius-Clapeyron

$$\frac{dp_s}{dT} = \frac{s''-s'}{v''-v'}. \tag{36}$$

These relations illustrate the complexity of the two-phase heat capacity which contains information about the whole isotherm reaching from ideal gas to compressed liquid. Thus, comparisons of this property are a sensitive test for an equation of state concerning the consistency of the whole data set.

Deviations between the measured values and values calculated from the EOS are shown in Fig. 31. They are less than ±1% in the whole temperature range of Magee's experiments. The good representation was achieved by using Magee's single-phase isochoric heat capacities as input values being related to the two-phase heat capacity $c_v^{(2)}$ by the relations indicated above. For temperatures below 190 K, Magee's $c_v^{(2)}$-values were used to establish the fundamental EOS because for these temperatures no single-phase c_v-values were available.

The equations of other authors reveal deviations which are below 1% at temperatures above 260 K but increase for lower temperatures. They become larger when approaching the triple point where the values predicted by the HM-EOS are too small while those predicted by the HE-EOS and the PNSW-EOS are larger than the measured values.

4.3. Critical Point

From the conditions of the critical point

$$\left(\frac{\partial p}{\partial v}\right)_c = 0 \qquad \text{and} \qquad \left(\frac{\partial^2 p}{\partial v^2}\right)_c = 0, \tag{37}$$

the critical parameters can be calculated. The critical point of the fundamental equation of state is located at:

$$T_c = 374.21\ \text{K} \quad \rho_c = 511.95\ \text{kg/m}^3 \quad p_c = 4.05928\ \text{MPa}.$$

Critical temperature and critical density are compared with measured critical parameters in Fig. 32. The critical temperature is very close to those of Kabata *et al.*[26] and of Fukushima *et al.*[16]. It is located within the estimated uncertainties of most researchers which are indicated by the rectangular areas in Fig. 32. The critical density agrees within ±1% with measured values being also within the estimated uncertainties.

5. Conclusion

A fundamental equation of state has been established for the Helmholtz free energy of HFC-134a. It covers the temperature range from 170 K to 455 K for pressures up to 70 MPa. The fundamental equation of state represents nearly all available measurements within their experimental uncertainties for the properties in the single-phase regions as well as for saturation properties. The only exception is the representation of heat capacity and speed of sound in the vicinity of the critical point because only very few experimental data are available in this part of the thermodynamic surface to support the equation of state. The results for the isobaric heat capacity at temperatures above 453 K show that extrapolation up to 523 K is possible within narrow limits of uncertainty. Comparisons with the HM-EOS at high pressure shows that reasonable results can be expected even at pressures up to 100 MPa.

Although there are about 4000 experimental data available, there are still some additional experimental data needed. Referring to the Secs. 4.1.4 and 4.1.5, there are only a few caloric measurements in the immediate vicinity of saturated vapor state which lead to different predictions from different equa-

ions of state. Furthermore, a set of liquid densities of high accuracy at temperatures below 240 K would be very valuable because the only set of densities available in this region (Hou *et al.*[23]) has been proven to be somewhat inconsistent with other reliable measurements. Due to these deficiencies in the experimental data, Annex 18 decided to reopen the process of data evaluation for HFC-134a in the future when new reliable measurements become available. Nevertheless, with this large amount of experimental information available, HFC-134a is already one of the fluids for which the thermodynamic properties are known at a superior level of accuracy.

6. Acknowledgements

The authors are grateful to all participants of Annex 18 for their fruitful discussions. Special thanks are dedicated to K. M. deReuck from IUPAC, London and to S.G. Penoncello from CATS, Moscow, Idaho who kindly corrected the English language and whose reports on the equations of state comparisons were very helpful during the preparation of this paper. We would also like to thank all authors from whom we received their experimental information prior to publication and M.O. McLinden who sent us his data base of thermodynamic properties. Furthermore, we thank the Deutsche Forschungsgemeinschaft (DFG) for her financial support.

7. References

[1] Ahrendts, J.; Baehr, H.D.: Direct application of experimental values for any thermodynamic variables of state in establishing canonical equations of state. Int. Chem. Eng. **21** (1981) 557.

[2] Arita, K.; Tomizawa, T.; Nagakawa, Y.; Yoshida, Y.: Vapour-Liquid Equilibrium of the non-azeotropic refrigerant mixture formed by chloro-fluoromethane and 1,1,1,2-tetrafluoroethane. Fluid Phase Equil. **63** (1991) 151.

[3] Baehr, H.D.; Tillner-Roth, R.: Measurements and correlation of the vapour pressures of 1,1,1,2-tetrafluoroethane (R 134a) and of 1,1-difluoroethane (R 152a). J. Chem. Thermodynamics, **23** (1991) 1063.

[4] Baroncini, C.; Giuliani, G.; Pacetti, M.; Polonara, F.: Experimental study of thermodynamic properties of 1,1,1,2-Tetrafluoroethane (R 134a). In: Thermophysical Properties of Pure Substances and Mixtures for Refrigeration. Proc. Meet. I.I.R. Comm. B1, Tel Aviv (1990) 1, 83.

[5] Basu, R.S.; Wilson, D.P.: Thermophysical properties of 1,1,1,2-tetrafluoroethane (R 134a). Int. J. Thermophy. **10** (1989) 3, 591.

[6] Beckermann, W.; Kohler, F.: Personal Communication, Ruhr-Universität Bochum 1993.

[7] Bender, E.: Zur Aufstellung von Zustandsgleichungen, aus denen sich die Sättigungsgrössen exakt berechnen lassen–gezeigt am Beispiel des Methans. Kältetechnik–Klimatisierung **23**, 1971.

[8] Bier, K.; Oellrich, M.; Türk, M.; Zhai, J.: Untersuchungen zum Phasengleichgewicht von neuen Kältemitteln und Kältemittelgemischen in einem grossen Temperaturbereich. DKV Tagungsbericht **17** (1990) 2, 233.

[9] Chen, S.S.; Rodgers, A.S.; Chao, J.; Wilhoit, R.C.; Zwolinski, B.J.: Ideal gas thermodynamic properties of six fluoroethanes. J. Phys. Chem. Ref. Data, **4** (1975) 2, 441 .

[10] Dennis, J.E.; Gay, M.; Welsch, R.E.: An adaptive nonlinear least-squares algorithm. Technical summary report No. 2010, Mathematics Research Center, Madison 1979.

[11] Döring, R.: Thermodynamic properties of the refrigerants R 134a (CH_2 F-CF_3) and R 123 ($CHCl_2$-CF_3). Proc. Meet. I.I.R. Comm. B1, Tel Aviv (1990) 1, 57.

[12] Dressner, M.; Bier, K.: Thermische Mischungseffekte in binären Gasmischungen mit neuen Kältemitteln. Fortschr.-Ber. VDI-Z., Reihe **3**, Nr. 332, Düsseldorf: VDI-Verlag 1993.

[13] Elhassan, A.E.; deReuck, K.M.: Preliminary report on equations of state for environmentally acceptable refrigerants. Prepared for IEA Annex 18 meeting, Purdue University 13th July 1992, IUPAC Thermodynamic Tables Project Centre, Imperial College, London 1992.

[14] Fukushima, M.; Watanabe, N.; Kamimura, T.: Measurements of the vapor-liquid coexistence curves and the critical parameters of HCFC 123 and HFC 134a. Trans. of the JAR, **7** (1990) 2, 85.

[15] Fukushima, M.; Watanabe, N; Kamimura, T: Measurements of PVT-properties of HCFC123 and HFC134a. Trans. of the JAR, **7** (1990) 2, 243.

[16] Fukushima, M.: Saturated liquid densities of HCFC 123, HFC 134a, CFC 11, and CFC 12. Trans. of the JAR, **8** (1991) 65.

[17] Goodwin, A.R.H.; Defibaugh, D.R.; Weber, L.A.: The vapor-pressure of 1,1,1,2-tetrafluoroethane (R 134a) and chlorodifluoromethane (R 22). Int. J. Thermophysics **13** (1993) 837.

[18] Goodwin, A.R.H.; Moldover, M.R.: Thermophysical properties of gaseous refrigerants from speed of sound measurements. I. Apparatus, model, and results for 1,1,1,2-tetrafluoroethane R134a. J. Chem. Phys. **93** (1990) 4, 2741.

[19] Guedes, H.J.R.; Zollweg, J.A.: Speed of sound in liquid R 134a. Int. J. Refrig. **15** (1992) 6, 381.

[20] Gürtner, J.; Ernst, G.: Personal Communication, Universität Karlsruhe 1992.

[21] Huber, M.L.; Ely, J.F.: An equation of state formulation of the thermodynamic properties of R 134a (1,1,1,2-tetrafluoroethane). Int. J. Refrig. **15** (1992) 6, 393.

[22] Huber, M.L.; McLinden, M.O.: Thermodynamic properties of R 134a (1,1,1,2-tetrafluoroethane). Proc. Int. Refrig. Conf., Purdue University, USA, Vol. II, (1992) pp. 453.

[23] Hou, H.; Holste, J.C.; Gammon, B. E.; Marsh, K. N.: Experimental densities for compressed R 134a. Int. J. Refrig. **15** (1992) 6, 365.

[24] Penoncello, S.G.; Jacobsen, R.T.; Williams, R.C. Lemmon, E.W.: Thermophysical Properties of the Environmentally Acceptable Refrigerants–Equation of State Comparisons for HFC-134a and HCFC-123. Final Report to the IEA-Annex 18, Center for Applied Thermodynamic Studies, University of Idaho, Moscow, 1993.

[25] Jacobsen, R.T.; Stewart, R.B.: Thermodynamic properties of nitrogen including liquid and vapor phases from 63 K to 2000 K with pressures to 10000 bar. J. Phys. Chem. Ref. Data **2** (1973) 757.

[26] Kabata, Y.; Tanikawa, S.; Uematsu, M.; Watanabe K.: Measurement of the vapor-liquid coexistence curve and the critical parameters for 1,1,1,2-tetrafluoroethane. Int. J. Thermophysics **10** (1989) 3, 605.

[27] Kesselman, P. M.; Zheleznyii, V. P.; Semenyuk, Y. V.: Thermophysikalische Grössen des Kältemittels R 134a in der flüssigen Phase. Kholod. Tekh. 7 (1991) 9.

[28] Klomfar, J.; Hruby, J.; Sifner, O.: Measurement of the p-v-T behaviour of refrigerant R 134a in the liquid phase. Int. J. Thermophysics, **14** (1993) 727.

[29] Kruse, H.: Personal Communication, Universität Hannover 1990.

[30] Kubota, H.; Yamashita, T.; Tanaka, Y.; Makita, T.: Vapor pressure of new fluorocarbons. Int. J. Thermophysics, **10** (1989) 629.

[31] Leuckel, W.; Leisenheimer, B.; Bier, K.: Verbrennungstechnische Eigenschaften des Kältemittels R 152a und seiner Mischungen mit R 134a bzw. R 23. Ki, Klima·Kälte-Heizung **4** (1992) 113.

[32] Maezawa, Y.; Sato, H.; Watanabe, K.: Saturated liquid densities of HCFC-123 and HFC-134a. J. Chem. Eng. Data **35** (1990) 225.

[33] Magee, J.W.: Measurements of molar heat capacity at constant volume (C_v) for 1,1,1,2-tetrafluoroethane (R 134a). Int. J. Refrig. **15** (1992) 6, 372.

[34] Magee, J.W.; Howley, J.B.: Vapor-pressure measurements on 1,1,1,2-tetrafluoroethane (R 134a) from 180 to 350 K. Int. J. Refrig. **15** (1992) 6, 362.

[35] Marx, V.; Pruss, A.; Wagner, W.: Neue Zustandsgleichungen für R 12, R 22, R 11 und R 113 - Beschreibung des thermodynamischen Zustandsverhaltens bei Temperaturen bis 525 K und Drücken bis 200 MPa. Fortschr.-Ber. VDI-Z., Reihe **19**, Nr. 57, Düsseldorf: VDI-Verlag 1992.

[36] McLinden, M.O.; Gallagher, J.S.; Weber, L.A.; Morrison, G.; Ward, D.K.; Goodwin, A.R.H.; Moldover, M.R.; Schmidt, J.W.; Chae, H.B.; Bruno, T.J.; Ely, J.F.; Huber, M.L.: Measurement and formulation of the thermodynamic properties of refrigerants 134a (1,1,1,2-tetrafluoroethane) and 123 (1,1-dichloro-2,2,2-trifluoroethane). ASHRAE Trans. 95 (1989) **2**, 263.

[37] Moldover, M.R.; Trusler, J.P.M.; Edwards, T.J.; Mehl, J.B.; Davis, R.S. Measurement of the universal gas constant R using a sperical acoustic resonator. J. Res. Natl. Bur. Stand. **93** (1988) 85.

[38] Morrison, G.; Ward, D.K.: Properties of two alternative refrigerants, 1,1-dichloro-2,2,2-trifluoroethane (R 123) and 1,1,1,2-tetrafluoroethane (R 134a). Fluid Phase Equil. **62** (1991) 65.

[39] Nakagawa, S.; Sato, H.; Watanabe, K.: Specific heat at constant pressure for liquid new refrigerants. Proc. 27th Nat. Heat Trans. Symp. Japan, Nagoya (1990) 421.

[40] Niesen, V.G.; vanPoolen, L.J.; Outcalt, S.L.; Holcomb, C.D.: Coexisting densities and vapor pressures of refrigerants R 22, R 134a, and R 124 at 300 to 395 K. Fluid Phase Equil. **97** (1994) 81.

[41] Nishiumi, H.; Yokoyama, T.: Vapor-liquid equilibrium for the system of R 134a-R 22. Proc. 11th Japan Symp. Therm. Prop., Paper B105 (1990) 95.

[42] Park, Y. J.: Bestimmung des thermischen Verhaltens neuer Arbeitsstoffe der Energietechnik mit Hilfe einer Burnett-Apparatur, Dissertation, Universität Karlsruhe 1993.

[43] Piao, C.C.; Sato., H.; Watanabe, K.: An experimental study for *PVT* properties of CFC alternative refrigerant 1,1,1,2-tetrafluoroethane (R 134a). ASHRAE Trans., **96** (1990) 132.

[44] Piao, C.C.; Noguchi, M.; Sato, H.; Watanabe, K.: Equation of state for HFC 134a. in: Penoncello, S.G.; Jacobsen, R.T.; Williams, R.C. Lemmon, E.W.: Thermophysical Properties of the Environmentally Acceptable Refrigerants–Equation of State Comparisons for HFC-134a and HCFC-123. Final Report to the IEA-Annex 18, Center for Applied Thermodynamic Studies, University of Idaho, Moscow, 1993.

[45] Quian, Z.Y.; Sato, H.; Watanabe, K.: Compressibility measurements of R 134a by the Burnett technique. Fluid Phase Equil. **78** (1993) 323–329.

[46] Saitoh, A.; Nakagawa, S.; Sato, H.; Watanabe, K.: Isobaric heat capacity data for liquid HFC-134a. J. Chem. Eng. Data **35** (1990) 107.

[47] Saul, A.; Wagner, W.: A fundamental equation for water covering the range from the melting line to 1273 K at pressures up to 25000 MPa. J. Phys. Chem. Ref. Data **18** (1989) 1537.

[48] Schmidt, R.; Wagner, W.: A new form of the equation of state for pure substances and its application to oxygen. Fluid Phase Equil. **19** (1985) 175.

[49] Schramm, B.; Hauck, J.; Kern, L.: Messungen der 2. Virialkoeffizienten einiger neuer Chlorfluorkohlenwasserstoffe und ihrer binären Mischungen bei Temperaturen von 296 K–475 K. Ber. Bunsenges. phys. Chemie, **96** (1992) 6, 745.

[50] Schramm, B.; Weber, C.: Measurements of the second virial coefficients of some new chlorofluorocarbons and of their mixtures at temperatures in the range from 230 K to 300 K. J. Chem. Thermodynamics **23** (1991) 281.

[51] Setzmann, U.; Wagner, W.: A new equation of state and tables of thermodynamic properties for methane covering the range from the melting line to 625 K at pressures up to 1000 MPa. J. Phys. Chem. Ref. Data **20** (1991) 1061.

[52] Takagi, T.: Thermophysical properties of environmentally acceptable fluorocarbons HFC 134 and HCFC 123. JAR and Japan Flon Gas Ass. (1991) 56.

[53] Tang, S.; Jin, G.X.; Sengers, J.V.: Thermodynamic properties of 1,1,1,2-tetrafluoroethane (R 134a) in the critical region. Int. J. Thermophysics **12** (1991) 515.

[13] Tillner-Roth, R.; Baehr, H.D.: Burnett measurements and correlation of gas-phase (p,ρ,T) of 1,1,1,2-tetrafluoroethane (R 134a) and of 1,1-difluoroethane (R 152a). J. Chem. Thermodynamics, **24** (1992) 413.

[15] Tillner-Roth, R.; Baehr, H.D.: Measurements of liquid, near-critical, and supercritical (p,ρ,T) of 1,1,1,2-tetrafluoroethane (R 134a) and of 1,1-difluoroethane (R 152a). J. Chem. Thermodynamics **25** (1993) 277.

[56] Tillner-Roth, R.: Die thermodynamischen Eigenschaften von R 134a, R 152a und ihren Gemischen–Messungen und Fundamentalgleichungen. Forsch.-Ber. DKV Nr. 41, Deutscher Kälte- und Klimatechnischer Verein, Stuttgart 1993..

[57] Wagner, W.: Eine mathematisch statistische Methode zum Aufstellen thermodynamischer Gleichungen–gezeigt am Beispiel der Dampfdruckkurve reiner fluider Stoffe. Fortschr.-Ber. VDI-Z., Reihe **3**, Nr. 39, Düsseldorf, VDI-Verlag: 1974.

[58] Weber, L.A.: Vapor pressure and gas phase *PVT* data for 1,1,1,2-tetrafluoroethane. Int. J. Thermophysics **10** (1989) 3, 617.

[59] Wirbser, H.: Hochdruckströmungskalorimetrie: Spezifische Wärmekapazitäten und differentieller Joule-Thomson-Koeffizient halogenierter Kohlenwasserstoffe. Dissertation, Universität Karlsruhe 1994.

[60] Yamashita, T.; Kubota, H.; Tanaka, Y.; Makita, T.; Kashiwagi, H.: Physical properties of new halogenated hydrocarbons. Proc. 10th Japan Symp. Therm. Prop. (1989) 75.

[61] Yokoyama, C.; Takahashi, S.: Saturated liquid densities of 2,2-dichloro-1,1,1-trifluoroethane (HCFC-123), 1,2-dichloro-1,2,2-trifluoroethane (HCFC-123a), 1,1,1,2-tetrafluoroethane (HFC-134a) and 1,1,1-trifluoroethane (HFC-143a). Fluid Phase Equil. **67** (1991) 227.

[62] Zhu, M.; Wu, J.; Fu, Y.D.: New experimental vapor pressure data and a new vapor pressure equation for HFC 134a. Fluid Phase Equil. **80** (1992) 99.

[63] Zhu, M.; Fu, Y.; Han, L.: An experimental study of *PVT* properties of CFC alternative HFC 134a. Fluid Phase Equil. **80** (1992) 149.

TABLE 1. Summary of experimental critical parameters. The sample purity is given in mass percent

Source	Year	Purity	T_c/K	p_c/MPa	ρ_c/(kg/m^3)
Basu and Wilson[5]	1989	99.95	374.22±0.15	4.067±0.027	512.2±5
McLinden *et al.*[36]	1989	99.94	374.18±0.01	4.056±0.01	515.3±1
Yamashita *et al.*[60*]	1989	99.9	374.24±0.05	4.065±0.005	—
Kubota *et al.*[30*]	1989	99.9	374.24±0.05	4.065±0.005	—
Kabata *et al.*[26]	1989	99.8	374.27±0.01	—	508.0±3
Bier *et al.*[8]	1990	99.9	374.09±0.05	4.052±0.06	514.0±10
Bier *et al.*[8]	1990	99.9	374.10±0.05	4.050±0.06	514.0±10
Fukushima *et al.*[14]	1991	99.99	374.16±0.02	4.067±0.005	507.0±5
Morrison and Ward[38]	1991	99.95	374.23±0.01	4.068±0.005	515.2±2

*The values reported by[60] and[30] probably result from the same measurements.

TABLE 2. Summary of measurements in the single phase (v: vapor, l: liquid)[1]

Source	Year		Purity	Number total/used	Range of data T/K	p/MPa	Uncertainties s_T	s_p	s_y
				(p,ρ,T)-measurements (y = ρ)					
Basu and Wilson[5]	1989	v	99.95	52/0	317–447	1–6.7	30 mK	0.001p	0.003ρ
Dressner and Bier[12]	1993	v	99.9	121/121	333–423	0.3–58	5 mK	0.0002p	0.001ρ
Döring[11]	1990	v	—	112/0	247–368	0.1–3.5	—	—	—
Weber[58]	1989	v	99.95	69/0	321–423	0.2–5.3	1 mK	$10^{-4}\,p$	0.0005ρ
Piao *et al.*[43]	1989	v,l	99.8	159/0	313–423	0.8–12	10 mK	2 kPa	0.002ρ
Maezawa *et al.*[32]	1990	l	99.99	10/0	280–340	0.5–2	15 mK	5 kPa	0.002ρ
Kesselmann *et al.*[27]	1991	l	99.9	65/0	212–345	0.4–21	20 mK	1.5 kPa	0.0008ρ
Morrison and Ward[38]	1991	l	99.95	120/0	278–367	0.7–5.8	5 mK	1 kPa	0.0003ρ
Hou *et al.*[23]	1992	l	99.98	429/0	180–380	0.9–70	10 mK	10 kPa	0.001ρ
Baroncini *et al.*[4]	1990	v	99.98	46/0	263–358	0.2–2.0	20 mK	0.003p	0.002ρ
Tillner-Roth and Baehr[54]	1992	v	99.97	411/393	293–453	0.1–16	5 mK	$10^{-4}\,p$	0.0003ρ
Tillner-Roth and Baehr[55]	1993	l,v	99.97	432/413	243–413	0.6–16	10 mK	0.0002p	0.0003ρ
Fukushima *et al.*[15]	1990	v	99.8	63/0	294–424	0.6–5.7	10 mK	3 kPa	0.002ρ
Magee[33]	1992	l	99.99	150/0	186–340	2.9–35	30 mK	0.0007p	0.0015ρ
Qian *et al.*[45]	1992	v	99.99	21/0	320–340	0.1–2	10 mK	0.3 kPa	0.002ρ
Zhu *et al.*[63]	1992	v	99.95	42/0	283–353	0.1–1.3	15 mK	2 kPa	—
Park[42]	1993	v	—	220/0	333–423	0.3–14	5 mK	0.0002p	0.001ρ
Klomfar *et al.*[28]	1993	l	99.9	89/0	204–298	1–56	50 mK	0.001p	0.001ρ
				Speed of sound (y = w)					
Beckermann and Kohler[6]	1993	v	99.9	230/0	253–410	0–0.6	10 mK	0.0002p	$2\cdot10^{-4}\,w$
Guedes and Zollweg[19]	1992	l	99.8	206/193	180–380	0.9–70	10 mK	0.0015p	<1m/s
Goodwin and Moldover[18]	1990	v	99.94	94/94	233–340	0–0.5	1 mK	50 Pa	$10^{-4}\,w$
Takagi[52]	1991	l	99.9	80/0	290–370	2–70	30 mK	0.001p	0.002w
				Isobaric heat capacity (y = c_p)					
Wirbser[59]	1993	l,v	99.95	151/117	273–523	0.5–30	5 mK	0.0002p	(0.001–0.1)c_p
Gürtner and Ernst[20]	1992	v	99.95	42/42	253–423	0–0.5	5 mK	0.0001p	0.002c_p
Nakagawa *et al.*[39]	1990	l	—	37/0	273–356	0.5–3	10 mK	3 kPa	0.003c_p
Saitoh *et al.*[46]	1990	l	99.97	31/0	275–356	1–3	10 mK	3 kPa	0.003c_p
				Isochoric heat capacity (y = c_v)					
Magee[33]	1992	l	99.99	150/150	186–340	2.9–35	30 mK	0.0007p	0.005c_v
				Joule-Thomson coefficient (y = μ)					
Wirbser[59]	1993	l,v	99.95	108/0	333–423	0.3–20	5 mK	0.0002p	(0.003–0.1)μ
				Second virial coefficient (y = B)					
Beckermann and Kohler[6]	1993	v	99.9	15/0	233–420	—	10 mK	—	0.01B
Goodwin and Moldover[18]	1990	v	99.94	10/0	235–440	—	1 mK	—	<0.01B
Schramm *et al.*[50]	1992	v	—	5/0	303–473	—	10 mK	—	<0.02B
Schramm and Weber[49]	1991	v	—	4/0	233–293	—	10 mK	—	<0.03B
Tillner-Roth and Baehr[54]	1992	v	99.97	19/0	293–453	—	5 mK	—	<0.015B
Dressner and Bier[12]	1993	v	99.9	4/0	333–423	—	5 mK	—	<0.01B
Weber[58]	1989	v	99.95	12/0	323–423	—	5 mK	—	<0.01B

[1]The sample purity is given in mass per cent

TABLE 3. Summary of measurements of saturation properties*

Source	Year	Purity	Number total/used	Temperature-range T/K	Uncertainties s_T	s_y
			Vapor pressure ($y = p_s$)			
Basu and Wilson[5]	1989	99.95	32/0	210–369	30 mK	0.001p
Weber[58]	1989	99.95	22/22	313–373	1 mK	0.1 kPa
Piao *et al.*[43]	1989	99.99	46/0	308–374	10 mK	2 kPa
Morrison and Ward[38]	1991	99.95	12/0	268–374	1 mK	1.5 kPa
Maezawa *et al.*[32]	1990	99.99	13/0	279–350	15 mK	7 kPa
Kubota *et al.*[30]	1989	99.9	25/0	253–373	50 mK	1.2 kPa
Bier[8]	1990	99.9	41/0	204–374	10 mK	(0.001–0.01)p
Döring[11]	1990	—	22/0	218–358	—	—
Baroncini *et al.*[4]	1990	99.98	64/0	242–358	20 mK	0.003p
Baehr and Tillner-Roth[3]	1993	99.94	37/37	303–374	5 mK	0.0002p
Fukushima *et al.*[15]	1990	99.99	41/0	262–371	10 mK	3 kPa
Nishiumi and Yokoyama[41]	1990	—	16/0	247–373	10 mK	0.0015p
Arita *et al.*[2]	1991	99.5	3/0	273–323	20 mK	0.7 kPa
Goodwin *et al.*[17]	1993	99.95	37/37	214–265	10 mK	20 Pa
		99.95	20/20	266–313	1 mK	0.1 kPa
Niesen *et al.*[40]	1993	99.9	12/0	316–370	0.1 K	3.5 kPa
Zhu *et al.*[62]	1992	99.95	43/0	279–363	10 mK	0.5 kPa
Magee and Howley[34]	1992	99.99	19/5	180–350	30 mK	0.02–1.8 kPa
			Saturated liquid density ($y = \rho'$)			
Basu and Wilson[5]	1989	99.95	9/0	238–371	30 mK	0.003ρ
Döring[11]	1990	—	20/0	243–338	—	—
Fukushima *et al.*[15]	1990	99.99	3/0	323–357	10 mK	0.002ρ
Fukushima *et al.*[14]	1991	99.99	8/0	369–374	20 mK	1.5 kg/m^3
Fukushima[16]	1991	99.99	7/0	244–291	20 mK	3 kg/m^3
Hou *et al.*[23]	1992	99.98	10/0	180–360	10 mK	0.001ρ
Kabata *et al.*[26]	1989	99.8	12/0	343–374	10 mK	0.0055ρ
Kruse[29]	1990	—	9/0	232–312	20 mK	0.001ρ
Maezawa *et al.*[32]	1990	99.99	25/0	199–370	15 mK	0.002ρ
Morrison and Ward[38]	1991	99.95	26/0	268–368	1 mK	0.003ρ
Niesen *et al.*[40]	1993	99.9	12/0	316–370	0.1 K	0.5 kg/m^3
Piao *et al.*[43]	1989	99.6	7/0	313–372	20 mK	0.005ρ
Tillner-Roth and Baehr[55]	1993	99.97	13/0	243–353	10 mK	0.0005ρ
Yokoyama and Takahashi[61]	1991	99.8	21/0	251–367	20 mK	0.003ρ
			Saturated vapor density ($y = \rho''$)			
Fukushima[16]	1991	99.99	6/0	293–371	20 mK	0.002ρ
Fukushima *et al.*[14]	1991	99.99	9/0	371–374	20 mK	1.5 kg/m^3
Kabata *et al.*[26]	1989	99.8	15/0	361–374	10 mK	0.0055ρ
Morrison and Ward[38]	1991	99.95	8/0	298–365	1 mK	0.003ρ
Niesen *et al.*[40]	1993	99.9	12/0	316–370	0.1 K	0.5 kg/m^3
Weber[58]	1989	99.95	5/0	320–365	1 mK	0.001ρ

*The sample puritie are given in mass per cent

TABLE 4. Coefficients of Eq. (4) for liquid HFC-134a

i	g_i	i	g_i	i	g_i	i	g_i
			Based on the data of Tillner-Roth and Baehr[55]				
1	14.4523550	4	$5.07020933 \cdot 10^{-4}$	7	22.22226808	10	—1.58754782
2	0.491185102	5	—2.7877891524	8	3.986022479		
3	—13.9840437	6	52.2926435	9	—66.2525696		
			Based on the data of Hou *et al.*[23]				
1	14.4937330	4	$5.84703389 \cdot 10^{-4}$	7	25.29622142	10	—2.95713405
2	0.505043520	5	—2.9525905643	8	4.745207617		
3	—13.9754460	6	62.3707965	9	—78.4183305		

TABLE 5. Relations between the dimensionless free energy and thermodynamic properties

Property			Relation
Pressure[1]	$p(\tau,\delta)$	=	$RT\rho(1+\delta\Phi_\delta^r)$
Internal Energy[1]	$\frac{u(\tau,\delta)}{RT}$	=	$\tau\,(\Phi_\tau^0 + \Phi_\tau^r)$
Enthalpy[1]	$\frac{h(\tau,\delta)}{RT}$	=	$1 + \tau(\Phi_\tau^0 + \Phi_\tau^r) + \delta\Phi_\delta^r$
Entropy[1]	$\frac{s(\tau,\delta)}{R}$	=	$\tau\,(\Phi_\tau^0 + \Phi_\tau^r) - \Phi^\circ - \Phi^r$
Gibbs Energy[1]	$\frac{g(\tau,\delta)}{RT}$	=	$1 + \delta\Phi_\delta^r + \Phi^\circ + \Phi^r$
Isochoric Heat Capacity[1]	$\frac{c_v(\tau,\delta)}{R}$	=	$-\tau^2(\Phi_{\tau\tau}^\circ + \Phi_{\tau\tau}^r)$
Isobaric Heat Capacity	$\frac{c_p(\tau,\delta)}{R}$	=	$(c_v/R) + \frac{(1 + \delta\Phi_\delta^r - \delta\tau\Phi_{\delta\tau}^r)^2}{1 + 2\delta\Phi_\delta^r + \delta^2\Phi_{\delta\delta}^r}$
Speed of Sound	$\frac{w^2(\tau,\delta)}{RT}$	=	$1 + 2\delta\Phi_\delta^r + \delta^2\Phi_{\delta\delta}^r + \frac{(1 + \delta\Phi_\delta^r - \delta\tau\,\Phi_{\delta\tau}^r)^2}{(c_v/R)}$
Joule-Thomson Coefficient	$\mu(\tau,\delta)\,R\,\rho$	=	$\frac{-(\delta\Phi_\delta^r + \delta^2\Phi_{\delta\delta}^r + \delta\tau\Phi_{\delta\tau}^r)}{(1 + \delta\Phi_\delta^r - \delta\tau\Phi_{\delta\tau}^r)^2 + (c_v/R)(1 + 2\delta\Phi_\delta^r + \delta^2\Phi_{\delta\delta}^r)}$
Maxwell Rule[1]	$\frac{p_s}{RT}\left(\frac{1}{\rho''} - \frac{1}{\rho'}\right)$	=	$\Phi^r(\tau,\delta') - \Phi^r(\tau,\delta'') + \ln\frac{\delta'}{\delta''}$
Second Virial Coefficient[1]	$B(\tau)\,\rho_c$	=	$\lim_{\delta\to 0}\Phi_\delta^r(\tau,\delta)$
Third Virial Coefficient[1]	$C(\tau)\,\rho_c^2$	=	$\lim_{\delta\to 0}\Phi_{\delta\delta}^r(\tau,\delta)$

[1]Depending linearly on the Helmholtz free energy.

Abbreviations: $\Phi_\delta = \left(\frac{\partial\Phi}{\partial\delta}\right)_\tau$, $\Phi_\tau = \left(\frac{\partial\Phi}{\partial\tau}\right)_\delta$, $\Phi_{\delta\delta} = \left(\frac{\partial^2\Phi}{\partial\delta^2}\right)$, $\Phi_{\delta\tau} = \left(\frac{\partial^2\Phi}{\partial\delta\partial\tau}\right)$, $\Phi_{\tau\tau} = \left(\frac{\partial^2\Phi}{\partial\tau^2}\right)$.

TABLE 6. Exponents of the terms in the bank of terms (Eq. (12))

Sort of term (Counter)	δ-Exponents (d_i) τ-Exponents (t_i)
$\tau^{t_i}\,\delta^{d_i}$ ($N_0 = 210$)	d_i = 1; 1.5; ... 7; 8 t_i = −0.5; 0; 0.5; ... 4; 5; 6; 7; 8; 10
$\exp(-\delta)\,\tau^{t_i}\delta^{d_i}$ ($N_1 = 353$)	d_i = 1; 1.5; ... 7 t_i = −0.5; 1; ... 4; 5; 6; 7; 8; 10; 12; 15
$\exp(-\delta^2)\,\tau^{t_i}\delta^{d_i}$ ($N_2 = 443$)	d_i = 1; 2; ... 6 t_i = 2; 2.5; ... 8; 9; 10
$\exp(-\delta^3)\,\tau^{t_i}\delta^{d_i}$ ($N_3 = 520$)	d_i = 3; 3.5; ... 6 t_i = 5; 7.5; ... 27.5; 30
$\exp(-\delta^4)\,\tau^{t_i}\delta^{d_i}$ ($N_4 = 565$)	d_i = 3; 4; 5; 6; 8 t_i = 1; 5; 10; ... 40
$\exp(-\delta^5)\,\tau^{t_i}\delta^{d_i}$ ($N_5 = 615$)	d_i = 3; 4; 5; 6; 8 t_i = 1; 5; 10; ... 45

TABLE 7. Coefficients and exponents of the residual part of the fundamental equation of state for HFC-134a

i	a_i	t_i	d_i	i	a_i	t_i	d_i
1	0.5586817E−1	−1/2	2	12	0.1017263E−3	1	4
2	0.4982230E+0	0	1	13	−0.5184567E+0	5	1
3	0.2458698E−1	0	3	14	−0.8692288E−1	5	4
4	0.8570145E−3	0	6	15	0.2057144E+0	6	1
5	0.4788584E−3	3/2	6	16	−0.5000457E−2	10	2
6	−0.1800808E+1	3/2	1	17	0.4603262E−3	10	4
7	0.2671641E+0	2	1	18	−0.3497836E−2	10	1
8	−0.4781652E−1	2	2	19	0.6995038E−2	18	5
9	0.1423987E−1	1	5	20	−0.1452184E−1	22	3
10	0.3324062E+0	3	2	21	−0.1285458E−3	50	10
11	−0.7485907E−2	5	2				

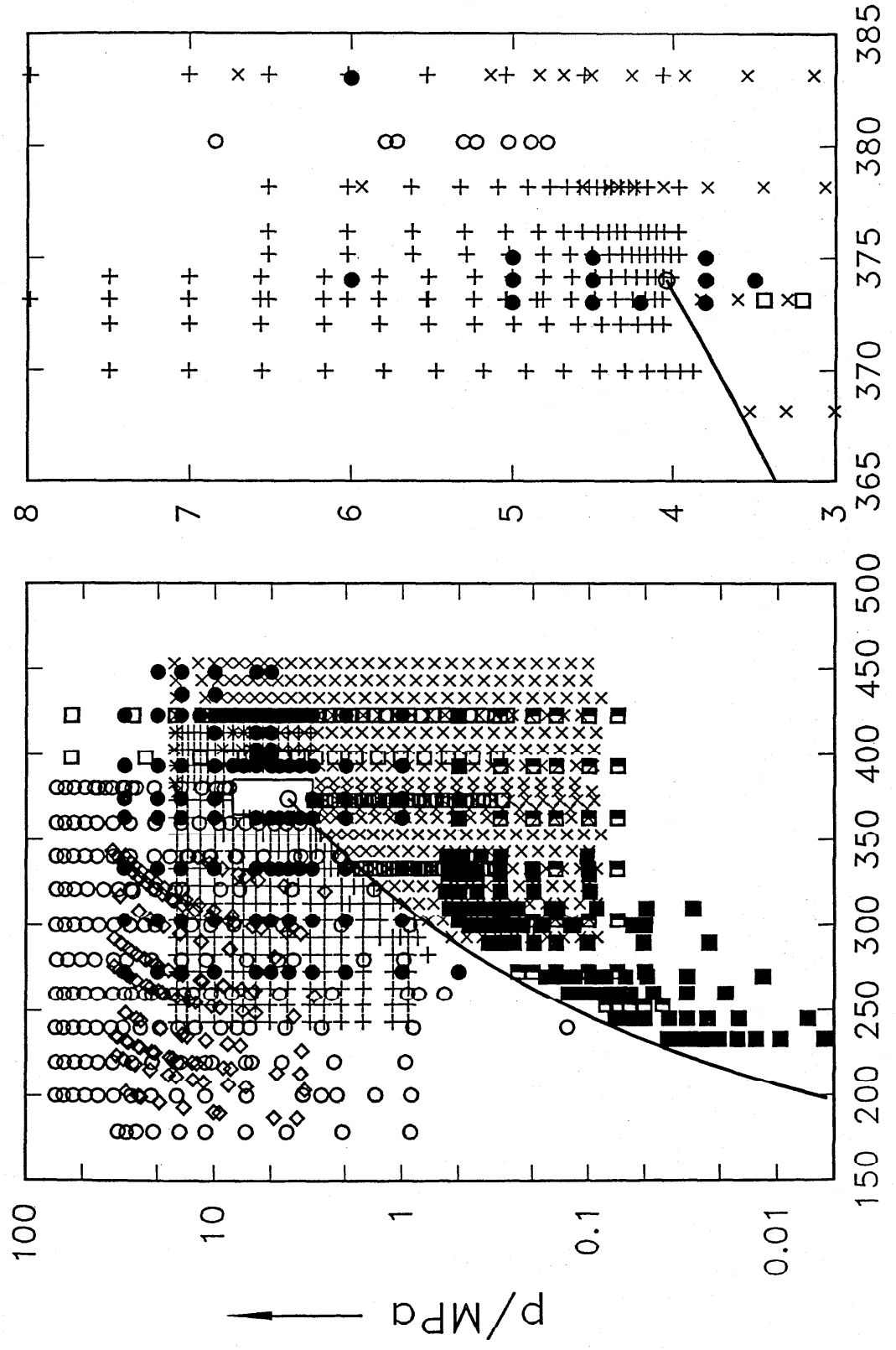

FIG. 1. Distribution of selected measurements in a (p,T)-diagram of HFC-134a. +: Tillner-Roth and Baehr[55] (p,ρ,T), ×: Tillner-Roth and Baehr[54] (p,ρ,T), □: Dressner and Bier[12] (p,ρ,T), ○: Guedes and Zollweg[19] (speed of sound), ■: Goodwin and Moldover[18] (speed of sound), ◇: Magee[33] (c_v), ◧: Gürtner and Ernst[20] (c_p), ●: Wirbser[59] (c_p).

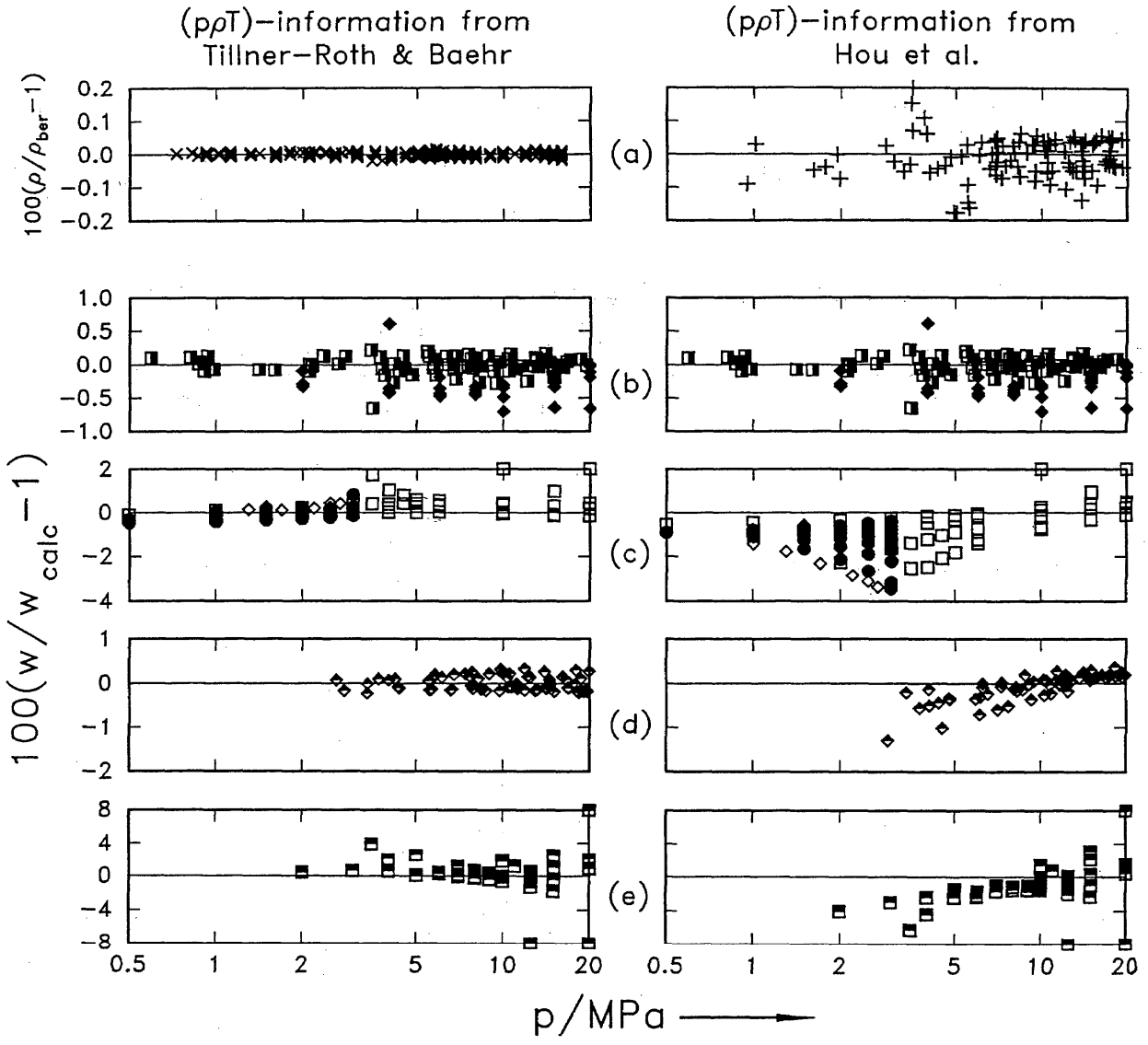

FIG. 2. Results of the consistency test in the liquid phase of HFC-134a. (a): Deviations of densities at $T<350$ K and $p<20$ MPa from Eq. (4) using the respective set of coefficients. ×: Tillner-Roth and Baehr[55], +: Hou *et al.*[23]. (b)–(e): Deviations of measured speed of sound from the correlation function reported by Guedes and Zollweg[19]. (b): Measured speed of sound: ◨: Guedes and Zollweg[19], ◆: Takagi[52]. (c): Speed of sound calculated from isobaric heat capacities: □: Wirbser[59], ◇: Saitoh *et al.*[46], ●: Nakagawa *et al.*[39]. (d): Speed of sound calculated from isochoric heat capacities: ◈: Magee[33]. (e): Speed of sound calculated from Joule-Thomson coefficients: ⬒: Wirbser[59].

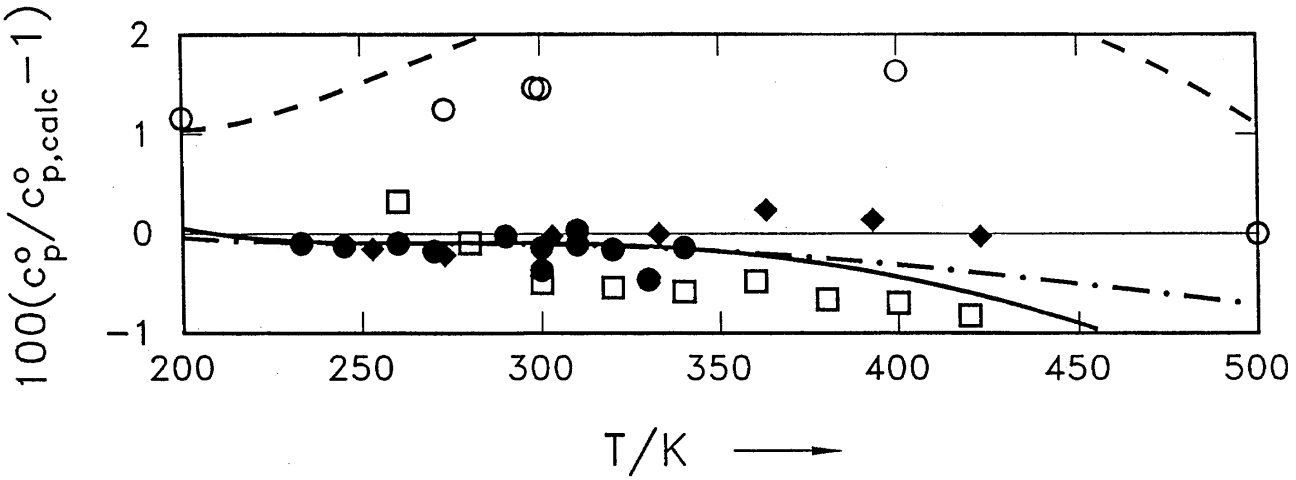

FIG. 3. Deviations of reported ideal gas heat capacity values from values calculated from Eq. (8). ◆: Gürtner and Ernst[20], ●: Goodwin and Moldover[18], □; Beckermann and Kohler[6], ○: Chen *et al.*[9], —— HM-EOS and HE-EOS, −·−·− PNSW-EOS, − − − Basu and Wilson[5].

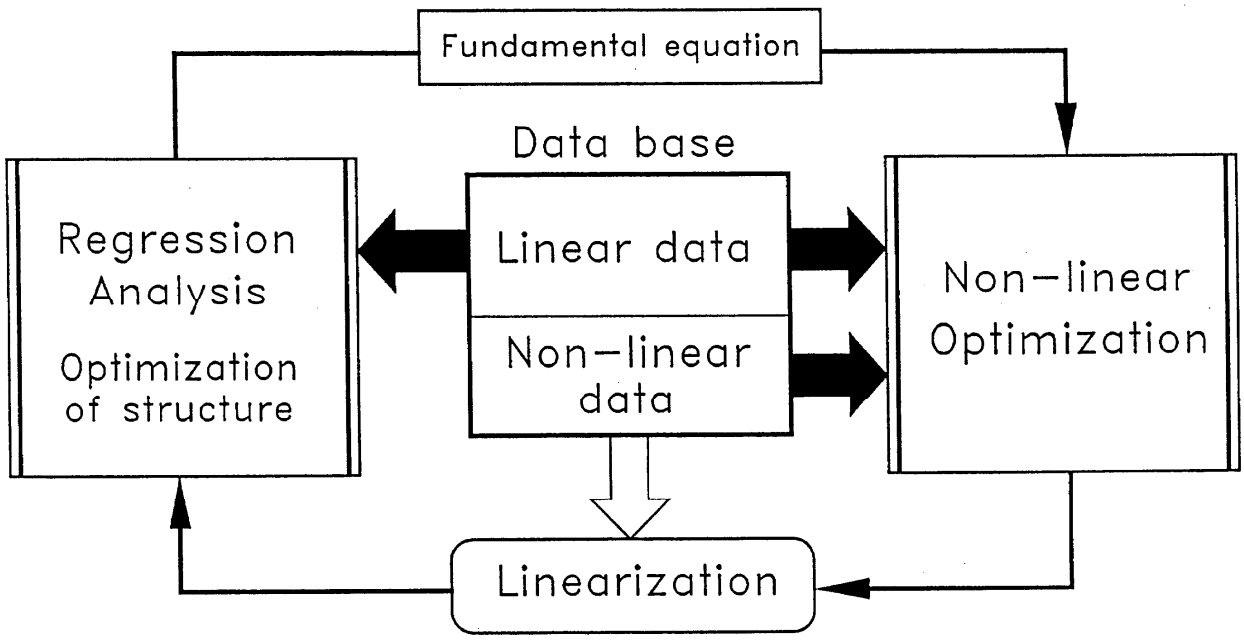

FIG. 4. Optimization cycle during the formulation of the residual part Φ^r of the fundamental equation.

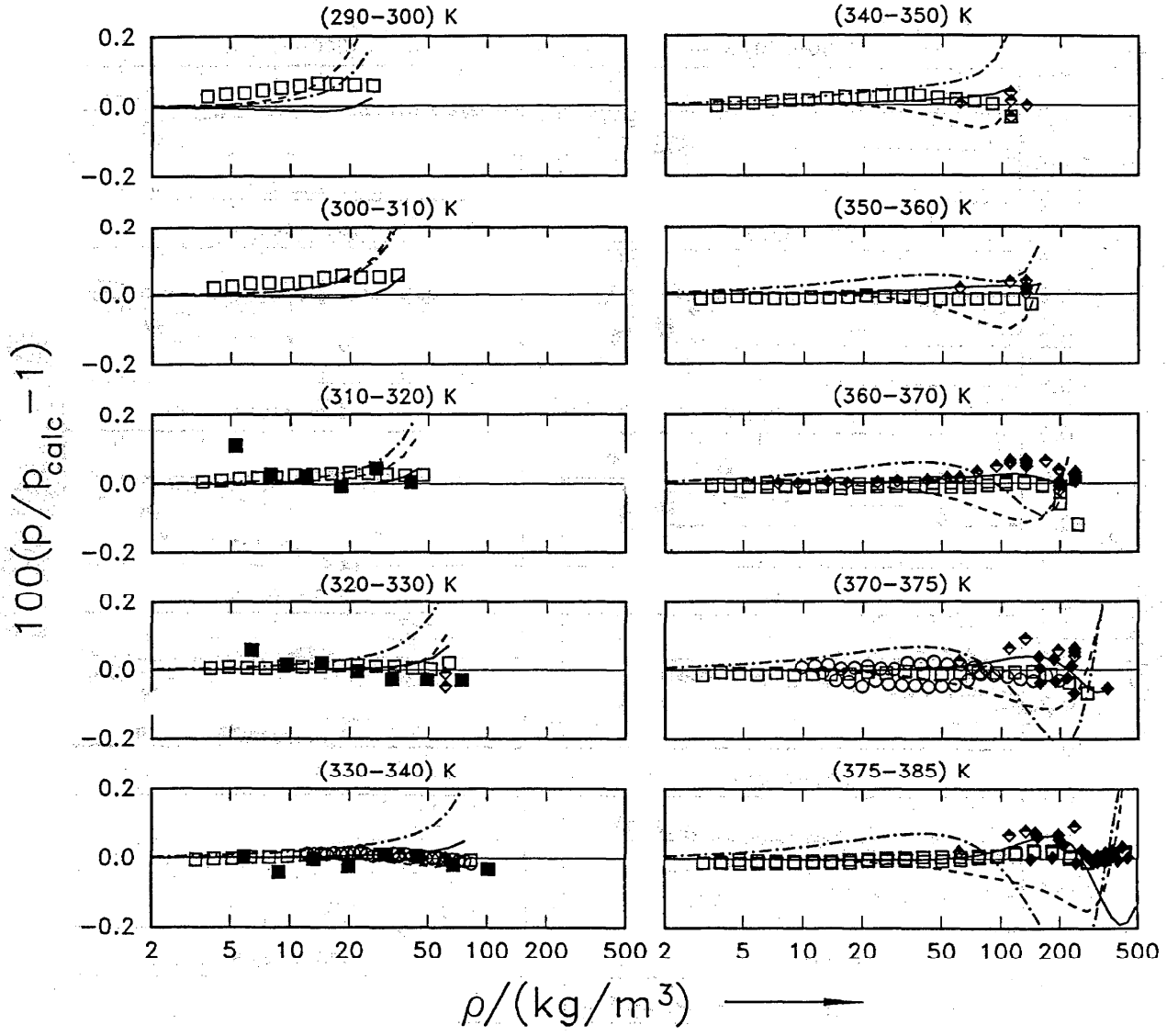

FIG. 5. Pressure deviations of (p,ρ,T)-properties in the gaseous phase from our own EOS. □: Tillner-Roth and Baehr[54], ◆: Tillner-Roth and Baehr[55], ■: Qian *et al.*[45], ○: Dressner and Bier[12], ◆: Weber[58], —— HM-EOS, – – – HE-EOS, –·–·– PNSW-EOS.

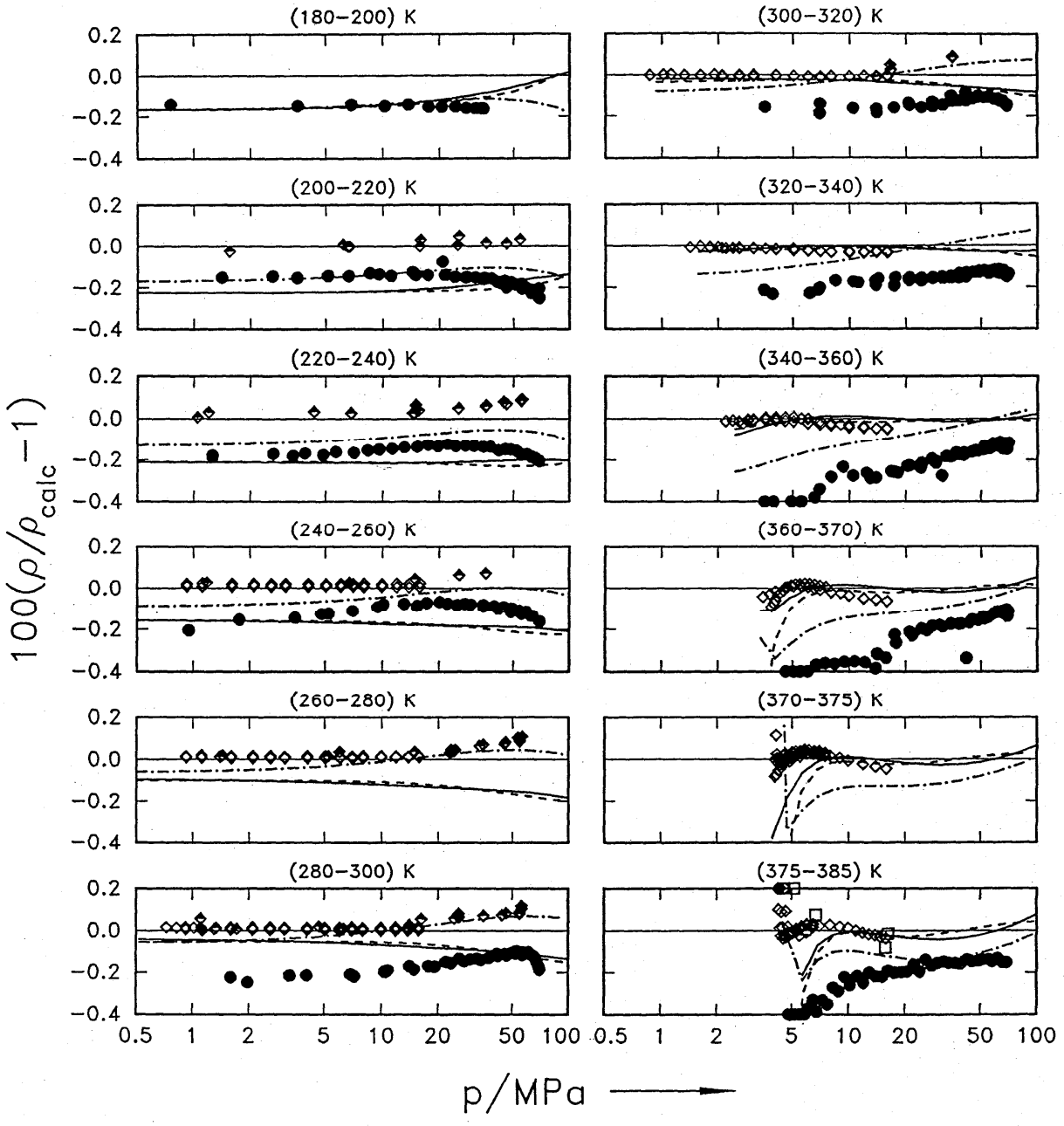

FIG. 6. Density deviations of (p,ρ,T)-properties in the liquid phase from our own EOS. □: Tillner-Roth and Baehr[54], ◇: Tillner-Roth and Baehr[55], ◆: Klomfar *et al.*[28], ●: Hou *et al.*[23], —— HM-EOS, – – – HE-EOS, –·–·– PNSW-EOS.

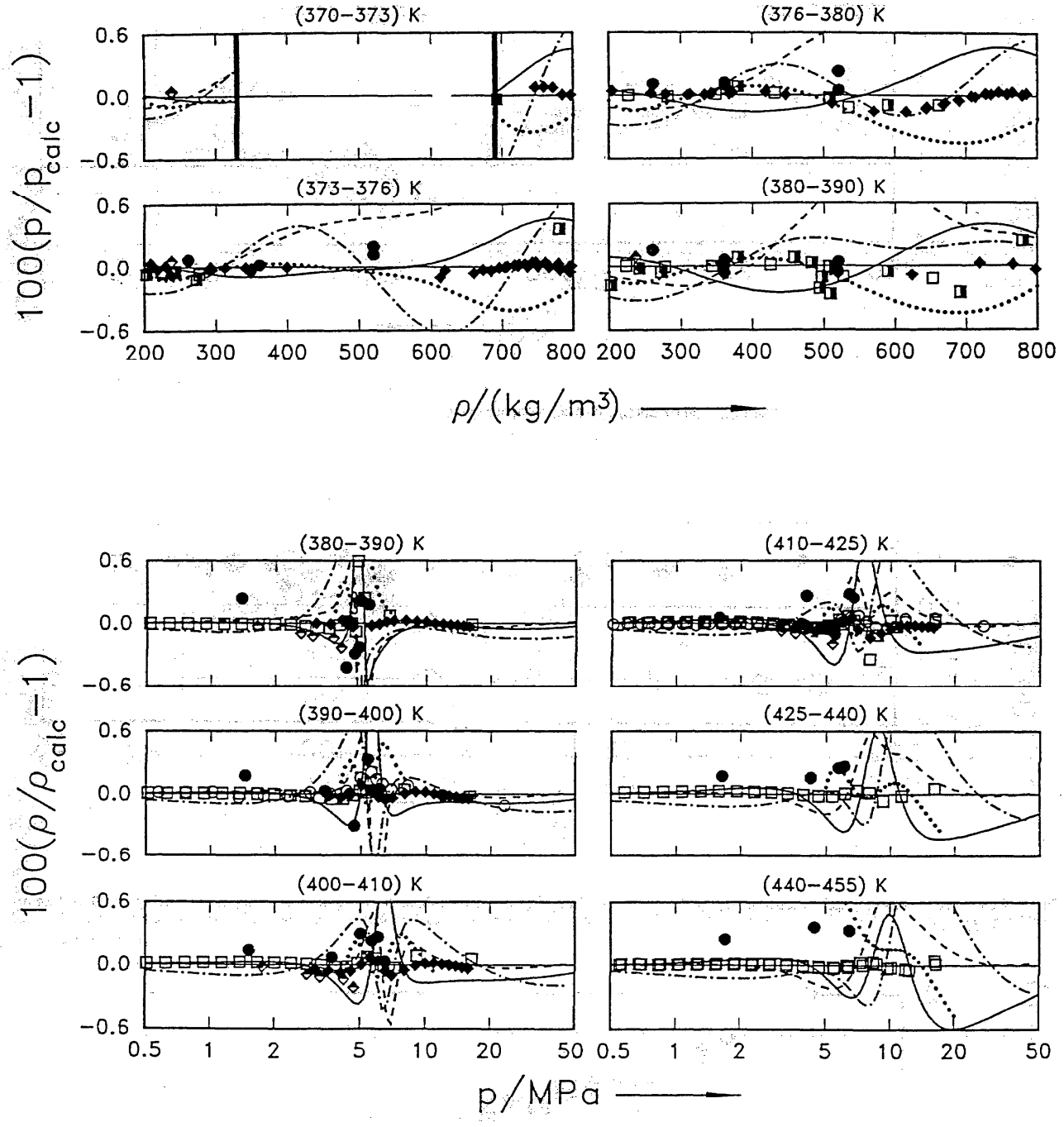

FIG. 7. Pressure and density deviations of (p,ρ,T)-properties in near-critical and supercritical states from our own EOS. □: Tillner-Roth and Baehr[54], ◆: Tillner-Roth and Baehr[55], ●: Basu and Wilson[5], ○: Dressner and Bier[12], ◨: Piao *et al.*[43], ◈. Weber[58], ◧: Saturation, —— HM-EOS, – – – HE-EOS, –·–·– PNSW-EOS, ····· Tang *et al.*[53].

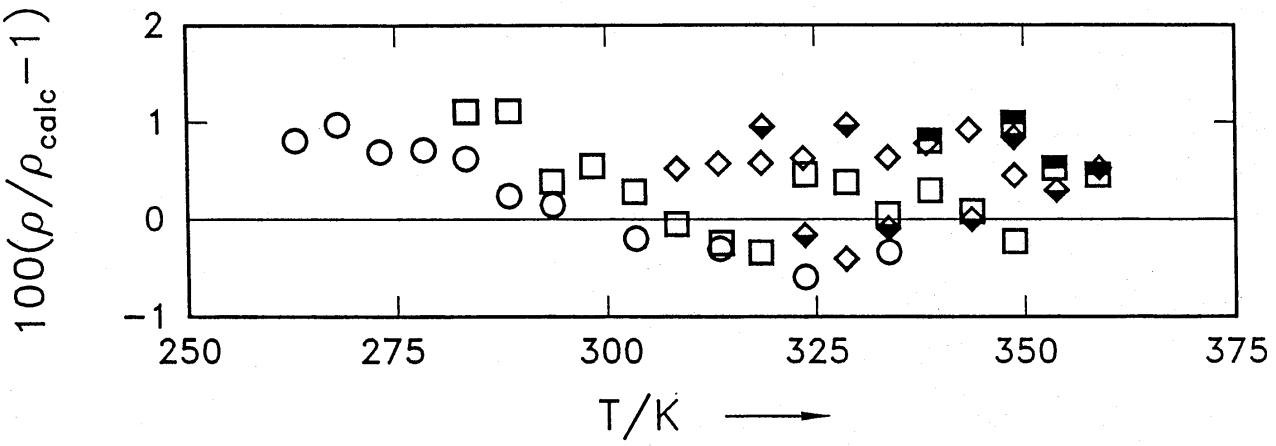

FIG. 8. Density deviations of (p,ρ,T)-properties reported by Baroncini *et al.*[4] from our own EOS. ○: 9 kg/m^3, □: 20 kg/m^3, ◇: 40 kg/m^3, ◆: 56 kg/m^3, ▣: 88 kg/m^3.

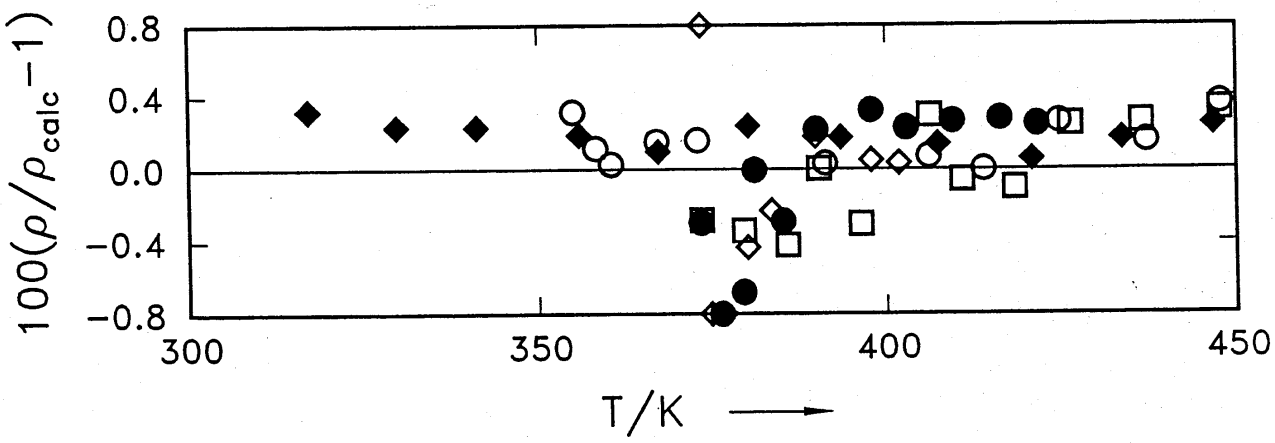

FIG. 9. Density deviations of (p,ρ,T)-properties reported by Basu and Wilson[5] from our own EOS. ◆: 51 kg/m^3, ○: 156 kg/m^3, □: 261 kg/m^3, ●: 361 kg/m^3, ◇: 520 kg/m^3.

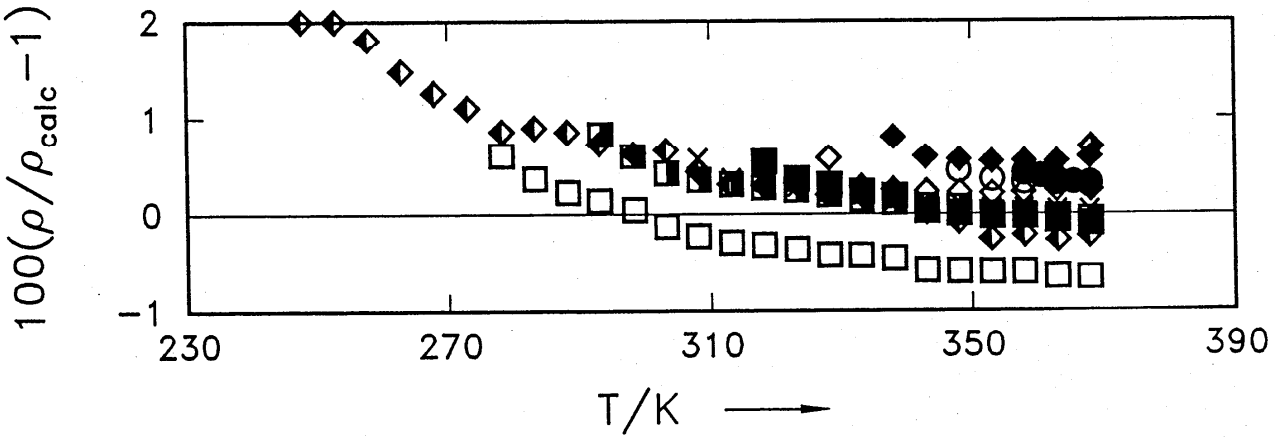

FIG. 10. Density deviations of (p,ρ,T)-properties reported by Doering[11] from our own EOS. ◆: 3.75 kg/m^3, □: 12.8 kg/m^3, ◨: 24.5 kg/m^3, ×: 35 kg/m^3, ■: 51 kg/m^3, ◇: 72 kg/m^3, ◆: 93.5 kg/m^3, ○: 114 kg/m^3, ●: 156 kg/m^3, ◆: 232 kg/m^3.

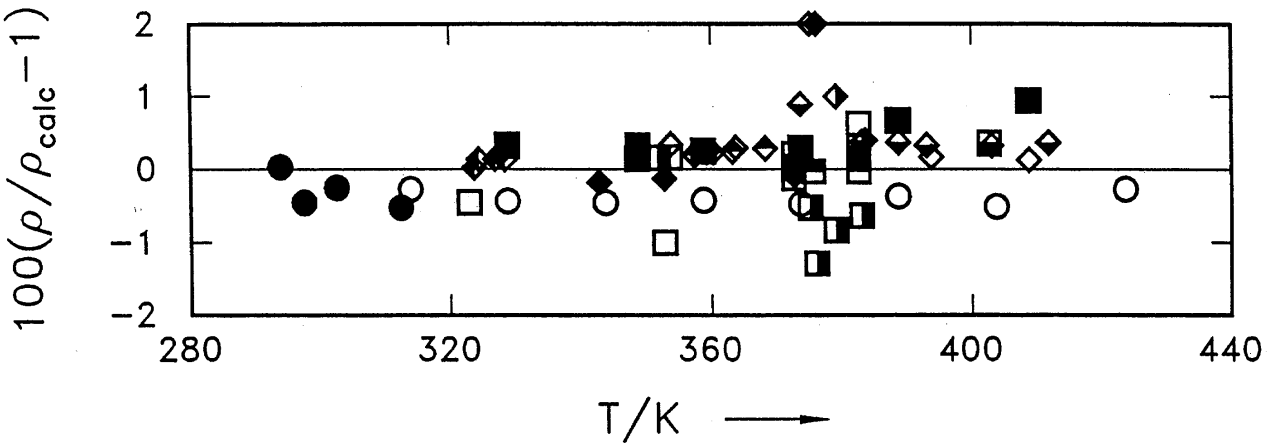

FIG. 11. Density deviations of (p,ρ,T)-properties reported by Fukushima *et al.*[15] from our own EOS. ○: 23 kg/m^3, ●:28 kg/m^3, □: 51 kg/m^3, ■: 75 kg/m^3, ◆: 109 kg/m^3, ◇: 152 kg/m^3, ⬓: 218 kg/m^3, ◆: 313 kg/m^3, ◨: 501 kg/m^3, ◆: 548 kg/m^3, ⬒: 700 kg/m^3, ◆: 897 kg/m^3, ◧: 968 kg/m^3, ◆: 1100 kg/m^3.

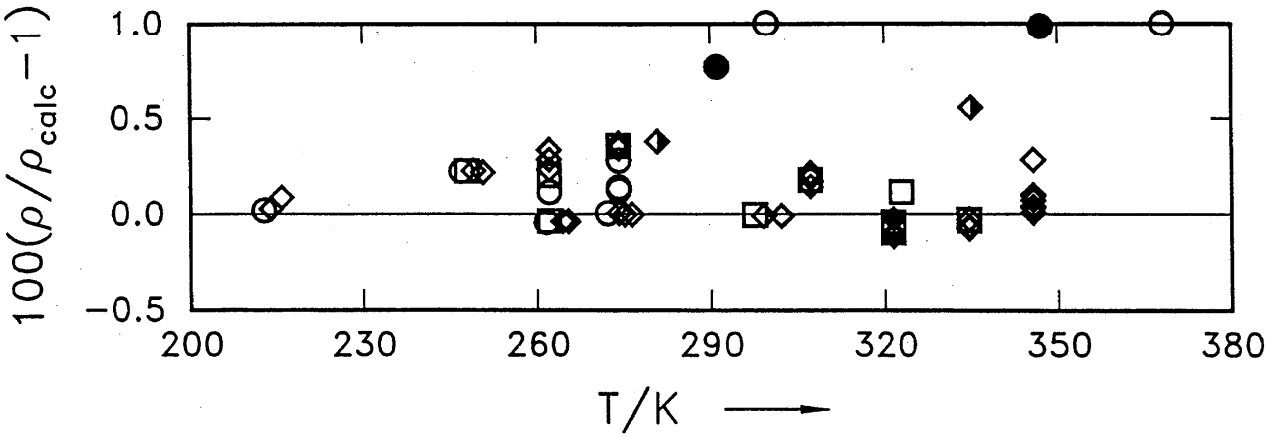

FIG. 12. Density deviations of (p,ρ,T)-properties reported by Kesselman *et al.*[27] from our own EOS. ○: <1 MPa, □: 1–2 MPa, ◇: 2–5 MPa, ◆: 5–10 MPa, ●: 10–20 MPa.

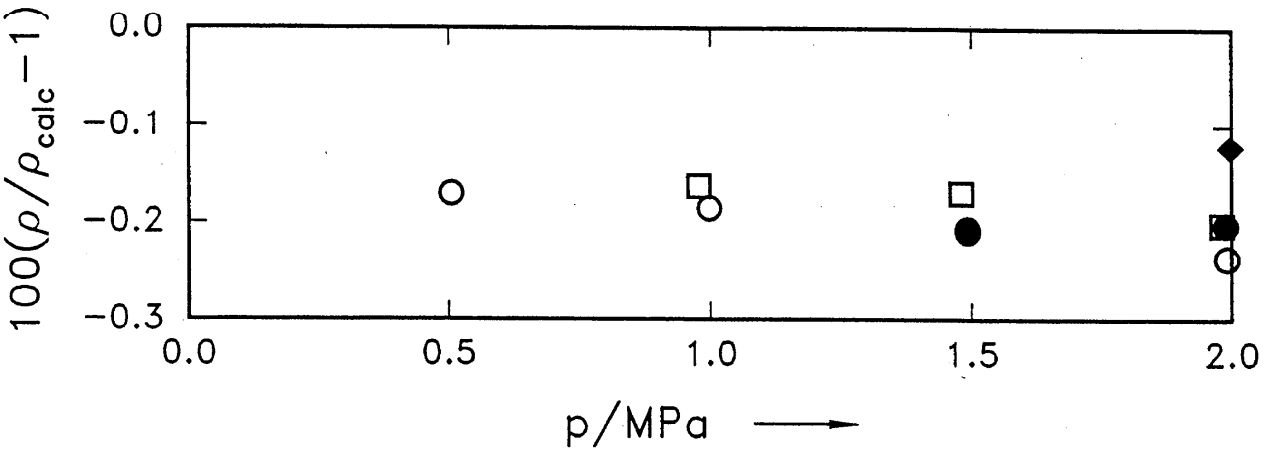

FIG. 13. Density deviations of (p,ρ,T)-properties reported by Maezawa *et al.*[32] from our own EOS. ○: 280 K, □: 300 K, ●: 320 K, ◆: 340 K.

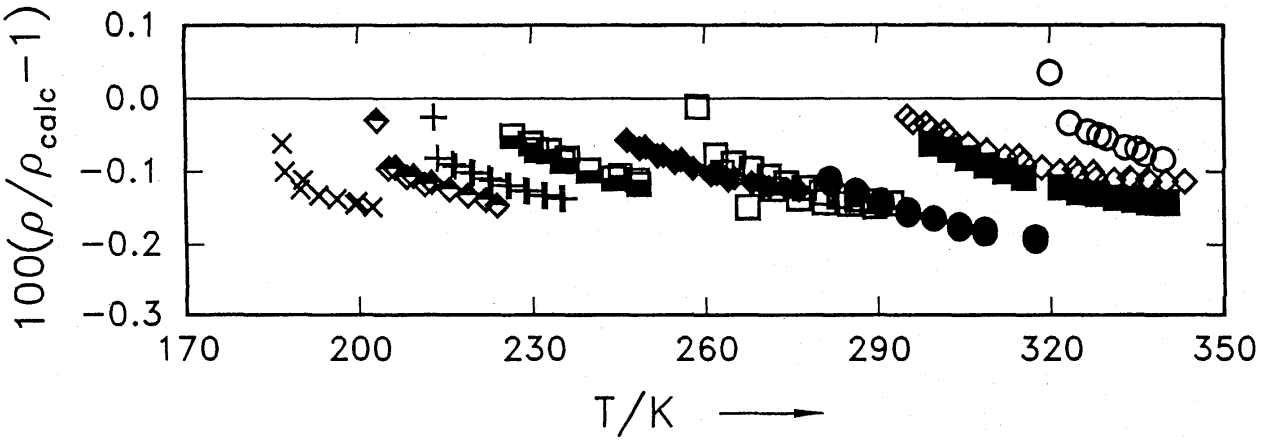

FIG. 14. Density deviations of (p,ρ,T)-properties reported by Magee[33] from our own EOS. ○: 1130 kg/m^3, ■: 1215 kg/m^3, ◇: 1225 kg/m^3, ●: 1280 kg/m^3, □: 1345 kg/m^3, ◆: 1385 kg/m^3, ◨: 1440 kg/m^3, +: 1475 kg/m^3, ◈: 1500 kg/m^3, ×: 1545 kg/m^3.

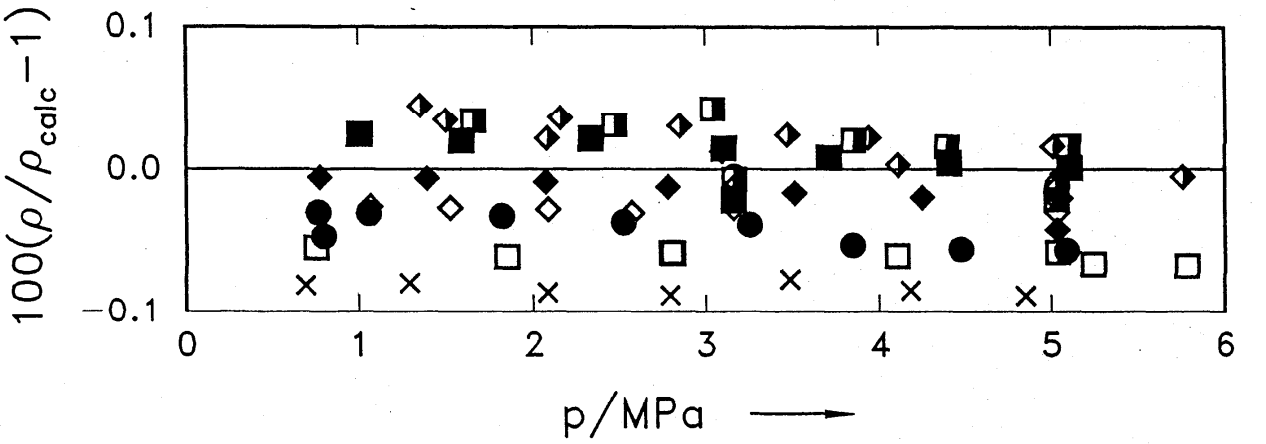

FIG. 15a. Density deviations of (p,ρ,T)-properties reported by Morrison and Ward[38]. ×: 279 K, ●: 288 K, □: 293 K, ◆: 298.5 K, ◇: 304.5 K, ■: 308 K, +: 314.5 K, ◈: 318 K, ○: 324 K, ◨: 328 K.

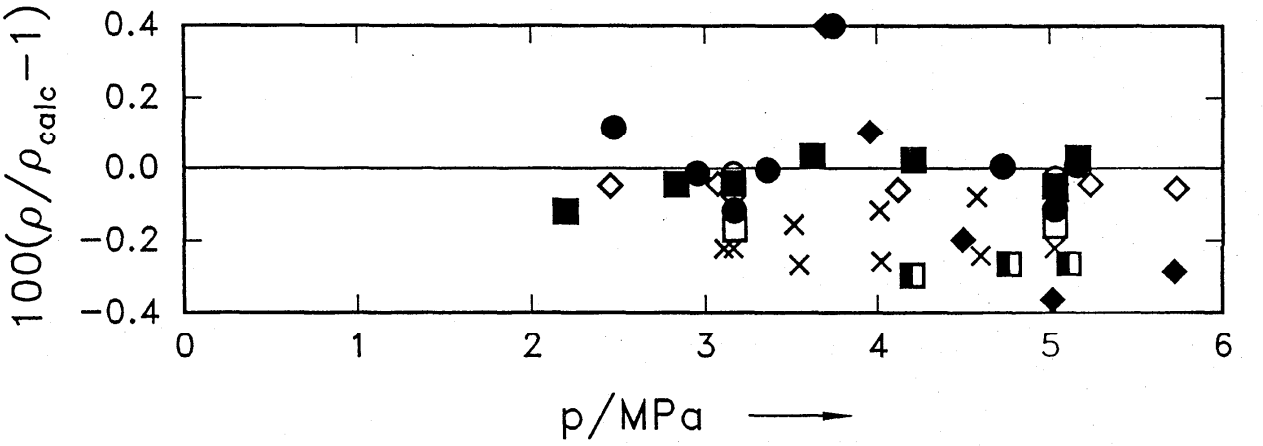

FIG. 15b. Density deviations of (p,ρ,T)-properties reported by Morrison and Ward[38] from our own EOS. ○: 333 K, ■: 337.5 K, ◇: 342.5 K, ●: 347.5 K, □: 352 K, ×: 357 K, ◆: 365 K, ◧: 367 K.

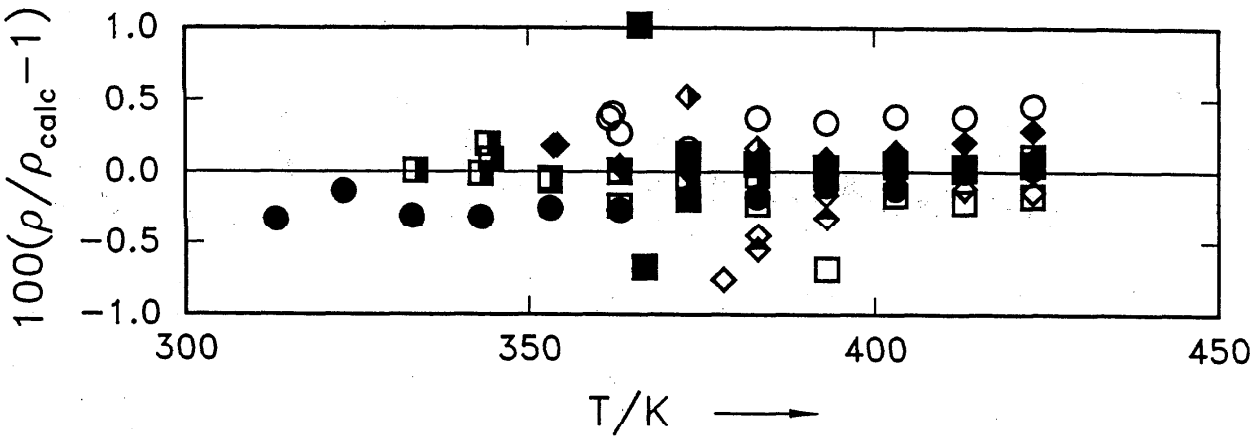

FIG. 16a. Density deviations of (p,ρ,T)-properties reported by Piao *et al.*[43] from our own EOS. ●: 37 kg/m^3, ◨: 87 kg/m^3, □: 151 kg/m^3, ◆: 155 kg/m^3, ○: 203 kg/m^3, ■: 242 kg/m^3, ◈: 273 kg/m^3, ◇: 380 kg/m^3, ◆: 459 kg/m^3.

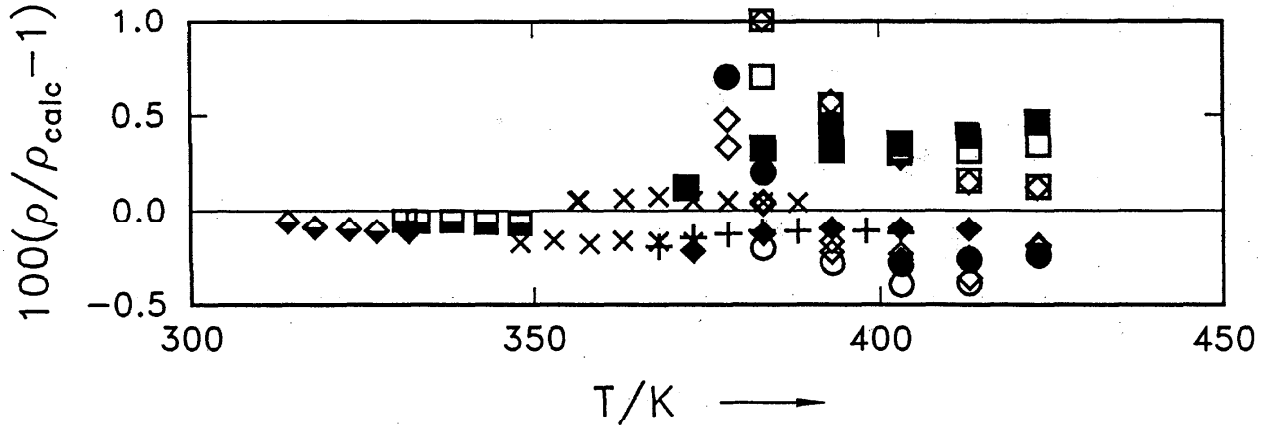

FIG. 16b. Density deviations of (p,ρ,T)-properties reported by Piao *et al.*[43] from our own EOS. ○: 483 kg/m^3, □: 495 kg/m^3, ◇: 508 kg/m^3, ●: 590 kg/m^3, ■: 691 kg/m^3, ◆: 780 kg/m^3, +: 839 kg/m^3, ×: 903 kg/m^3, ◨: 1064 kg/m^3, ◈: 1143 kg/m^3.

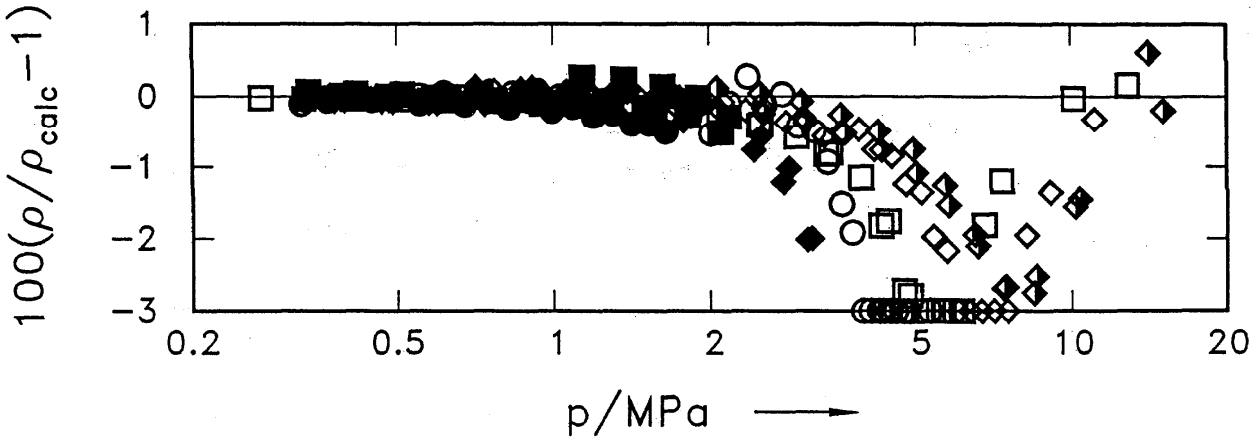

FIG. 17. Density deviations of (p,ρ,T)-properties reported by Park[42] from our own EOS. ●: 333 K, ■: 348 K, ◆: 363 K, ○: 378 K, □: 393 K, ◇: 408 K, ◈: 423 K.

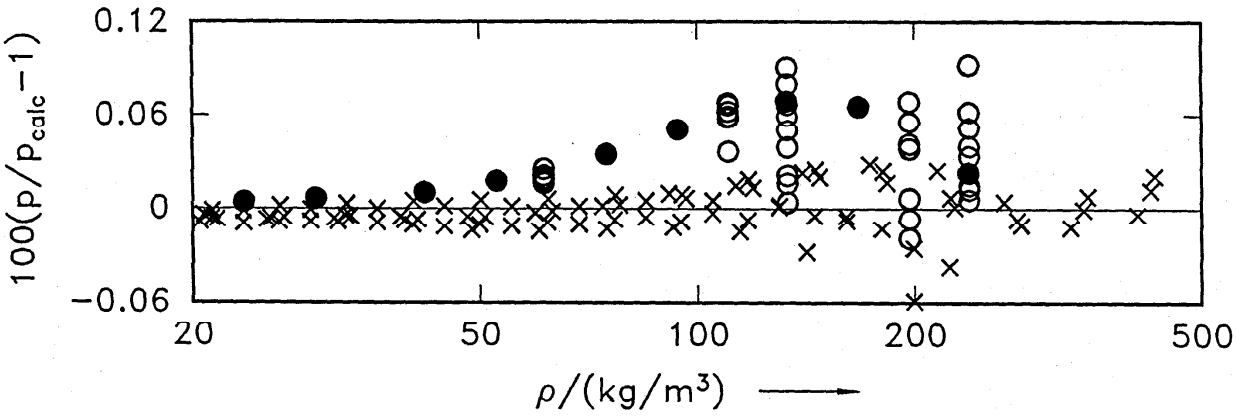

FIG. 18. Pressure deviations of (p,ρ,T)-properties between 350 K and 400 K from our own EOS. ●: Weber (Burnett-measurements)[58], ○: Weber (isochoric measurements)[58], ×: Tillner-Roth and Baehr[54].

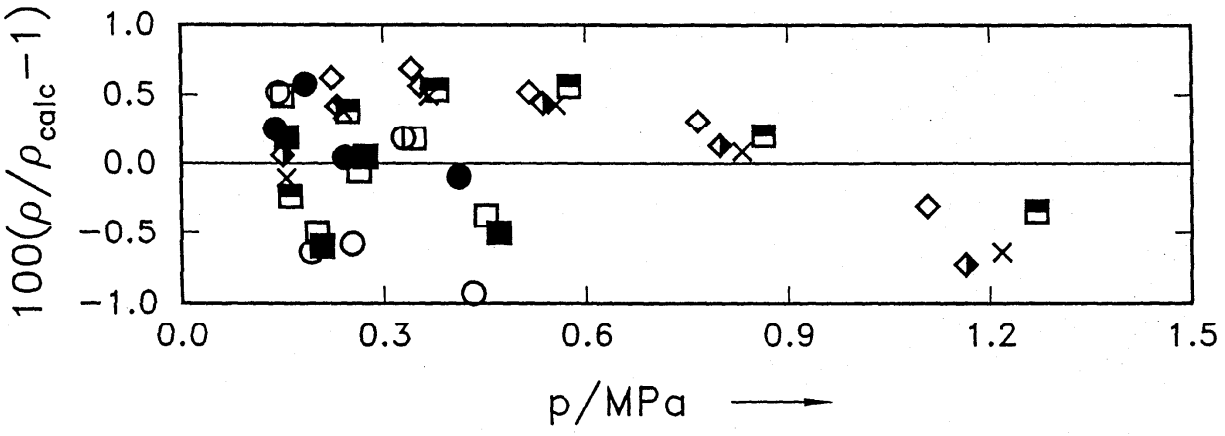

FIG. 19. Density deviations of (p,ρ,T)-properties reported by Zhu *et al.*[63] from our own EOS. ●: 283 K, ○: 293 K, □: 303 K, ■: 313 K, ◇: 325 K, ◆: 333 K, ×: 343 K, ⬒: 353 K.

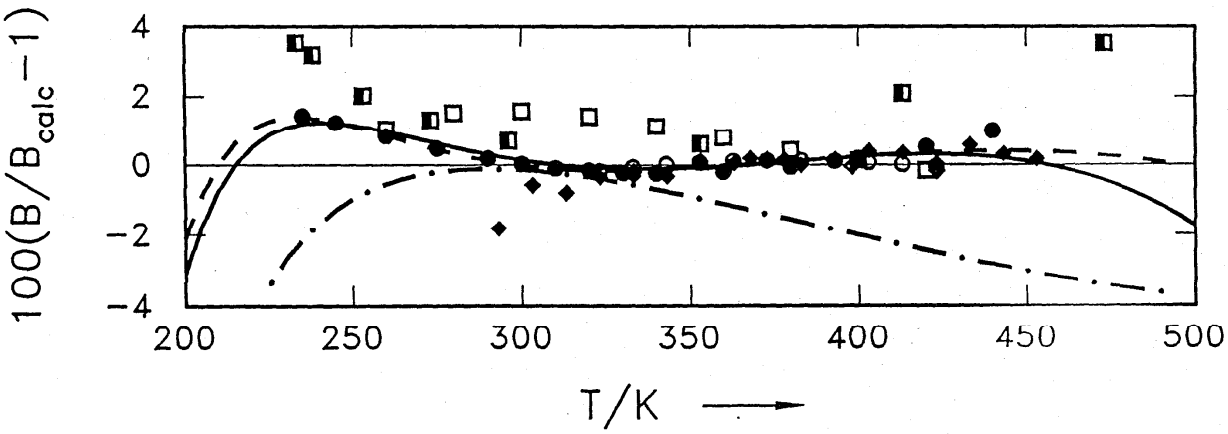

FIG. 20. Deviations of second virial coefficients from the EOS. ◆: Tillner-Roth and Baehr[54], ○: Dressner and Bier[12], ●: Goodwin and Moldover[18], □: Beckermann and Kohler[6], ◧: Schramm *et al.*[50,49], —— HM-EOS, – – – HE-EOS, –·–·– PNSW-EOS.

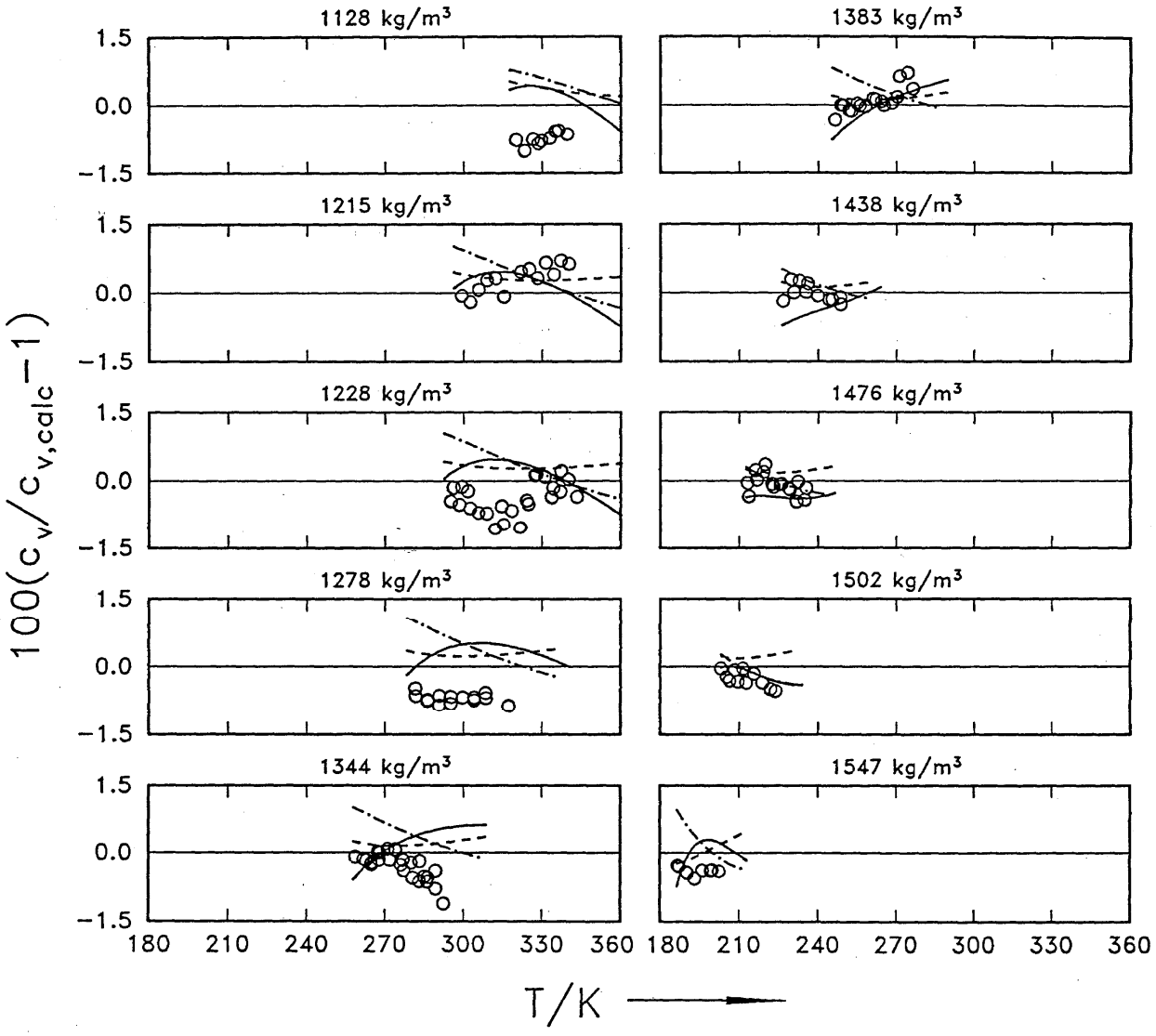

FIG. 21. Deviations of isochoric heat capacities measured by Magee[33] from our own EOS. ○: Magee[33], —— HM-EOS, — — — HE-EOS, –·–·– PNSW-EOS.

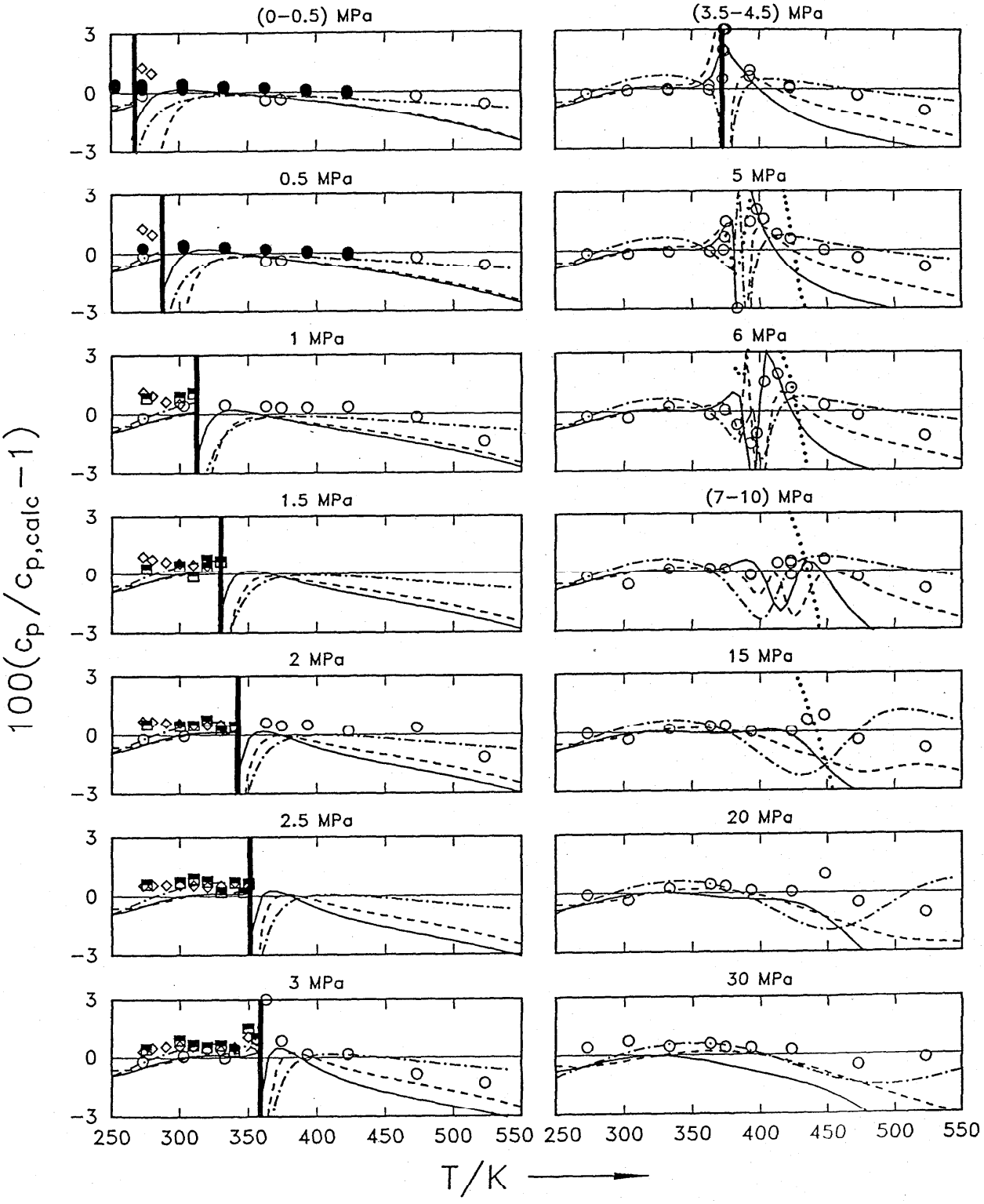

FIG. 22. Deviations of isobaric heat capacities from values calculated from our own EOS. ◇: Saitoh *et al.*[46], ▭: Nakagawa *et al.*[47], ●: Gürtner and Ernst[20], ○: Wirbser[59], ▮: saturation boundary, ——— HM-EOS, — — — HE-EOS, –·–·– PNSW-EOS, ·····Tang *et al.*[53].

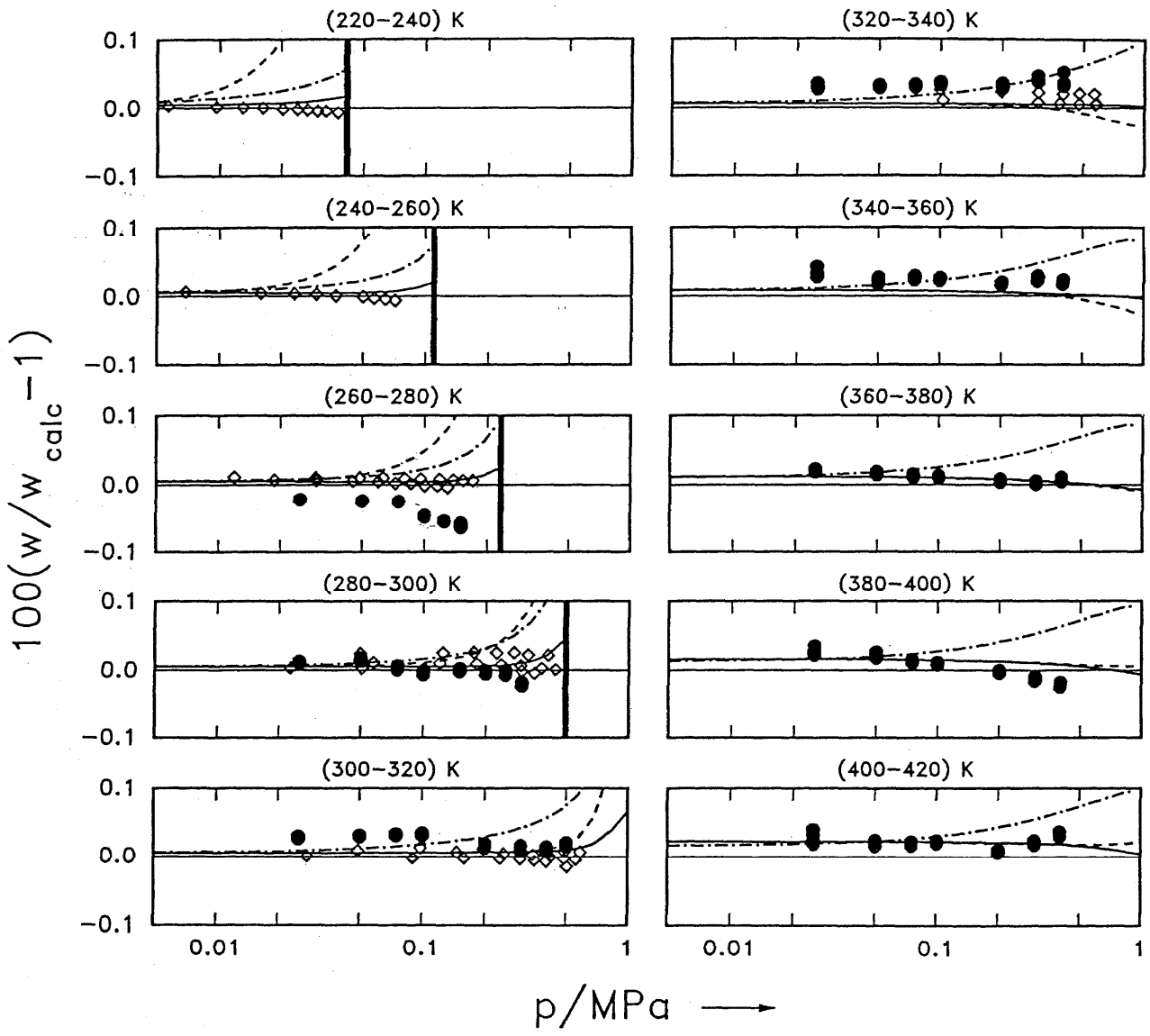

FIG. 23. Deviations of speed of sound values in the gaseous phase from our own EOS. ◇: Goodwin and Moldover[18], ●: Beckermann and Kohler[6], ▮: saturation boundary, —— HM-EOS, — — — HE-EOS, –·–·– PNSW-EOS.

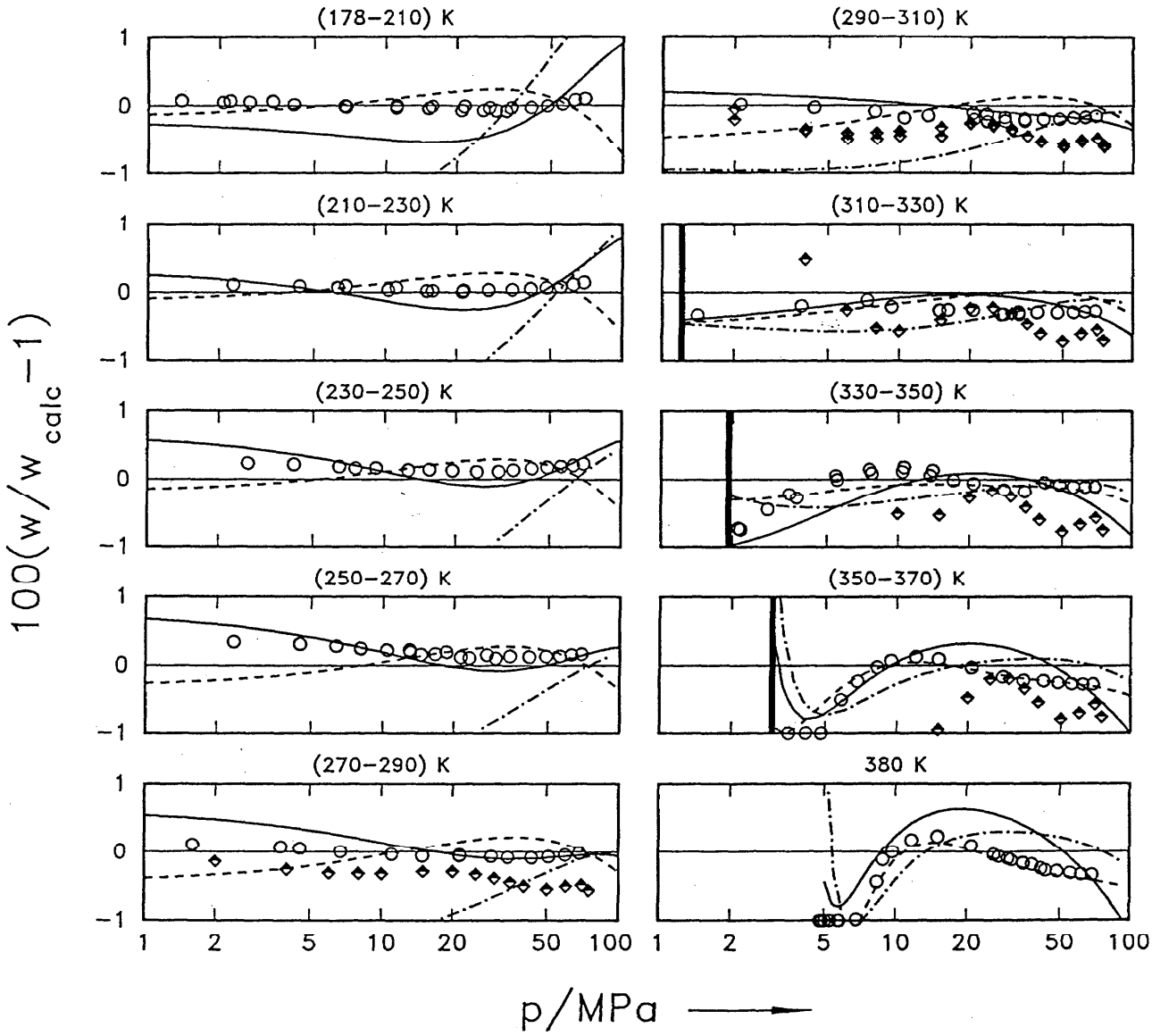

FIG. 24. Deviations of speed of sound values in the liquid region from our own EOS. ◆: Takagi[52], ○: Guedes and Zollweg[19], ▮: saturation boundary, —— HM-EOS, — — — HE-EOS, –·–·– PNSW-EOS.

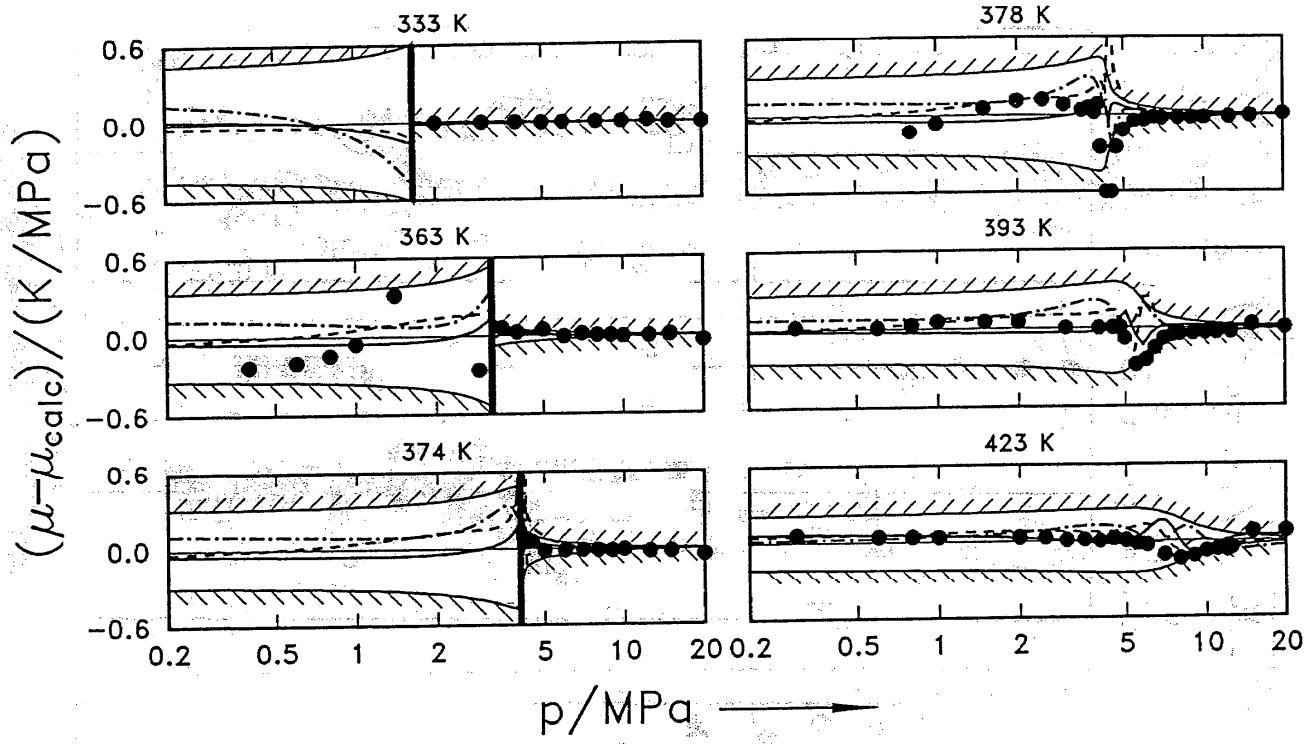

FIG. 25. Deviations of Joule-Thomson coefficients from our own EOS. ●: Wirbser[59], ▮: saturation boundary, ////// ±3%-boundary, —— HM-EOS, – – – HE-EOS, –·–·– PNSW-EOS.

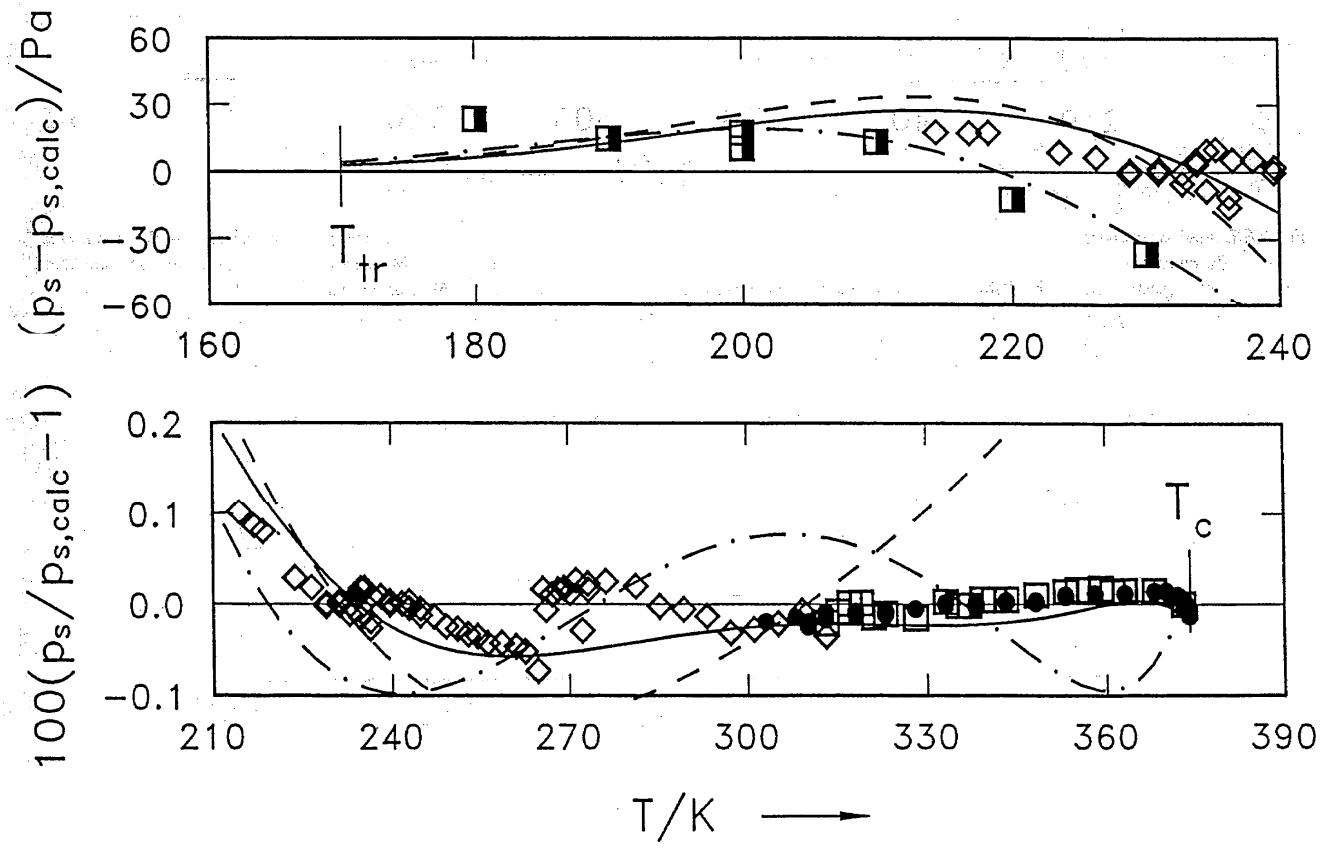

FIG. 26. Deviations of selected vapor pressures from the fundamental equation of state. ◨: Magee and Howley[34], ◇: Goodwin *et al.*[17], ●: Baehr and Tillner-Roth[11], □: Weber[58], —— HM-EOS, – – – HE-EOS, –·–·– PNSW-EOS.

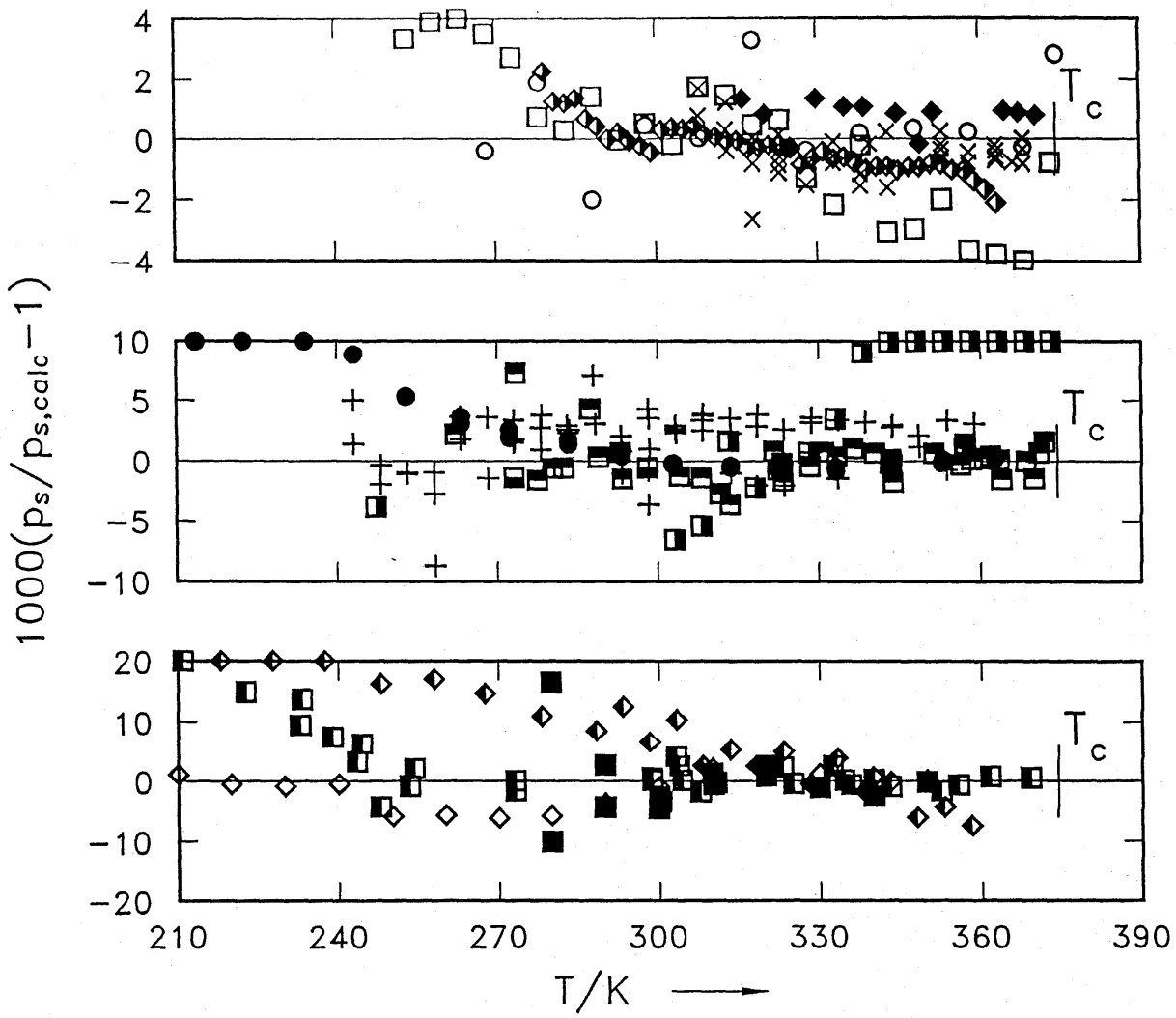

FIG. 27. Deviations of measured vapor pressures from the fundamental EOS not being used during the correlation process. ⬓: Arita *et al.*[2], +: Baroncini *et al.*[4], ⬒: Fukushima *et al.*[15], ●: Bier *et al.*[8], ×: Piao *et al.*[43], □: Kubota *et al.*[30], ■: Maezawa *et al.*[32], ◇: Magee and Howley[34], ○: Morrison and Ward[38], ◆: Niesen *et al.*[40], ◨: Nishiumi and Yokoyama[41], ◧: Basu and Wilson[5], ◈: Zhu *et al.*[62], ◈: Döring *et al.*[11].

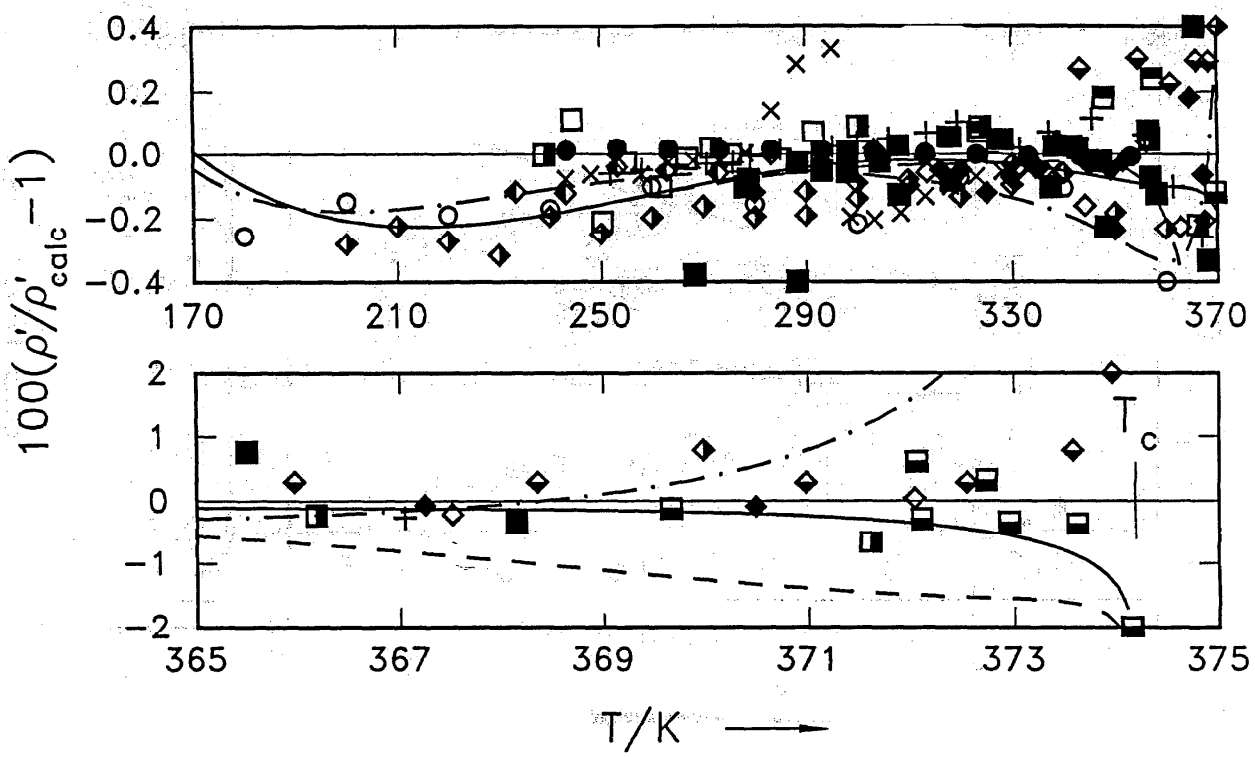

FIG. 28. Deviations of saturated liquid densities from the fundamental equation of state. ×: Döring *et al.*[11], □, ◪, ⬒: Fukushima *et al.*[15,14,16], ○: Hou *et al.*[23], +: Yokoyama and Takahashi[61], ◆: Kabata *et al.*[26], ◆: Maezawa *et al.*[32], ◆: Kruse[29], ■: Morrison and Ward[38], ◆: Niesen *et al.*[40], ◇: Piao *et al.*[43], ◨: Basu and Wilson[5], ●: Tillner-Roth and Baehr[55], —— HM-EOS, — — — HE-EOS, —·—·— PNSW-EOS.

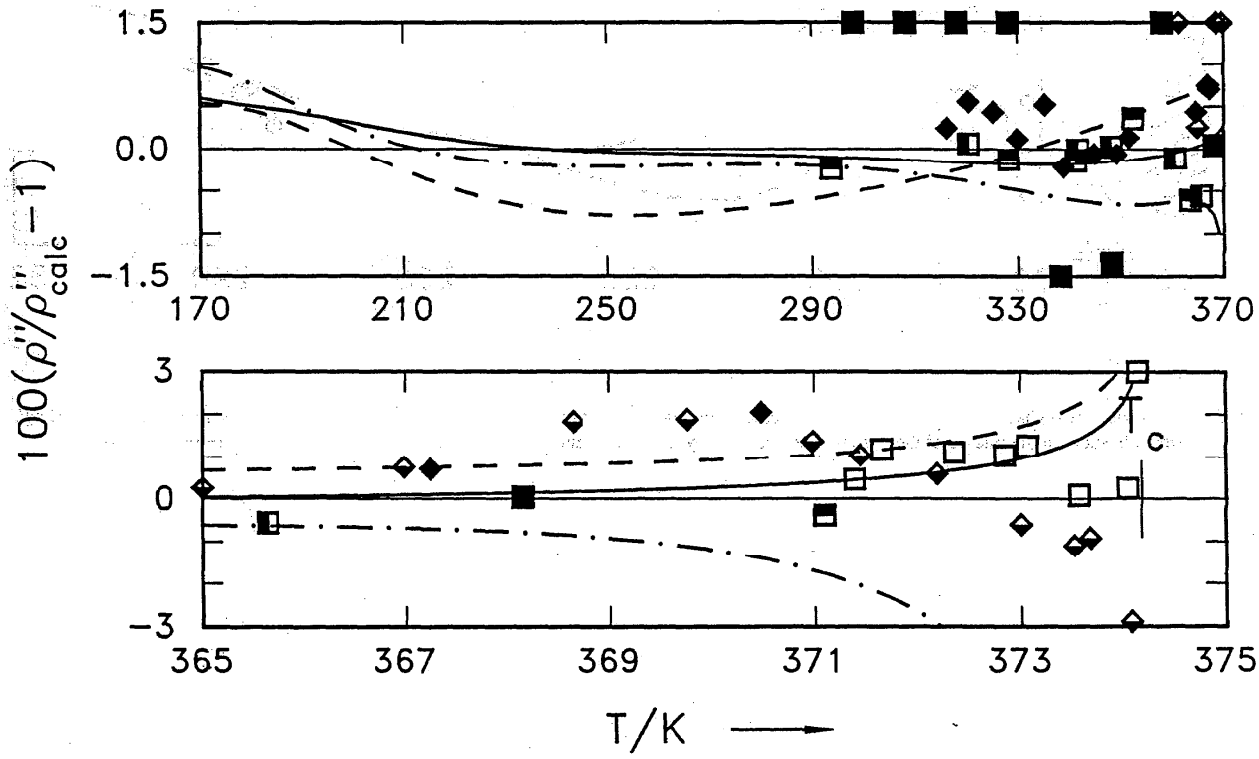

FIG. 29. Deviations of saturated vapor densities from the fundamental equation of state. □, ⬒: Fukushima *et al.*[14,16], ◆: Kabata *et al.*[26], ■: Morrison and Ward[38], ◆: Niesen *et al.*[40], ◧: Weber[58], —— HM-EOS, — — — HE-EOS, —·—·— PNSW-EOS.

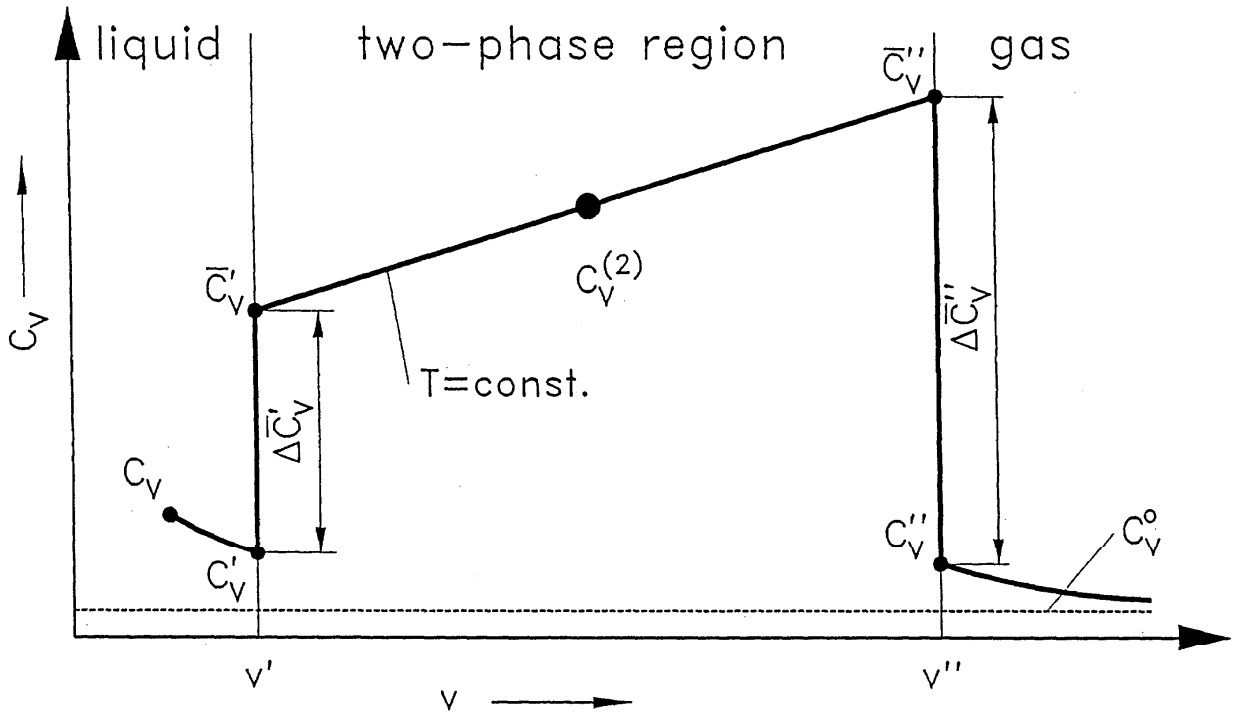

FIG. 30. Qualitative plot of the isochoric heat capacity on an isotherm.

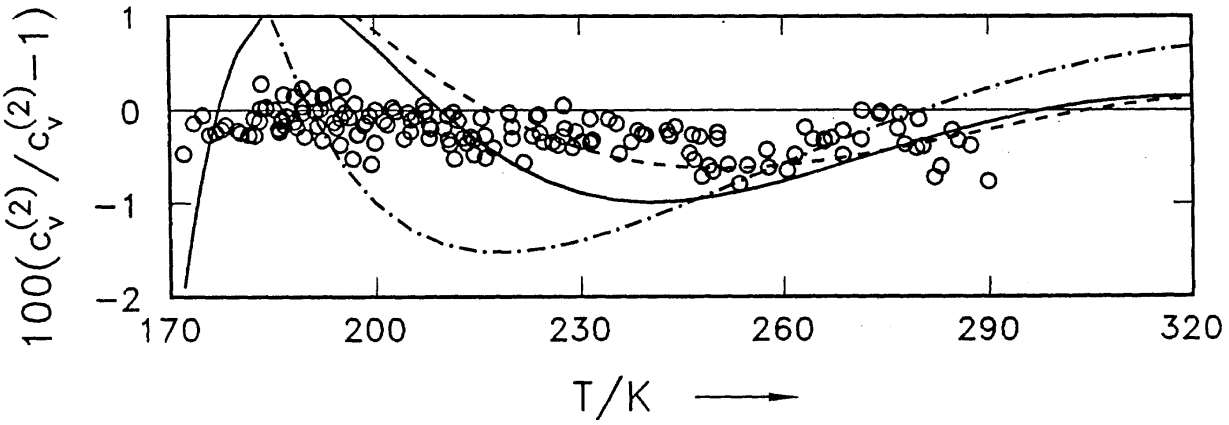

FIG. 31. Deviations of two-phase isochoric heat capacities measured by Magee[33] from our own EOS. The other equations of state were evaluated at 1100 kg/m^3 which is about in the middle of the density range covered by the experiments. —— HM-EOS, — — — HE-EOS, –·–·– PNSW-EOS.

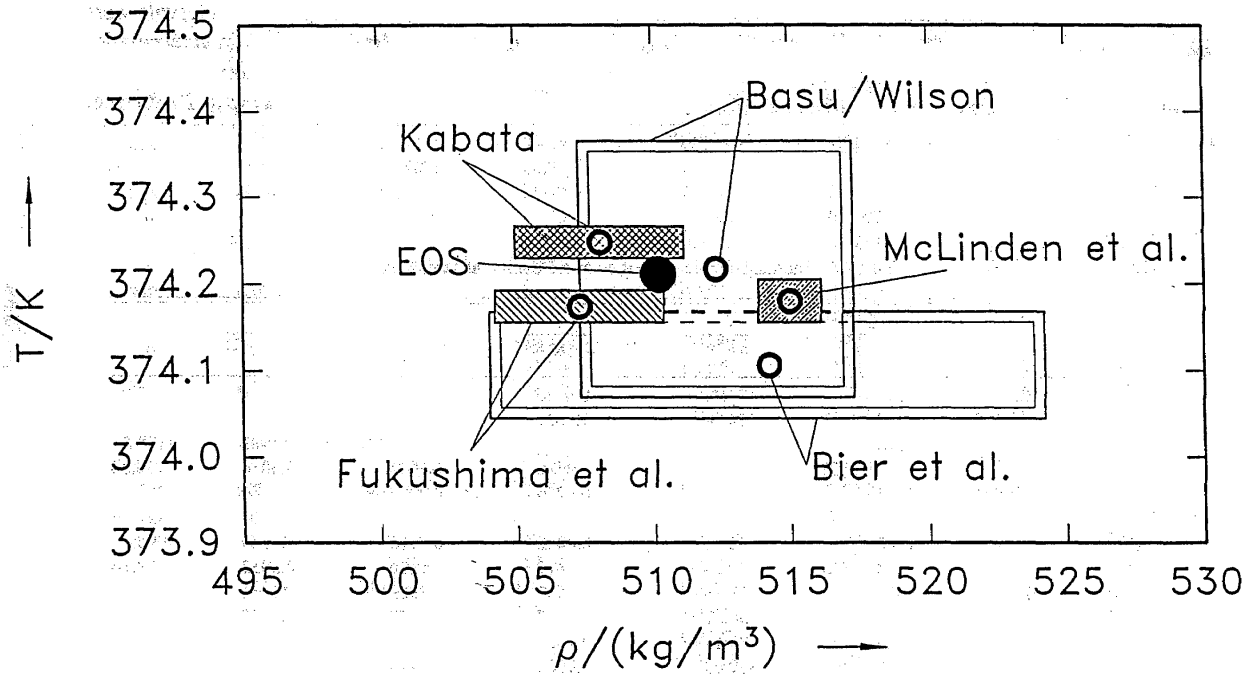

FIG. 32. Comparison of measured critical parameters T_c and ρ_c with values calculated from our own EOS. The rectangles indicate the uncertainty of the respective experimental value.

8. Appendix
Tables of Thermodynamic Properties

All values in Tables 8 and 9 were calculated from the fundamental equation of state to preserve thermodynamic consistency. Temperature and pressure intervals were chosen in order to minimize the inaccuracy in interpolation. However, interpolation in the critical region is not recommended because of the extreme shape of the (p,ρ,T)-surface.

TABLE 8. Thermodynamic properties of HFC-134a at saturation

T / K	p_s / MPa	ρ / kg/m^3	h / kJ/kg	s / kJ/(kgK)	c_v / kJ/(kgK)	c_p / kJ/(kgK)	w / m/s
169.85[a]	0.00039	1591.1	71.454	0.4126	0.7922	1.1838	1119.9
		0.02817	334.94	1.9639	0.5029	0.5853	126.79
170	0.00040	1590.7	71.632	0.4136	0.7921	1.1838	1119.2
		0.02862	335.02	1.9630	0.5033	0.5856	126.84
172	0.00049	1585.4	74.000	0.4275	0.7914	1.1840	1109.0
		0.03529	336.18	1.9518	0.5080	0.5904	127.49
174	0.00061	1580.1	76.368	0.4412	0.7910	1.1844	1098.8
		0.04325	337.34	1.9410	0.5126	0.5952	128.14
176	0.00075	1574.8	78.738	0.4547	0.7909	1.1851	1088.6
		0.05270	338.51	1.9307	0.5173	0.6000	128.78
178	0.00092	1569.5	81.109	0.4681	0.7909	1.1860	1078.5
		0.06388	339.69	1.9208	0.5220	0.6048	129.42
180	0.00113	1564.2	83.482	0.4813	0.7912	1.1871	1068.3
		0.07701	340.88	1.9113	0.5267	0.6096	130.05
182	0.00137	1558.9	85.858	0.4945	0.7916	1.1884	1058.1
		0.09239	342.07	1.9022	0.5313	0.6145	130.67
184	0.00165	1553.5	88.236	0.5075	0.7923	1.1898	1048.0
		0.11030	343.26	1.8935	0.5360	0.6193	131.29
186	0.00198	1548.2	90.618	0.5203	0.7930	1.1914	1037.8
		0.13106	344.47	1.8852	0.5407	0.6242	131.90
188	0.00237	1542.8	93.002	0.5331	0.7939	1.1931	1027.7
		0.15503	345.68	1.8771	0.5453	0.6290	132.51
190	0.00282	1537.5	95.391	0.5457	0.7949	1.1949	1017.6
		0.18259	346.89	1.8695	0.5500	0.6339	133.11
192	0.00334	1532.1	97.783	0.5582	0.7961	1.1969	1007.5
		0.21416	348.12	1.8621	0.5546	0.6388	133.70
194	0.00394	1526.7	100.17	0.5707	0.7973	1.1989	997.55
		0.25017	349.34	1.8550	0.5593	0.6437	134.28
196	0.00463	1521.3	102.57	0.5830	0.7986	1.2011	987.54
		0.29110	350.57	1.8483	0.5639	0.6486	134.85
198	0.00541	1515.9	104.98	0.5952	0.8000	1.2034	977.55
		0.33745	351.81	1.8418	0.5685	0.6536	135.42
200	0.00631	1510.4	107.39	0.6073	0.8015	1.2057	967.60
		0.38977	353.05	1.8356	0.5732	0.6586	135.98
202	0.00733	1505.0	109.80	0.6193	0.8031	1.2081	957.68
		0.44864	354.30	1.8297	0.5779	0.6636	136.53
204	0.00849	1499.5	112.22	0.6312	0.8047	1.2106	947.80
		0.51465	355.55	1.8240	0.5825	0.6687	137.07
206	0.00979	1494.0	114.65	0.6430	0.8063	1.2132	937.94
		0.58846	356.80	1.8185	0.5872	0.6737	137.60
208	0.01126	1488.5	117.08	0.6548	0.8081	1.2159	928.12
		0.67075	358.06	1.8133	0.5919	0.6789	138.12
210	0.01291	1483.0	119.51	0.6664	0.8098	1.2186	918.33
		0.76222	359.32	1.8083	0.5966	0.6841	138.63
212	0.01475	1477.5	121.95	0.6780	0.8116	1.2214	908.57
		0.86364	360.58	1.8036	0.6013	0.6893	139.12
214	0.01681	1471.9	124.40	0.6894	0.8135	1.2242	898.84
		0.97578	361.84	1.7990	0.6060	0.6946	139.61
216	0.01909	1466.3	126.85	0.7008	0.8154	1.2271	889.15
		1.0994	363.11	1.7946	0.6108	0.7000	140.09
218	0.02163	1460.8	129.31	0.7122	0.8173	1.2301	879.48
		1.2355	364.38	1.7905	0.6155	0.7054	140.55
220	0.02443	1455.1	131.77	0.7234	0.8193	1.2331	869.85
		1.3850	365.65	1.7865	0.6203	0.7109	141.00

TABLE 8. Thermodynamic properties of HFC-134a at saturation — Continued

$\frac{T}{K}$	$\frac{p_s}{MPa}$	$\frac{\rho}{kg/m^3}$	$\frac{h}{kJ/kg}$	$\frac{s}{kJ/(kgK)}$	$\frac{c_v}{kJ/(kgK)}$	$\frac{c_p}{kJ/(kgK)}$	$\frac{w}{m/s}$
222	0.02753	1449.5	134.25	0.7346	0.8212	1.2362	860.24
		1.5486	366.92	1.7826	0.6251	0.7164	141.44
224	0.03094	1443.9	136.72	0.7457	0.8233	1.2394	850.67
		1.7275	368.19	1.7790	0.6300	0.7221	141.86
226	0.03469	1438.2	139.21	0.7567	0.8253	1.2426	841.12
		1.9227	369.46	1.7755	0.6348	0.7278	142.27
228	0.03879	1432.5	141.70	0.7677	0.8274	1.2459	831.60
		2.1351	370.73	1.7722	0.6398	0.7336	142.67
230	0.04329	1426.7	144.19	0.7785	0.8295	1.2492	822.10
		2.3659	372.00	1.7690	0.6447	0.7395	143.05
232	0.04819	1421.0	146.70	0.7894	0.8316	1.2526	812.63
		2.6162	373.27	1.7660	0.6497	0.7455	143.42
234	0.05354	1415.2	149.21	0.8001	0.8337	1.2561	803.19
		2.8872	374.54	1.7631	0.6547	0.7516	143.77
236	0.05935	1409.4	151.72	0.8108	0.8359	1.2596	793.77
		3.1801	375.80	1.7603	0.6597	0.7578	144.11
238	0.06565	1403.5	154.25	0.8215	0.8380	1.2632	784.37
		3.4962	377.07	1.7577	0.6648	0.7641	144.43
240	0.07248	1397.7	156.78	0.8320	0.8402	1.2669	774.99
		3.8367	378.33	1.7552	0.6699	0.7705	144.73
242	0.07987	1391.8	159.32	0.8426	0.8424	1.2706	765.63
		4.2030	379.59	1.7528	0.6751	0.7770	145.02
244	0.08784	1385.8	161.87	0.8530	0.8447	1.2745	756.29
		4.5965	380.85	1.7505	0.6803	0.7837	145.28
246	0.09643	1379.9	164.43	0.8634	0.8469	1.2784	746.97
		5.0185	382.10	1.7483	0.6855	0.7904	145.53
246.78[b]	0.10000	1377.5	165.44	0.8675	0.8478	1.2799	743.30
		5.1932	382.59	1.7474	0.6876	0.7931	145.63
248	0.10568	1373.8	166.99	0.8738	0.8492	1.2824	737.67
		5.4707	383.35	1.7462	0.6908	0.7973	145.77
250	0.11561	1367.8	169.56	0.8841	0.8514	1.2864	728.38
		5.9545	384.60	1.7442	0.6961	0.8044	145.98
252	0.12627	1361.7	172.14	0.8943	0.8537	1.2906	719.11
		6.4715	385.84	1.7423	0.7015	0.8116	146.17
254	0.13768	1355.6	174.73	0.9045	0.8560	1.2948	709.85
		7.0233	387.07	1.7405	0.7069	0.8189	146.35
256	0.14989	1349.5	177.33	0.9147	0.8584	1.2992	700.60
		7.6117	388.31	1.7388	0.7123	0.8263	146.50
258	0.16293	1343.2	179.94	0.9248	0.8607	1.3036	691.36
		8.2384	389.53	1.7372	0.7178	0.8340	146.63
260	0.17684	1337.0	182.55	0.9348	0.8631	1.3081	682.14
		8.9051	390.75	1.7356	0.7234	0.8417	146.75
262	0.19166	1330.7	185.18	0.9449	0.8655	1.3128	672.92
		9.6138	391.97	1.7341	0.7289	0.8497	146.84
264	0.20742	1324.4	187.81	0.9548	0.8679	1.3176	663.71
		10.366	393.17	1.7327	0.7346	0.8578	146.91
266	0.22418	1318.0	190.46	0.9648	0.8703	1.3224	654.51
		11.165	394.37	1.7314	0.7402	0.8660	146.95
268	0.24197	1311.6	193.11	0.9747	0.8727	1.3275	645.31
		12.011	395.56	1.7301	0.7459	0.8745	146.98
270	0.26082	1305.1	195.78	0.9845	0.8752	1.3326	636.12
		12.908	396.75	1.7289	0.7517	0.8832	146.98
272	0.28080	1298.5	198.45	0.9943	0.8776	1.3379	626.93
		13.857	397.93	1.7277	0.7574	0.8920	146.96
274	0.30193	1291.9	201.14	1.0041	0.8801	1.3433	617.74
		14.861	399.09	1.7266	0.7633	0.9011	146.91
276	0.32426	1285.3	203.84	1.0139	0.8826	1.3489	608.55
		15.923	400.25	1.7255	0.7691	0.9103	146.84
278	0.34784	1278.5	206.54	1.0236	0.8851	1.3547	599.36
		17.044	401.40	1.7245	0.7750	0.9198	146.74
280	0.37271	1271.7	209.26	1.0332	0.8877	1.3606	590.17
		18.227	402.54	1.7235	0.7809	0.9296	146.62
282	0.39892	1264.9	212.00	1.0429	0.8902	1.3667	580.98
		19.476	403.67	1.7226	0.7869	0.9396	146.47

TABLE 8. Thermodynamic properties of HFC-134a at saturation — Continued

T / K	p_s / MPa	ρ / kg/m^3	h / kJ/kg	s / kJ/(kgK)	c_v / kJ/(kgK)	c_p / kJ/(kgK)	w / m/s
284	0.42651	1258.0	214.74	1.0525	0.8928	1.3730	571.78
		20.794	404.79	1.7217	0.7929	0.9498	146.30
286	0.45553	1251.0	217.50	1.0621	0.8954	1.3796	562.57
		22.182	405.89	1.7208	0.7990	0.9603	146.10
288	0.48603	1243.9	220.27	1.0717	0.8981	1.3863	553.36
		23.645	406.99	1.7200	0.8051	0.9712	145.87
290	0.51805	1236.7	223.05	1.0812	0.9007	1.3933	544.14
		25.186	408.07	1.7192	0.8112	0.9823	145.61
292	0.55165	1229.5	225.85	1.0907	0.9034	1.4005	534.91
		26.808	409.14	1.7184	0.8174	0.9938	145.32
294	0.58688	1222.2	228.66	1.1002	0.9061	1.4080	525.68
		28.516	410.19	1.7177	0.8236	1.0057	145.01
296	0.62378	1214.7	231.49	1.1097	0.9088	1.4158	516.42
		30.313	411.23	1.7169	0.8299	1.0180	144.66
298	0.66241	1207.2	234.33	1.1192	0.9116	1.4239	507.16
		32.204	412.25	1.7162	0.8362	1.0306	144.28
300	0.70282	1199.6	237.18	1.1286	0.9144	1.4324	497.88
		34.192	413.26	1.7155	0.8426	1.0438	143.87
302	0.74506	1191.9	240.06	1.1380	0.9172	1.4412	488.59
		36.284	414.25	1.7148	0.8490	1.0574	143.43
304	0.78918	1184.1	242.95	1.1475	0.9201	1.4504	479.28
		38.483	415.22	1.7142	0.8554	1.0715	142.95
306	0.83524	1176.1	245.86	1.1569	0.9230	1.4600	469.95
		40.796	416.18	1.7135	0.8620	1.0862	142.44
308	0.88330	1168.1	248.78	1.1663	0.9259	1.4701	460.60
		43.228	417.11	1.7128	0.8685	1.1016	141.90
310	0.93340	1159.9	251.73	1.1756	0.9288	1.4806	451.23
		45.785	418.03	1.7121	0.8751	1.1176	141.32
312	0.98560	1151.5	254.69	1.1850	0.9318	1.4917	441.83
		48.475	418.92	1.7114	0.8818	1.1344	140.70
314	1.0399	1143.1	257.68	1.1944	0.9349	1.5034	432.42
		51.305	419.79	1.7107	0.8886	1.1521	140.05
316	1.0965	1134.5	260.68	1.2038	0.9380	1.5157	422.97
		54.282	420.63	1.7100	0.8954	1.1706	139.36
318	1.1554	1125.7	263.71	1.2132	0.9411	1.5288	413.50
		57.415	421.45	1.7092	0.9023	1.1902	138.62
320	1.2166	1116.7	266.76	1.2226	0.9443	1.5426	403.99
		60.714	422.25	1.7085	0.9093	1.2108	137.85
322	1.2802	1107.6	269.84	1.2320	0.9475	1.5572	394.45
		64.189	423.01	1.7077	0.9163	1.2328	137.03
324	1.3462	1098.3	272.94	1.2414	0.9508	1.5729	384.88
		67.851	423.74	1.7068	0.9235	1.2561	136.18
326	1.4148	1088.7	276.07	1.2508	0.9542	1.5896	375.26
		71.713	424.44	1.7060	0.9307	1.2811	135.27
328	1.4860	1079.0	279.23	1.2603	0.9576	1.6074	365.60
		75.789	425.10	1.7050	0.9381	1.3078	134.32
330	1.5599	1069.0	282.41	1.2698	0.9611	1.6267	355.89
		80.093	425.72	1.7041	0.9456	1.3366	133.32
332	1.6364	1058.8	285.63	1.2793	0.9647	1.6474	346.13
		84.644	426.31	1.7030	0.9532	1.3677	132.28
334	1.7158	1048.3	288.89	1.2888	0.9684	1.6699	336.30
		89.459	426.85	1.7019	0.9609	1.4015	131.18
336	1.7981	1037.5	292.18	1.2984	0.9722	1.6944	326.41
		94.563	427.34	1.7007	0.9688	1.4384	130.03
338	1.8833	1026.4	295.51	1.3081	0.9761	1.7212	316.43
		99.978	427.78	1.6994	0.9769	1.4789	128.83
340	1.9715	1015.0	298.88	1.3177	0.9801	1.7507	306.36
		105.73	428.17	1.6980	0.9851	1.5237	127.56
342	2.0628	1003.2	302.29	1.3275	0.9843	1.7834	296.19
		111.86	428.49	1.6965	0.9936	1.5736	126.24
344	2.1574	990.99	305.76	1.3373	0.9888	1.8199	285.89
		118.40	428.74	1.6948	1.0023	1.6296	124.86
346	2.2552	978.30	309.27	1.3472	0.9934	1.8610	275.45
		125.40	428.92	1.6930	1.0112	1.6930	123.42

TABLE 8. Thermodynamic properties of HFC-134a at saturation — Continued

T / K	p_s / MPa	ρ / kg/m^3	h / kJ/kg	s / kJ/(kgK)	c_v / kJ/(kgK)	c_p / kJ/(kgK)	w / m/s
348	2.3563	965.10	312.85	1.3572	0.9984	1.9077	264.85
		132.90	429.02	1.6911	1.0205	1.7655	121.91
350	2.4610	951.31	316.49	1.3674	1.0036	1.9613	254.05
		140.99	429.02	1.6889	1.0300	1.8493	120.33
352	2.5693	936.88	320.21	1.3776	1.0094	2.0239	243.03
		149.72	428.92	1.6865	1.0400	1.9476	118.67
354	2.6812	921.68	324.01	1.3880	1.0156	2.0978	231.76
		159.20	428.70	1.6838	1.0504	2.0645	116.94
356	2.7969	905.61	327.91	1.3987	1.0225	2.1870	220.20
		169.56	428.33	1.6808	1.0614	2.2063	115.13
358	2.9166	888.49	331.91	1.4095	1.0302	2.2971	208.31
		180.95	427.80	1.6774	1.0730	2.3822	113.23
360	3.0404	870.11	336.05	1.4207	1.0389	2.4367	196.04
		193.58	427.07	1.6735	1.0853	2.6063	111.24
362	3.1685	850.16	340.36	1.4322	1.0490	2.6206	183.36
		207.75	426.10	1.6690	1.0986	2.9026	109.15
364	3.3010	828.21	344.87	1.4442	1.0608	2.8751	170.21
		223.89	424.82	1.6638	1.1131	3.3131	106.94
366	3.4382	803.56	349.65	1.4568	1.0749	3.2526	156.54
		242.67	423.14	1.6576	1.1291	3.9212	104.60
368	3.5803	775.05	354.83	1.4704	1.0923	3.8750	142.26
		265.24	420.87	1.6499	1.1474	4.9182	102.10
370	3.7278	740.31	360.64	1.4856	1.1145	5.1048	127.23
		293.89	417.68	1.6398	1.1690	6.8621	99.370
372	3.8811	693.10	367.71	1.5041	1.1459	8.7028	111.10
		334.83	412.67	1.6250	1.1965	12.375	96.219
374	4.0416	587.91	380.85	1.5387	1.2120	101.66	92.401
		434.05	399.50	1.5885	1.2409	137.23	91.389
374.21[c]	4.0593	511.95	389.63	1.5620	—	—	—
		511.95	389.63	1.5620	—	—	—

[a]Triple point.
[b]Normal boiling point.
[c]Critical point.

TABLE 9. Thermodynamic properties of HFC-134a in the single-phase region

T/K	ρ/kg/m^3	h/kJ/kg	s/kJ/(kgK)	c_v/kJ/(kgK)	c_p/kJ/(kgK)	w/m/s	T/K	ρ/kg/m^3	h/kJ/kg	s/kJ/(kgK)	c_v/kJ/(kgK)	c_p/kJ/(kgK)	w/m/s
		0.01 MPa							**0.02 MPa**				
170	1590.7	71.636	0.4136	0.7921	1.1838	1119.2	170	1590.7	71.641	0.4136	0.7921	1.1838	1119.2
175	1577.5	77.557	0.4479	0.7909	1.1847	1093.8	175	1577.5	77.562	0.4479	0.7909	1.1847	1093.8
180	1564.2	83.486	0.4813	0.7912	1.1871	1068.3	180	1564.2	83.491	0.4813	0.7912	1.1871	1068.3
185	1550.9	89.430	0.5139	0.7926	1.1906	1042.9	185	1550.9	89.435	0.5139	0.7926	1.1905	1043.0
190	1537.5	95.394	0.5457	0.7949	1.1949	1017.6	190	1537.5	95.398	0.5457	0.7950	1.1949	1017.7
195	1524.0	101.38	0.5768	0.7980	1.2000	992.56	195	1524.0	101.38	0.5768	0.7980	1.2000	992.61
200	1510.4	107.39	0.6073	0.8015	1.2057	967.62	200	1510.4	107.40	0.6073	0.8015	1.2057	967.67
205	1496.8	113.43	0.6371	0.8055	1.2119	942.87	205	1496.8	113.44	0.6371	0.8055	1.2119	942.92
206.29	1493.2	115.00	0.6448	0.8066	1.2136	936.50	210	1483.0	119.52	0.6664	0.8098	1.2186	918.36
206.29	0.60000	356.99	1.8177	0.5879	0.6745	137.67	215	1469.1	125.63	0.6952	0.8144	1.2256	894.00
210	0.58902	359.49	1.8298	0.5937	0.6797	138.86	216.74	1464.3	127.76	0.7050	0.8161	1.2282	885.57
215	0.57487	362.91	1.8459	0.6020	0.6874	140.42	216.74	1.1483	363.58	1.7931	0.6125	0.7019	140.26
220	0.56142	366.37	1.8618	0.6107	0.6956	141.97	220	1.1303	365.87	1.8036	0.6171	0.7058	141.30
225	0.54863	369.87	1.8775	0.6196	0.7041	143.49	225	1.1038	369.42	1.8195	0.6247	0.7125	142.88
230	0.53643	373.41	1.8931	0.6287	0.7128	144.99	230	1.0787	373.00	1.8352	0.6329	0.7199	144.42
235	0.52478	377.00	1.9085	0.6378	0.7217	146.47	235	1.0548	376.62	1.8508	0.6413	0.7278	145.94
240	0.51364	380.63	1.9238	0.6470	0.7307	147.94	240	1.0320	380.28	1.8662	0.6500	0.7360	147.44
245	0.50298	384.31	1.9390	0.6563	0.7397	149.38	245	1.0102	383.98	1.8815	0.6588	0.7444	148.92
250	0.49277	388.03	1.9540	0.6655	0.7488	150.81	250	0.98939	387.72	1.8966	0.6677	0.7529	150.38
255	0.48297	391.79	1.9689	0.6747	0.7579	152.22	255	0.96944	391.51	1.9116	0.6767	0.7615	151.82
260	0.47356	395.61	1.9837	0.6839	0.7669	153.62	260	0.95030	395.34	1.9265	0.6856	0.7702	153.24
265	0.46452	399.46	1.9984	0.6931	0.7760	155.00	265	0.93194	399.21	1.9412	0.6946	0.7789	154.64
270	0.45582	403.37	2.0130	0.7022	0.7850	156.37	270	0.91429	403.13	1.9559	0.7036	0.7877	156.03
275	0.44744	407.31	2.0275	0.7113	0.7940	157.73	275	0.89732	407.09	1.9704	0.7125	0.7964	157.41
280	0.43938	411.31	2.0419	0.7203	0.8029	159.07	280	0.88098	411.09	1.9848	0.7214	0.8052	158.77
285	0.43160	415.34	2.0562	0.7293	0.8118	160.40	285	0.86525	415.14	1.9992	0.7303	0.8139	160.11
290	0.42410	419.43	2.0704	0.7382	0.8207	161.72	290	0.85008	419.23	2.0134	0.7392	0.8226	161.45
295	0.41685	423.55	2.0845	0.7471	0.8295	163.03	295	0.83544	423.37	2.0275	0.7480	0.8313	162.77
300	0.40985	427.72	2.0985	0.7560	0.8383	164.32	300	0.82131	427.55	2.0416	0.7567	0.8399	164.08
305	0.40309	431.93	2.1124	0.7647	0.8470	165.61	305	0.80766	431.77	2.0555	0.7655	0.8486	165.37
310	0.39654	436.19	2.1263	0.7735	0.8557	166.88	310	0.79447	436.03	2.0694	0.7742	0.8572	166.66
315	0.39021	440.49	2.1400	0.7822	0.8644	168.14	315	0.78170	440.34	2.0832	0.7828	0.8657	167.93
320	0.38408	444.84	2.1537	0.7908	0.8730	169.40	320	0.76935	444.69	2.0969	0.7914	0.8742	169.19
325	0.37814	449.22	2.1673	0.7994	0.8816	170.64	325	0.75738	449.08	2.1105	0.8000	0.8827	170.44
330	0.37238	453.65	2.1808	0.8080	0.8901	171.87	330	0.74579	453.52	2.1241	0.8085	0.8912	171.69
335	0.36680	458.12	2.1943	0.8165	0.8986	173.09	335	0.73455	457.99	2.1375	0.8170	0.8996	172.92
340	0.36138	462.64	2.2077	0.8250	0.9070	174.31	340	0.72365	462.51	2.1509	0.8254	0.9080	174.14
345	0.35612	467.19	2.2210	0.8334	0.9154	175.51	345	0.71307	467.07	2.1642	0.8338	0.9163	175.35
350	0.35101	471.79	2.2342	0.8418	0.9238	176.71	350	0.70280	471.68	2.1775	0.8422	0.9246	176.56
355	0.34605	476.43	2.2474	0.8501	0.9321	177.90	355	0.69282	476.32	2.1906	0.8505	0.9329	177.75
360	0.34122	481.11	2.2604	0.8584	0.9404	179.08	360	0.68313	481.01	2.2037	0.8588	0.9411	178.94
365	0.33653	485.84	2.2735	0.8667	0.9486	180.25	365	0.67371	485.73	2.2168	0.8670	0.9493	180.11
370	0.33197	490.60	2.2864	0.8749	0.9568	181.41	370	0.66454	490.50	2.2298	0.8752	0.9575	181.28

TABLE 9. Thermodynamic properties of HFC-134a in the single-phase region — Continued

T/K	ρ/kg/m^3	h/kJ/kg	s/kJ/(kgK)	c_v/kJ/(kgK)	c_p/kJ/(kgK)	w/m/s	T/K	ρ/kg/m^3	h/kJ/kg	s/kJ/(kgK)	c_v/kJ/(kgK)	c_p/kJ/(kgK)	w/m/s
			0.01 MPa							**0.02 MPa**			
375	0.32753	495.40	2.2993	0.8831	0.9649	182.57	375	0.65562	495.31	2.2427	0.8834	0.9656	182.44
380	0.32320	500.25	2.3122	0.8912	0.9731	183.72	380	0.64694	500.16	2.2555	0.8915	0.9737	183.60
385	0.31899	505.13	2.3249	0.8993	0.9811	184.86	385	0.63849	505.04	2.2683	0.8996	0.9817	184.74
390	0.31489	510.06	2.3377	0.9074	0.9892	185.99	390	0.63026	509.97	2.2810	0.9076	0.9898	185.88
395	0.31090	515.03	2.3503	0.9154	0.9972	187.12	395	0.62224	514.94	2.2937	0.9156	0.9977	187.01
400	0.30700	520.03	2.3629	0.9234	1.0052	188.23	400	0.61442	519.95	2.3063	0.9236	1.0057	188.13
410	0.29949	530.17	2.3879	0.9393	1.0210	190.45	410	0.59936	530.09	2.3313	0.9394	1.0215	190.36
420	0.29235	540.45	2.4127	0.9550	1.0367	192.64	420	0.58503	540.38	2.3561	0.9551	1.0371	192.55
430	0.28554	550.90	2.4373	0.9706	1.0523	194.80	430	0.57137	550.83	2.3807	0.9707	1.0527	194.72
440	0.27903	561.50	2.4617	0.9860	1.0677	196.94	440	0.55834	561.44	2.4051	0.9862	1.0681	196.87
450	0.27282	572.26	2.4858	1.0014	1.0831	199.06	450	0.54589	572.19	2.4292	1.0015	1.0834	198.99
460	0.26688	583.16	2.5098	1.0166	1.0982	201.15	460	0.53398	583.10	2.4532	1.0167	1.0985	201.09
			0.03 MPa							**0.04 MPa**			
170	1590.7	71.645	0.4136	0.7921	1.1833	1119.3	170	1590.7	71.650	0.4136	0.7921	1.1837	1119.3
175	1577.5	77.566	0.4479	0.7909	1.1847	1093.8	175	1577.5	77.571	0.4479	0.7909	1.1847	1093.9
180	1564.2	83.495	0.4813	0.7912	1.1871	1068.4	180	1564.2	83.500	0.4813	0.7912	1.1870	1068.4
185	1550.9	89.439	0.5139	0.7926	1.1905	1043.0	185	1550.9	89.443	0.5139	0.7926	1.1905	1043.0
190	1537.5	95.402	0.5457	0.7950	1.1949	1017.7	190	1537.5	95.407	0.5457	0.7950	1.1949	1017.8
195	1524.0	101.39	0.5768	0.7980	1.2000	992.65	195	1524.0	101.39	0.5768	0.7980	1.2000	992.69
200	1510.5	107.40	0.6073	0.8015	1.2057	967.71	200	1510.5	107.40	0.6072	0.8015	1.2057	967.76
205	1496.8	113.44	0.6371	0.8055	1.2119	942.96	205	1496.8	113.45	0.6371	0.8055	1.2119	943.01
210	1483.0	119.52	0.6664	0.8098	1.2185	918.41	210	1483.1	119.52	0.6664	0.8098	1.2185	918.46
215	1469.2	125.63	0.6951	0.8144	1.2255	894.05	215	1469.2	125.63	0.6951	0.8144	1.2256	894.10
220	1455.2	131.78	0.7234	0.8193	1.2331	869.88	220	1455.2	131.78	0.7234	0.8193	1.2331	869.93
223.46	1445.4	136.06	0.7427	0.8227	1.2385	853.21	225	1441.0	137.97	0.7512	0.8243	1.2410	845.93
223.46	1.6784	367.85	1.7800	0.6287	0.7205	141.75	228.55	1430.9	142.39	0.7707	0.8279	1.2468	828.96
225	1.6660	368.95	1.7849	0.6306	0.7220	142.25	228.55	2.1972	371.08	1.7713	0.6411	0.7352	142.78
230	1.6272	372.58	1.8008	0.6375	0.7277	143.84	230	2.1821	372.14	1.7759	0.6428	0.7364	143.25
235	1.5903	376.23	1.8165	0.6451	0.7343	145.40	235	2.1315	375.84	1.7918	0.6493	0.7413	144.86
240	1.5552	379.92	1.8321	0.6532	0.7415	146.94	240	2.0835	379.56	1.8075	0.6565	0.7474	146.43
245	1.5218	383.65	1.8474	0.6615	0.7492	148.45	245	2.0380	383.31	1.8230	0.6643	0.7542	147.98
250	1.4899	387.41	1.8627	0.6700	0.7571	149.94	250	1.9946	387.10	1.8383	0.6724	0.7615	149.50
255	1.4594	391.22	1.8777	0.6787	0.7653	151.40	255	1.9532	390.93	1.8534	0.6807	0.7691	150.99
260	1.4303	395.07	1.8927	0.6874	0.7736	152.85	260	1.9136	394.80	1.8684	0.6892	0.7770	152.46
265	1.4023	398.96	1.9075	0.6962	0.7820	154.28	265	1.8757	398.70	1.8833	0.6977	0.7851	153.91
270	1.3754	402.89	1.9222	0.7050	0.7904	155.69	270	1.8393	402.65	1.8981	0.7064	0.7932	155.34
275	1.3496	406.86	1.9368	0.7138	0.7989	157.08	275	1.8045	406.63	1.9127	0.7150	0.8015	156.76
280	1.3248	410.88	1.9512	0.7226	0.8075	158.46	280	1.7710	410.66	1.9272	0.7237	0.8098	158.15
285	1.3009	414.94	1.9656	0.7313	0.8160	159.82	285	1.7388	414.73	1.9416	0.7324	0.8181	159.53

TABLE 9. Thermodynamic properties of HFC-134a in the single-phase region — Continued

T/K	ρ/kg/m^3	h/kJ/kg	s/kJ/(kgK)	c_v/kJ/(kgK)	c_p/kJ/(kgK)	w/m/s
			0.03 MPa			
290	1.2779	419.04	1.9799	0.7401	0.8245	161.17
295	1.2558	423.18	1.9940	0.7488	0.8331	162.51
300	1.2344	427.37	2.0081	0.7575	0.8416	163.83
305	1.2137	431.60	2.0221	0.7662	0.8501	165.14
310	1.1937	435.87	2.0360	0.7748	0.8586	166.43
315	1.1744	440.19	2.0498	0.7834	0.8671	167.72
320	1.1558	444.54	2.0635	0.7920	0.8755	168.99
325	1.1377	448.94	2.0772	0.8005	0.8839	170.25
330	1.1202	453.38	2.0907	0.8090	0.8923	171.50
335	1.1032	457.86	2.1042	0.8175	0.9006	172.74
340	1.0868	462.39	2.1176	0.8259	0.9090	173.97
345	1.0708	466.95	2.1309	0.8342	0.9172	175.19
350	1.0553	471.56	2.1442	0.8426	0.9255	176.40
355	1.0403	476.21	2.1574	0.8509	0.9337	177.60
360	1.0257	480.90	2.1705	0.8591	0.9419	178.79
365	1.0115	485.63	2.1835	0.8673	0.9500	179.98
370	0.99772	490.40	2.1965	0.8755	0.9582	181.15
375	0.98429	495.21	2.2094	0.8836	0.9663	182.32
380	0.97122	500.06	2.2223	0.8917	0.9743	183.48
385	0.95850	504.95	2.2351	0.8998	0.9823	184.62
390	0.94610	509.89	2.2478	0.9078	0.9903	185.77
395	0.93403	514.86	2.2605	0.9158	0.9983	186.90
400	0.92227	519.87	2.2731	0.9238	1.0062	188.03
410	0.89961	530.01	2.2981	0.9396	1.0219	190.26
420	0.87805	540.31	2.3229	0.9553	1.0376	192.46
430	0.85751	550.76	2.3475	0.9709	1.0531	194.64
440	0.83791	561.37	2.3719	0.9863	1.0684	196.79
450	0.81919	572.13	2.3961	1.0016	1.0837	198.92
460	0.80130	583.05	2.4201	1.0168	1.0988	201.02
			0.06 MPa			
170	1590.7	71.659	0.4136	0.7921	1.1837	1119.4
175	1577.5	77.580	0.4479	0.7909	1.1847	1094.0
180	1564.3	83.509	0.4813	0.7912	1.1870	1068.5
185	1550.9	89.452	0.5139	0.7926	1.1905	1043.1
190	1537.5	95.416	0.5457	0.7950	1.1949	1017.8
195	1524.1	101.40	0.5768	0.7980	1.2000	992.78
200	1510.5	107.41	0.6072	0.8015	1.2056	967.85
205	1496.8	113.46	0.6371	0.8055	1.2118	943.10
210	1483.1	119.53	0.6663	0.8098	1.2185	918.56
215	1469.2	125.54	0.6951	0.8144	1.2256	894.21
220	1455.2	131.79	0.7234	0.8193	1.2331	870.04

T/K	ρ/kg/m^3	h/kJ/kg	s/kJ/(kgK)	c_v/kJ/(kgK)	c_p/kJ/(kgK)	w/m/s
			0.04 MPa			
290	1.7078	418.84	1.9559	0.7411	0.8265	160.90
295	1.6779	423.00	1.9701	0.7497	0.8349	162.24
300	1.6491	427.19	1.9842	0.7583	0.8433	163.58
305	1.6213	431.43	1.9982	0.7669	0.8517	164.90
310	1.5945	435.71	2.0122	0.7755	0.8601	166.21
315	1.5685	440.03	2.0260	0.7841	0.8684	167.50
320	1.5434	444.40	2.0397	0.7926	0.8768	168.78
325	1.5192	448.80	2.0534	0.8011	0.8851	170.05
330	1.4957	453.25	2.0670	0.8095	0.8934	171.31
335	1.4729	457.73	2.0805	0.8179	0.9017	172.56
340	1.4509	462.26	2.0939	0.8263	0.9099	173.80
345	1.4295	466.83	2.1072	0.8346	0.9182	175.03
350	1.4087	471.45	2.1205	0.8429	0.9264	176.24
355	1.3886	476.10	2.1337	0.8512	0.9345	177.45
360	1.3690	480.79	2.1468	0.8594	0.9427	178.65
365	1.3500	485.53	2.1599	0.8676	0.9508	179.84
370	1.3315	490.30	2.1729	0.8758	0.9589	181.02
375	1.3135	495.11	2.1858	0.8839	0.9669	182.19
380	1.2960	499.97	2.1987	0.8920	0.9749	183.35
385	1.2790	504.86	2.2115	0.9001	0.9829	184.51
390	1.2624	509.80	2.2242	0.9081	0.9909	185.66
395	1.2462	514.77	2.2369	0.9161	0.9988	186.79
400	1.2305	519.79	2.2495	0.9240	1.0067	187.93
410	1.2002	529.93	2.2745	0.9398	1.0224	190.17
420	1.1714	540.24	2.2994	0.9555	1.0380	192.38
430	1.1439	550.69	2.3240	0.9710	1.0535	194.56
440	1.1177	561.31	2.3484	0.9864	1.0688	196.72
450	1.0927	572.07	2.3726	1.0017	1.0840	198.85
460	1.0688	582.99	2.3966	1.0169	1.0991	200.96
			0.08 MPa			
170	1590.8	71.668	0.4135	0.7921	1.1837	1119.4
175	1577.5	77.589	0.4479	0.7909	1.1847	1094.0
180	1564.3	83.517	0.4813	0.7912	1.1870	1068.6
185	1551.0	89.461	0.5138	0.7926	1.1905	1043.2
190	1537.6	95.424	0.5456	0.7950	1.1948	1017.9
195	1524.1	101.41	0.5767	0.7980	1.1999	992.87
200	1510.5	107.42	0.6072	0.8015	1.2056	967.94
205	1496.9	113.46	0.6370	0.8055	1.2118	943.20
210	1483.1	119.54	0.6663	0.8098	1.2185	918.66
215	1469.3	125.65	0.6951	0.8144	1.2256	894.31
220	1455.3	131.80	0.7233	0.8193	1.2330	870.14

TABLE 9. Thermodynamic properties of HFC-134a in the single-phase region — Continued

T / K	ρ / kg/m³	h / kJ/kg	s / kJ/(kgK)	c_v / kJ/(kgK)	c_p / kJ/(kgK)	w / m/s
			0.06 MPa			
225	1441.1	137.97	0.7512	0.8243	1.2409	846.04
230	1426.8	144.20	0.7785	0.8295	1.2492	822.20
235	1412.3	150.47	0.8055	0.8348	1.2578	798.50
236.21	1408.8	152.00	0.8120	0.8361	1.2600	792.75
236.21	3.2130	375.94	1.7600	0.6603	0.7584	144.14
240	3.1560	378.81	1.7721	0.6642	0.7608	145.39
245	3.0844	382.63	1.7878	0.6705	0.7653	147.01
250	3.0165	386.47	1.8033	0.6775	0.7709	148.60
255	2.9519	390.34	1.8187	0.6851	0.7773	150.15
260	2.8904	394.24	1.8338	0.6929	0.7842	151.67
265	2.8317	398.18	1.8488	0.7010	0.7915	153.17
270	2.7756	402.16	1.8637	0.7093	0.7990	154.65
275	2.7219	406.17	1.8784	0.7176	0.8067	156.10
280	2.6703	410.23	1.8930	0.7260	0.8145	157.53
285	2.6209	414.32	1.9075	0.7345	0.8225	158.94
290	2.5733	418.45	1.9219	0.7430	0.8305	160.34
295	2.5276	422.63	1.9362	0.7515	0.8386	161.72
300	2.4836	426.84	1.9503	0.7599	0.8467	163.08
305	2.4411	431.09	1.9644	0.7684	0.8548	164.42
310	2.4002	435.39	1.9784	0.7769	0.8630	165.75
315	2.3607	439.72	1.9922	0.7853	0.8712	167.07
320	2.3225	444.10	2.0060	0.7938	0.8793	168.37
325	2.2856	448.52	2.0197	0.8022	0.8875	169.66
330	2.2498	452.98	2.0333	0.8105	0.8956	170.94
335	2.2153	457.47	2.0469	0.8189	0.9038	172.20
340	2.1818	462.01	2.0603	0.8272	0.9119	173.46
345	2.1493	466.59	2.0737	0.8355	0.9200	174.70
350	2.1179	471.21	2.0870	0.8437	0.9281	175.93
355	2.0873	475.88	2.1002	0.8519	0.9362	177.15
360	2.0577	480.58	2.1134	0.8601	0.9442	178.36
365	2.0289	485.32	2.1264	0.8683	0.9523	179.57
370	2.0009	490.10	2.1394	0.8764	0.9603	180.76
375	1.9737	494.92	2.1524	0.8845	0.9682	181.94
380	1.9472	499.78	2.1653	0.8925	0.9762	183.11
385	1.9215	504.68	2.1781	0.9006	0.9841	184.28
390	1.8965	509.62	2.1908	0.9085	0.9920	185.43
395	1.8721	514.60	2.2035	0.9165	0.9999	186.58
400	1.8483	519.62	2.2161	0.9244	1.0077	187.72
410	1.8026	529.78	2.2412	0.9402	1.0233	189.97
420	1.7591	540.09	2.2661	0.9558	1.0388	192.20
430	1.7177	550.56	2.2907	0.9713	1.0542	194.40
440	1.6782	561.18	2.3151	0.9867	1.0695	196.57
450	1.6405	571.95	2.3393	1.0020	1.0847	198.71
460	1.6045	582.87	2.3633	1.0171	1.0997	200.83
			0.08 MPa			
225	1441.1	137.98	0.7511	0.8243	1.2409	846.15
230	1426.8	144.21	0.7785	0.8295	1.2491	822.31
235	1412.3	150.47	0.8055	0.8348	1.2578	798.62
240	1397.7	156.79	0.8320	0.8402	1.2669	775.04
242.03	1391.7	159.37	0.8427	0.8425	1.2707	765.47
242.03	4.2096	379.61	1.7527	0.6752	0.7771	145.02
245	4.1507	381.92	1.7622	0.6778	0.7782	146.02
250	4.0560	385.82	1.7779	0.6833	0.7815	147.68
255	3.9564	389.74	1.7935	0.6898	0.7863	149.29
260	3.8814	393.68	1.8088	0.6969	0.7919	150.87
265	3.8006	397.66	1.8239	0.7045	0.7983	152.42
270	3.7234	401.67	1.8389	0.7123	0.8050	153.94
275	3.6498	405.71	1.8537	0.7203	0.8121	155.43
280	3.5793	409.79	1.8684	0.7284	0.8195	156.90
285	3.5117	413.90	1.8830	0.7366	0.8270	158.35
290	3.4469	418.06	1.8975	0.7449	0.8346	159.78
295	3.3847	422.25	1.9118	0.7532	0.8424	161.18
300	3.3248	426.48	1.9260	0.7616	0.8502	162.57
305	3.2672	430.75	1.9401	0.7699	0.8581	163.94
310	3.2117	435.06	1.9542	0.7783	0.8660	165.30
315	3.1581	439.41	1.9681	0.7866	0.8739	166.64
320	3.1065	443.80	1.9819	0.7949	0.8819	167.96
325	3.0565	448.23	1.9956	0.8033	0.8899	169.27
330	3.0083	452.70	2.0093	0.8115	0.8979	170.56
335	2.9616	457.21	2.0229	0.8198	0.9059	171.85
340	2.9164	461.76	2.0363	0.8281	0.9139	173.12
345	2.8726	466.35	2.0497	0.8363	0.9219	174.37
350	302	470.98	2.0631	0.8445	0.9299	175.62
355	2.7891	475.65	2.0763	0.8527	0.9379	176.85
360	2.7492	480.36	2.0895	0.8608	0.9458	178.08
365	2.7104	485.11	2.1026	0.8689	0.9537	179.29
370	2.6728	489.90	2.1156	0.8770	0.9617	180.49
375	2.6362	494.73	2.1286	0.8850	0.9696	181.69
380	2.6007	499.59	2.1415	0.8931	0.9774	182.87
385	2.5661	504.50	2.1543	0.9011	0.9853	184.04
390	2.5325	509.45	2.1671	0.9090	0.9931	185.21
395	2.4997	514.43	2.1798	0.9169	1.0010	186.36
400	2.4678	519.46	2.1924	0.9248	1.0088	187.51
410	2.4065	529.62	2.2175	0.9406	1.0243	189.78
420	2.3482	539.94	2.2424	0.9561	1.0397	192.02
430	2.2927	550.42	2.2670	0.9716	1.0550	194.23
440	2.2398	561.04	2.2914	0.9870	1.0702	196.41
450	2.1893	571.82	2.3157	1.0022	1.0853	198.57
460	2.1411	582.75	2.3397	1.0173	1.1004	200.69

TABLE 9. Thermodynamic properties of HFC-134a in the single-phase region — Continued

T/K	ρ kg/m³	h kJ/kg	s kJ/(kgK)	c_v kJ/(kgK)	c_p kJ/(kgK)	w m/s	T/K	ρ kg/m³	h kJ/kg	s kJ/(kgK)	c_v kJ/(kgK)	c_p kJ/(kgK)	w m/s
			0.10 MPa							**0.12 MPa**			
170	1590.8	71.677	0.4135	0.7921	1.1837	1119.5	170	1590.8	71.686	0.4135	0.7921	1.1837	1119.6
175	1577.6	77.597	0.4478	0.7909	1.1846	1094.1	175	1577.6	77.606	0.4478	0.7909	1.1846	1094.2
180	1564.3	83.526	0.4812	0.7912	1.1870	1068.7	180	1564.3	83.535	0.4812	0.7912	1.1870	1068.7
185	1551.0	89.470	0.5138	0.7927	1.1905	1043.3	185	1551.0	89.479	0.5138	0.7927	1.1904	1043.4
190	1537.6	95.433	0.5456	0.7950	1.1948	1018.0	190	1537.6	95.442	0.5456	0.7950	1.1948	1018.1
195	1524.1	101.42	0.5767	0.7980	1.1999	992.95	195	1524.2	101.42	0.5767	0.7980	1.1999	993.04
200	1510.6	107.43	0.6072	0.8015	1.2056	968.03	200	1510.6	107.44	0.6071	0.8015	1.2056	968.12
205	1496.9	113.47	0.6370	0.8055	1.2118	943.29	205	1497.0	113.48	0.6370	0.8055	1.2118	943.39
210	1483.2	119.55	0.6663	0.8098	1.2184	918.75	210	1483.2	119.56	0.6663	0.8099	1.2184	918.85
215	1469.3	125.66	0.6950	0.8144	1.2255	894.41	215	1469.3	125.67	0.6950	0.8145	1.2255	894.51
220	1455.3	131.80	0.7233	0.8193	1.2330	870.25	220	1455.3	131.81	0.7233	0.8193	1.2329	870.35
225	1441.2	137.99	0.7511	0.8243	1.2408	846.26	225	1441.2	138.00	0.7511	0.8243	1.2408	846.37
230	1426.9	144.21	0.7785	0.8295	1.2491	822.43	230	1426.9	144.22	0.7784	0.8295	1.2490	822.54
235	1412.4	150.48	0.8054	0.8348	1.2577	798.74	235	1412.4	150.49	0.8054	0.8348	1.2577	798.85
240	1397.7	156.79	0.8320	0.8402	1.2668	775.16	240	1397.8	156.80	0.8320	0.8402	1.2668	775.29
245	1382.9	163.15	0.8582	0.8458	1.2764	751.68	245	1382.9	163.16	0.8582	0.8458	1.2763	751.81
246.78	1377.5	165.44	0.8675	0.8478	1.2799	743.30	250	1367.8	169.56	0.8841	0.8514	1.2864	728.41
246.78	5.1932	382.59	1.7474	0.6876	0.7931	145.63	250.84	1365.3	170.65	0.8884	0.8524	1.2882	724.48
250	5.1144	385.14	1.7577	0.6901	0.7936	146.73	250.84	6.1676	385.12	1.7434	0.6984	0.8074	146.06
255	4.9976	389.12	1.7734	0.6952	0.7962	148.42	255	6.0465	388.48	1.7567	0.7012	0.8074	147.52
260	4.8873	393.11	1.7889	0.7013	0.8003	150.05	260	5.9088	392.52	1.7724	0.7062	0.8095	149.22
265	4.7827	397.12	1.8042	0.7082	0.8055	151.66	265	5.7788	396.57	1.7878	0.7122	0.8133	150.88
270	4.6833	401.16	1.8193	0.7155	0.8114	153.22	270	5.6557	400.65	1.8031	0.7188	0.8181	152.49
275	4.5886	405.24	1.8343	0.7231	0.8178	154.76	275	5.5387	404.76	1.8181	0.7260	0.8237	154.07
280	4.4981	409.34	1.8491	0.7309	0.8246	156.27	280	5.4272	408.89	1.8330	0.7334	0.8299	155.62
285	4.4116	413.48	1.8637	0.7389	0.8316	157.75	285	5.3209	413.06	1.8478	0.7411	0.8364	157.14
290	4.3288	417.66	1.8783	0.7469	0.8388	159.21	290	5.2192	417.26	1.8624	0.7490	0.8432	158.64
295	4.2494	421.87	1.8927	0.7550	0.8462	160.65	295	5.1218	421.49	1.8769	0.7569	0.8502	160.10
300	4.1731	426.12	1.9070	0.7632	0.8537	162.06	300	5.0284	425.76	1.8912	0.7649	0.8574	161.55
305	4.0997	430.41	1.9211	0.7714	0.8614	163.46	305	4.9387	430.06	1.9055	0.7730	0.8647	162.97
310	4.0291	434.74	1.9352	0.7797	0.8690	164.84	310	4.8525	434.41	1.9196	0.7811	0.8721	164.37
315	3.9611	439.10	1.9492	0.7879	0.8768	166.20	315	4.7696	438.79	1.9336	0.7892	0.8797	165.76
320	3.8955	443.50	1.9630	0.7961	0.8846	167.54	320	4.6897	443.20	1.9475	0.7973	0.8872	167.12
325	3.8322	447.95	1.9768	0.8044	0.8924	168.87	325	4.6126	447.66	1.9613	0.8055	0.8949	168.47
330	3.7711	452.43	1.9905	0.8126	0.9002	170.19	330	4.5382	452.15	1.9750	0.8136	0.9025	169.81
335	3.7120	456.95	2.0041	0.8208	0.9081	171.49	335	4.4664	456.69	1.9887	0.8217	0.9103	171.12
340	3.6548	461.51	2.0176	0.8290	0.9159	172.77	340	4.3970	461.26	2.0022	0.8298	0.9180	172.43
345	3.5995	466.11	2.0310	0.8371	0.9238	174.04	345	4.3298	465.87	2.0157	0.8379	0.9257	173.71
350	3.5459	470.75	2.0444	0.8453	0.9317	175.30	350	4.2648	470.51	2.0290	0.8460	0.9335	174.99
355	3.4939	475.43	2.0577	0.8534	0.9395	176.55	355	4.2018	475.20	2.0423	0.8541	0.9412	176.25
360	3.4435	480.14	2.0709	0.8615	0.9474	177.79	360	4.1408	479.93	2.0556	0.8622	0.9490	177.50
365	3.3947	484.90	2.0840	0.8695	0.9552	179.01	365	4.0816	484.69	2.0687	0.8702	0.9568	178.74
370	3.3472	489.70	2.0970	0.8776	0.9631	180.23	370	4.0242	489.49	2.0818	0.8782	0.9645	179.96

TABLE 9. Thermodynamic properties of HFC-134a in the single-phase region — Continued

T/K	ρ/kg/m³	h/kJ/kg	s/kJ/(kgK)	c_v/kJ/(kgK)	c_p/kJ/(kgK)	w/m/s	T/K	ρ/kg/m³	h/kJ/kg	s/kJ/(kgK)	c_v/kJ/(kgK)	c_p/kJ/(kgK)	w/m/s
			0.10 MPa							**0.12 MPa**			
375	3.3011	494.53	2.1100	0.8856	0.9709	181.43	375	3.9684	494.34	2.0948	0.8862	0.9723	181.18
380	3.2563	499.41	2.1229	0.8936	0.9787	182.63	380	3.9142	499.22	2.1077	0.8941	0.9800	182.38
385	3.2128	504.32	2.1358	0.9016	0.9865	183.81	385	3.8615	504.14	2.1206	0.9021	0.9877	183.58
390	3.1704	509.27	2.1486	0.9095	0.9943	184.98	390	3.8103	509.10	2.1334	0.9100	0.9954	184.76
395	3.1292	514.26	2.1613	0.9174	1.0021	186.15	395	3.7605	514.09	2.1461	0.9178	1.0031	185.93
400	3.0891	519.29	2.1739	0.9253	1.0098	187.31	400	3.7121	519.13	2.1588	0.9257	1.0108	187.10
410	3.0119	529.47	2.1990	0.9409	1.0252	189.59	410	3.6189	529.31	2.1839	0.9413	1.0262	189.40
420	2.9386	539.80	2.2239	0.9565	1.0405	191.85	420	3.5304	539.65	2.2088	0.9568	1.0414	191.67
430	2.8689	550.28	2.2486	0.9719	1.0558	194.07	430	3.4463	550.14	2.2335	0.9722	1.0566	193.91
440	2.8024	560.91	2.2730	0.9872	1.0709	196.26	440	3.3662	560.78	2.2580	0.9875	1.0717	196.11
450	2.7391	571.70	2.2973	1.0025	1.0860	198.43	450	3.2898	571.58	2.2822	1.0027	1.0867	198.29
460	2.6786	582.53	2.3213	1.0176	1.1010	200.56	460	3.2169	582.52	2.3063	1.0178	1.1016	200.43
			0.14 MPa							**0.16 MPa**			
170	1590.8	71.595	0.4135	0.7921	1.1837	1119.7	170	1590.9	71.704	0.4135	0.7921	1.1837	1119.7
175	1577.6	77.515	0.4478	0.7909	1.1846	1094.3	175	1577.6	77.624	0.4478	0.7910	1.1846	1094.3
180	1564.4	83.544	0.4812	0.7912	1.1870	1068.8	180	1564.4	83.553	0.4812	0.7912	1.1869	1068.9
185	1551.0	89.487	0.5138	0.7927	1.1904	1043.4	185	1551.1	89.496	0.5137	0.7927	1.1904	1043.5
190	1537.7	95.450	0.5456	0.7950	1.1948	1018.2	190	1537.7	95.459	0.5455	0.7950	1.1948	1018.3
195	1524.2	101.43	0.5767	0.7980	1.1999	993.13	195	1524.2	101.44	0.5766	0.7980	1.1998	993.22
200	1510.6	107.45	0.6071	0.8015	1.2055	968.21	200	1510.7	107.45	0.6071	0.8016	1.2055	968.30
205	1497.0	113.49	0.6370	0.8055	1.2117	943.48	205	1497.0	113.50	0.6369	0.8055	1.2117	943.57
210	1483.2	119.56	0.6662	0.8099	1.2184	918.95	210	1483.3	119.57	0.6662	0.8099	1.2184	919.05
215	1469.4	125.57	0.6950	0.8145	1.2255	894.61	215	1469.4	125.68	0.6950	0.8145	1.2254	894.71
220	1455.4	131.82	0.7233	0.8193	1.2329	870.46	220	1455.4	131.83	0.7232	0.8193	1.2329	870.56
225	1441.2	138.00	0.7510	0.8243	1.2408	846.48	225	1441.3	138.01	0.7510	0.8243	1.2407	846.59
230	1426.9	144.23	0.7784	0.8295	1.2490	822.66	230	1427.0	144.24	0.7784	0.8295	1.2490	822.77
235	1412.5	150.50	0.8054	0.8348	1.2576	798.97	235	1412.5	150.50	0.8053	0.8348	1.2576	799.09
240	1397.8	156.81	0.8319	0.8402	1.2667	775.41	240	1397.9	156.81	0.8319	0.8402	1.2667	775.53
245	1383.0	163.16	0.8582	0.8458	1.2763	751.94	245	1383.0	163.17	0.8581	0.8458	1.2762	752.07
250	1367.9	169.57	0.8840	0.8514	1.2863	728.55	250	1367.9	169.58	0.8840	0.8514	1.2863	728.68
254.39	1354.4	175.24	0.9065	0.8565	1.2957	708.04	255	1352.6	176.03	0.9096	0.8572	1.2969	705.34
254.39	7.1353	387.31	1.7402	0.7080	0.8203	146.38	257.56	1344.6	179.37	0.9226	0.8602	1.3026	693.39
255	7.1141	387.81	1.7421	0.7082	0.8201	146.60	257.56	8.0978	389.26	1.7375	0.7166	0.8323	146.61
260	6.9468	391.91	1.7581	0.7116	0.8197	148.37	260	8.0022	391.29	1.7454	0.7176	0.8311	147.50
265	6.7895	396.02	1.7737	0.7165	0.8217	150.08	265	7.8156	395.45	1.7612	0.7212	0.8310	149.28
270	6.6411	400.13	1.7891	0.7224	0.8253	151.75	270	7.6401	399.60	1.7767	0.7263	0.8331	151.00
275	6.5005	404.27	1.8043	0.7290	0.8300	153.38	275	7.4744	403.78	1.7920	0.7323	0.8366	152.68
280	6.3669	408.44	1.8193	0.7361	0.8354	154.97	280	7.3175	407.97	1.8072	0.7389	0.8412	154.31
285	6.2396	412.63	1.8341	0.7435	0.8413	156.53	285	7.1683	412.19	1.8221	0.7459	0.8465	155.91
290	6.1182	416.85	1.8488	0.7510	0.8476	158.06	290	7.0263	416.44	1.8369	0.7532	0.8523	157.47
295	6.0021	421.10	1.8633	0.7588	0.8543	159.56	295	6.8907	420.72	1.8515	0.7607	0.8584	159.00

TABLE 9. Thermodynamic properties of HFC-134a in the single-phase region — Continued

T/K	ρ/kg/m³	h/kJ/kg	s/kJ/(kgK)	c_v/kJ/(kgK)	c_p/kJ/(kgK)	w/m/s
			0.14 MPa			
300	5.8910	425.39	1.8778	0.7666	0.8611	161.03
305	5.7844	429.72	1.8921	0.7745	0.8681	162.48
310	5.6821	434.08	1.9062	0.7825	0.8753	163.91
315	5.5837	438.47	1.9203	0.7905	0.8826	165.32
320	5.4890	442.90	1.9343	0.7985	0.8900	166.70
325	5.3978	447.37	1.9481	0.8066	0.8974	168.07
330	5.3099	451.88	1.9619	0.8146	0.9049	169.42
335	5.2250	456.42	1.9755	0.8227	0.9125	170.76
340	5.1430	461.00	1.9891	0.8307	0.9200	172.08
345	5.0638	465.62	2.0026	0.8388	0.9277	173.38
350	4.9871	470.28	2.0160	0.8468	0.9353	174.67
355	4.9129	474.97	2.0293	0.8548	0.9430	175.95
360	4.8410	479.71	2.0426	0.8628	0.9506	177.21
365	4.7712	484.48	2.0557	0.8708	0.9583	178.46
370	4.7036	489.29	2.0688	0.8788	0.9660	179.70
375	4.6380	494.14	2.0818	0.8867	0.9736	180.92
380	4.5743	499.03	2.0948	0.8947	0.9813	182.14
385	4.5124	503.95	2.1077	0.9026	0.9890	183.34
390	4.4522	508.92	2.1205	0.9104	0.9966	184.53
395	4.3937	513.92	2.1332	0.9183	1.0043	185.72
400	4.3368	518.96	2.1459	0.9261	1.0119	186.89
410	4.2274	529.16	2.1711	0.9417	1.0271	189.21
420	4.1236	539.50	2.1960	0.9572	1.0423	191.49
430	4.0250	550.00	2.2207	0.9725	1.0574	193.74
440	3.9310	560.65	2.2452	0.9878	1.0724	195.96
450	3.8416	571.45	2.2695	1.0030	1.0873	198.15
460	3.7561	582.40	2.2935	1.0180	1.1022	200.30
			0.18 MPa			
170	1590.9	71.713	0.4134	0.7922	1.1836	1119.8
175	1577.7	77.633	0.4478	0.7910	1.1846	1094.4
180	1564.4	83.562	0.4812	0.7912	1.1869	1069.0
185	1551.1	89.505	0.5137	0.7927	1.1904	1043.6
190	1537.7	95.468	0.5455	0.7950	1.1947	1018.4
195	1524.2	101.45	0.5766	0.7980	1.1998	993.30
200	1510.7	107.46	0.6071	0.8016	1.2055	968.39
205	1497.1	113.51	0.6369	0.8055	1.2117	943.67
210	1483.3	119.58	0.6662	0.8099	1.2183	919.14
215	1469.4	125.69	0.6949	0.8145	1.2254	894.81
220	1455.5	131.84	0.7232	0.8193	1.2328	870.67
225	1441.3	138.02	0.7510	0.8243	1.2407	846.70
230	1427.0	144.24	0.7784	0.8295	1.2489	822.88

T/K	ρ/kg/m³	h/kJ/kg	s/kJ/(kgK)	c_v/kJ/(kgK)	c_p/kJ/(kgK)	w/m/s
			0.16 MPa			
300	6.7611	425.02	1.8660	0.7683	0.8649	160.51
305	6.6369	429.37	1.8803	0.7761	0.8716	161.99
310	6.5179	433.74	1.8946	0.7839	0.8785	163.44
315	6.4036	438.15	1.9087	0.7918	0.8856	164.87
320	6.2937	442.60	1.9227	0.7998	0.8927	166.28
325	6.1880	447.08	1.9366	0.8077	0.9000	167.67
330	6.0861	451.60	1.9504	0.8157	0.9073	169.04
335	5.9878	456.15	1.9641	0.8237	0.9147	170.39
340	5.8930	460.75	1.9777	0.8316	0.9221	171.73
345	5.8014	465.38	1.9912	0.8396	0.9296	173.05
350	5.7128	470.04	2.0046	0.8476	0.9371	174.35
355	5.6270	474.75	2.0180	0.8556	0.9447	175.64
360	5.5441	479.49	2.0312	0.8635	0.9522	176.92
365	5.4636	484.27	2.0444	0.8715	0.9598	178.18
370	5.3857	489.09	2.0575	0.8794	0.9674	179.43
375	5.3101	493.94	2.0706	0.8873	0.9750	180.67
380	5.2367	498.84	2.0835	0.8952	0.9826	181.89
385	5.1654	503.77	2.0964	0.9031	0.9902	183.11
390	5.0961	508.74	2.1093	0.9109	0.9978	184.31
395	5.0288	513.75	2.1220	0.9187	1.0054	185.50
400	4.9633	518.80	2.1347	0.9265	1.0129	186.68
410	4.8375	529.00	2.1599	0.9421	1.0281	189.02
420	4.7182	539.36	2.1849	0.9575	1.0431	191.32
430	4.6048	549.86	2.2096	0.9728	1.0582	193.58
440	4.4970	560.52	2.2341	0.9881	1.0731	195.81
450	4.3943	571.33	2.2584	1.0032	1.0880	198.01
460	4.2963	582.28	2.2824	1.0182	1.1028	200.17
			0.20 MPa			
170	1590.9	71.722	0.4134	0.7922	1.1836	1119.9
175	1577.7	77.642	0.4477	0.7910	1.1846	1094.5
180	1564.4	83.571	0.4811	0.7913	1.1869	1069.1
185	1551.1	89.514	0.5137	0.7927	1.1904	1043.7
190	1537.7	95.476	0.5455	0.7950	1.1947	1018.4
195	1524.3	101.46	0.5766	0.7980	1.1998	993.39
200	1510.7	107.47	0.6070	0.8016	1.2055	968.48
205	1497.1	113.51	0.6369	0.8055	1.2117	943.76
210	1483.3	119.59	0.6662	0.8099	1.2183	919.24
215	1469.5	125.70	0.6949	0.8145	1.2254	894.91
220	1455.5	131.84	0.7232	0.8193	1.2328	870.77
225	1441.4	138.03	0.7510	0.8243	1.2406	846.81
230	1427.1	144.25	0.7783	0.8295	1.2489	823.00

TABLE 9. Thermodynamic properties of HFC-134a in the single-phase region — Continued

T/K	ρ kg/m³	h kJ/kg	s kJ/(kgK)	c_v kJ/(kgK)	c_p kJ/(kgK)	w m/s	T/K	ρ kg/m³	h kJ/kg	s kJ/(kgK)	c_v kJ/(kgK)	c_p kJ/(kgK)	w m/s
			0.18 MPa							**0.20 MPa**			
235	1412.6	150.51	0.8053	0.8348	1.2576	799.21	235	1412.6	150.52	0.8053	0.8348	1.2575	799.33
240	1397.9	156.82	0.8319	0.8402	1.2666	775.66	240	1398.0	156.83	0.8318	0.8402	1.2666	775.78
245	1383.1	163.18	0.8581	0.8458	1.2762	752.20	245	1383.1	163.18	0.8581	0.8458	1.2761	752.33
250	1368.0	169.58	0.8840	0.8514	1.2862	728.82	250	1368.0	169.59	0.8839	0.8514	1.2861	728.95
255	1352.6	176.04	0.9096	0.8572	1.2968	705.48	255	1352.7	176.05	0.9095	0.8572	1.2968	705.62
260	1337.0	182.55	0.9348	0.8631	1.3081	682.16	260	1337.1	182.56	0.9348	0.8631	1.3080	682.31
260.43	1335.6	183.13	0.9370	0.8636	1.3091	680.12	263.07	1327.3	186.59	0.9502	0.8667	1.3153	667.98
260.43	9.0565	391.02	1.7353	0.7246	0.8435	146.77	263.07	10.012	392.61	1.7334	0.7320	0.8540	146.88
265	8.8578	394.86	1.7499	0.7265	0.8411	148.45	265	9.9171	394.26	1.7396	0.7323	0.8523	147.61
270	8.6534	399.06	1.7656	0.7305	0.8414	150.23	270	9.6815	398.51	1.7555	0.7350	0.8504	149.45
275	8.4611	403.28	1.7811	0.7357	0.8437	151.96	275	9.4609	402.77	1.7711	0.7394	0.8512	151.23
280	8.2794	407.50	1.7963	0.7418	0.8473	153.64	280	9.2530	407.03	1.7865	0.7448	0.8537	152.96
285	8.1072	411.75	1.8114	0.7484	0.8518	155.28	285	9.0566	411.31	1.8016	0.7510	0.8574	154.64
290	7.9435	416.02	1.8262	0.7554	0.8570	156.88	290	8.8703	415.60	1.8166	0.7577	0.8620	156.28
295	7.7876	420.32	1.8409	0.7626	0.8628	158.44	295	8.6931	419.93	1.8313	0.7647	0.8672	157.88
300	7.6388	424.65	1.8555	0.7701	0.8688	159.98	300	8.5243	424.28	1.8460	0.7719	0.8729	159.45
305	7.4965	429.01	1.8699	0.7777	0.8752	161.49	305	8.3631	428.66	1.8604	0.7793	0.8789	160.98
310	7.3602	433.41	1.8842	0.7854	0.8818	162.97	310	8.2089	433.07	1.8748	0.7869	0.8852	162.49
315	7.2294	437.83	1.8983	0.7932	0.8886	164.42	315	8.0612	437.51	1.8890	0.7945	0.8917	163.97
320	7.1039	442.29	1.9124	0.8010	0.8955	165.85	320	7.9195	441.98	1.9031	0.8022	0.8984	165.42
325	6.9831	446.79	1.9263	0.8088	0.9026	167.26	325	7.7834	446.49	1.9171	0.8100	0.9052	166.86
330	6.8669	451.32	1.9402	0.8167	0.9097	168.65	330	7.6524	451.04	1.9309	0.8178	0.9122	168.27
335	6.7549	455.89	1.9539	0.8246	0.9170	170.02	335	7.5263	455.62	1.9447	0.8256	0.9193	169.66
340	6.6469	460.49	1.9675	0.8326	0.9243	171.38	340	7.4048	460.23	1.9584	0.8335	0.9264	171.03
345	6.5426	465.13	1.9811	0.8405	0.9316	172.71	345	7.2876	464.88	1.9720	0.8413	0.9336	172.38
350	6.4419	469.81	1.9945	0.8484	0.9390	174.03	350	7.1744	469.57	1.9855	0.8492	0.9409	173.71
355	6.3444	474.52	2.0079	0.8563	0.9464	175.34	355	7.0650	474.29	1.9988	0.8570	0.9482	175.03
360	6.2501	479.27	2.0212	0.8642	0.9539	176.63	360	6.9592	479.05	2.0122	0.8649	0.9556	176.33
365	6.1588	484.06	2.0344	0.8721	0.9614	177.90	365	6.8568	483.85	2.0254	0.8728	0.9629	177.62
370	6.0703	488.88	2.0475	0.8800	0.9689	179.16	370	6.7576	488.68	2.0385	0.8806	0.9704	178.89
375	5.9845	493.75	2.0606	0.8879	0.9764	180.41	375	6.6615	493.55	2.0516	0.8884	0.9778	180.15
380	5.9013	498.65	2.0736	0.8957	0.9839	181.65	380	6.5682	498.46	2.0646	0.8963	0.9852	181.40
385	5.8205	503.59	2.0865	0.9036	0.9914	182.87	385	6.4777	503.40	2.0776	0.9041	0.9927	182.63
390	5.7420	508.56	2.0993	0.9114	0.9990	184.08	390	6.3899	508.39	2.0904	0.9118	1.0001	183.86
395	5.6657	513.58	2.1121	0.9192	1.0065	185.28	395	6.3045	513.40	2.1032	0.9196	1.0076	185.07
400	5.5915	518.63	2.1248	0.9269	1.0140	186.48	400	6.2215	518.46	2.1159	0.9274	1.0151	186.27
410	5.4491	528.84	2.1500	0.9424	1.0290	188.83	410	6.0623	528.69	2.1412	0.9428	1.0300	188.63
420	5.3141	539.21	2.1750	0.9578	1.0440	191.14	420	5.9115	539.06	2.1662	0.9582	1.0449	190.96
430	5.1860	549.73	2.1998	0.9731	1.0589	193.41	430	5.7683	549.59	2.1909	0.9734	1.0597	193.25
440	5.0641	560.39	2.2243	0.9883	1.0738	195.66	440	5.6322	560.26	2.2155	0.9886	1.0746	195.50
450	4.9480	571.20	2.2486	1.0034	1.0887	197.86	450	5.5027	571.08	2.2398	1.0037	1.0893	197.72
460	4.8373	582.16	2.2727	1.0185	1.1034	200.04	460	5.3791	582.05	2.2639	1.0187	1.1040	199.91

TABLE 9. Thermodynamic properties of HFC-134a in the single-phase region — Continued

T / K	ρ / kg/m^3	h / kJ/kg	s / kJ/(kgK)	c_v / kJ/(kgK)	c_p / kJ/(kgK)	w / m/s	T / K	ρ / kg/m^3	h / kJ/kg	s / kJ/(kgK)	c_v / kJ/(kgK)	c_p / kJ/(kgK)	w / m/s
			0.25 MPa							**0.30 MPa**			
170	1591.0	71.745	0.4134	0.7922	1.1836	1120.1	170	1591.0	71.767	0.4133	0.7922	1.1836	1120.3
175	1577.8	77.665	0.4477	0.7910	1.1845	1094.7	175	1577.8	77.687	0.4476	0.7910	1.1845	1094.9
180	1564.5	83.593	0.4811	0.7913	1.1869	1069.3	180	1564.6	83.615	0.4810	0.7913	1.1868	1069.4
185	1551.2	89.536	0.5136	0.7927	1.1903	1043.9	185	1551.3	89.558	0.5136	0.7927	1.1903	1044.1
190	1537.8	95.498	0.5454	0.7950	1.1947	1018.6	190	1537.9	95.520	0.5454	0.7950	1.1946	1018.9
195	1524.4	101.48	0.5765	0.7980	1.1997	993.61	195	1524.4	101.50	0.5765	0.7980	1.1997	993.83
200	1510.8	107.49	0.6070	0.8016	1.2054	968.70	200	1510.9	107.51	0.6069	0.8016	1.2054	968.93
205	1497.2	113.54	0.6368	0.8056	1.2116	944.00	205	1497.3	113.56	0.6368	0.8056	1.2115	944.23
210	1483.4	119.61	0.6661	0.8099	1.2182	919.48	210	1483.5	119.63	0.6660	0.8099	1.2182	919.73
215	1469.6	125.72	0.6949	0.8145	1.2253	895.17	215	1469.7	125.74	0.6948	0.8145	1.2252	895.42
220	1455.6	131.86	0.7231	0.8193	1.2327	871.04	220	1455.7	131.88	0.7230	0.8193	1.2326	871.30
225	1441.5	138.05	0.7509	0.8243	1.2406	847.08	225	1441.6	138.07	0.7508	0.8243	1.2405	847.35
230	1427.2	144.27	0.7783	0.8295	1.2488	823.28	230	1427.3	144.29	0.7782	0.8295	1.2487	823.57
235	1412.7	150.54	0.8052	0.8348	1.2574	799.63	235	1412.9	150.55	0.8051	0.8348	1.2573	799.92
240	1398.1	156.85	0.8318	0.8402	1.2664	776.09	240	1398.2	156.86	0.8317	0.8402	1.2663	776.40
245	1383.3	163.20	0.8580	0.8458	1.2760	752.66	245	1383.4	163.22	0.8579	0.8458	1.2758	752.98
250	1368.2	169.61	0.8839	0.8514	1.2860	729.29	250	1368.3	169.62	0.8838	0.8515	1.2858	729.63
255	1352.9	176.06	0.9094	0.8572	1.2966	705.98	255	1353.0	176.08	0.9093	0.8572	1.2964	706.34
260	1337.2	182.57	0.9347	0.8631	1.3078	682.69	260	1337.4	182.59	0.9346	0.8631	1.3076	683.06
265	1321.3	189.14	0.9597	0.8691	1.3198	659.38	265	1321.5	189.16	0.9597	0.8691	1.3196	659.77
268.86	1308.7	194.26	0.9789	0.8738	1.3297	641.33	270	1305.2	195.79	0.9844	0.8751	1.3324	636.44
268.86	12.393	396.08	1.7295	0.7484	0.8782	146.98	273.82	1292.5	200.90	1.0032	0.8799	1.3428	618.56
270	12.322	397.07	1.7332	0.7483	0.8766	147.43	273.82	14.770	398.99	1.7267	0.7627	0.9002	146.92
275	12.022	401.44	1.7493	0.7498	0.8724	149.36	275	14.679	400.05	1.7305	0.7625	0.8981	147.40
280	11.741	405.80	1.7650	0.7533	0.8714	151.22	280	14.314	404.52	1.7467	0.7631	0.8921	149.41
285	11.478	410.16	1.7804	0.7580	0.8726	153.01	285	13.975	408.98	1.7624	0.7660	0.8899	151.33
290	11.230	414.53	1.7956	0.7637	0.8753	154.75	290	13.657	413.43	1.7779	0.7704	0.8900	153.18
295	10.996	418.92	1.8106	0.7699	0.8790	156.44	295	13.358	417.88	1.7931	0.7756	0.8918	154.97
300	10.773	423.32	1.8254	0.7766	0.8834	158.09	300	13.076	422.35	1.8081	0.7815	0.8948	156.71
305	10.562	427.75	1.8401	0.7835	0.8884	159.70	305	12.809	426.83	1.8230	0.7879	0.8986	158.40
310	10.360	432.21	1.8546	0.7907	0.8939	161.28	310	12.555	431.34	1.8376	0.7946	0.9031	160.05
315	10.167	436.69	1.8689	0.7980	0.8997	162.82	315	12.314	435.86	1.8521	0.8015	0.9081	161.66
320	9.9833	441.21	1.8831	0.8054	0.9058	164.34	320	12.084	440.42	1.8664	0.8086	0.9135	163.23
325	9.8067	445.75	1.8972	0.8129	0.9120	165.82	325	11.863	445.00	1.8806	0.8159	0.9191	164.78
330	9.6372	450.33	1.9112	0.8205	0.9185	167.29	330	11.653	449.61	1.8947	0.8232	0.9251	166.29
335	9.4743	454.94	1.9250	0.8281	0.9251	168.72	335	11.450	454.25	1.9087	0.8306	0.9312	167.78
340	9.3176	459.58	1.9388	0.8358	0.9319	170.14	340	11.256	458.92	1.9225	0.8381	0.9375	169.24
345	9.1667	464.26	1.9525	0.8435	0.9387	171.53	345	11.070	463.63	1.9363	0.8456	0.9440	170.67
350	9.0213	468.97	1.9660	0.8512	0.9457	172.90	350	10.890	468.36	1.9499	0.8532	0.9506	172.09
355	8.8809	473.71	1.9795	0.8589	0.9527	174.26	355	10.717	473.13	1.9634	0.8608	0.9573	173.48
360	8.7453	478.50	1.9929	0.8667	0.9598	175.60	360	10.550	477.94	1.9769	0.8684	0.9641	174.85
365	8.6142	483.31	2.0061	0.8744	0.9669	176.92	365	10.389	482.77	1.9902	0.8760	0.9710	176.21
370	8.4874	488.17	2.0193	0.8821	0.9741	178.22	370	10.234	487.65	2.0035	0.8837	0.9779	177.54

TABLE 9. Thermodynamic properties of HFC-134a in the single-phase region — Continued

T/K	ρ kg/m³	h kJ/kg	s kJ/(kgK)	c_v kJ/(kgK)	c_p kJ/(kgK)	w m/s	T/K	ρ kg/m³	h kJ/kg	s kJ/(kgK)	c_v kJ/(kgK)	c_p kJ/(kgK)	w m/s
			0.25 MPa							**0.30 MPa**			
375	8.3647	493.05	2.0325	0.8899	0.9813	179.51	375	10.083	492.55	2.0166	0.8913	0.9849	178.86
380	8.2457	497.98	2.0455	0.8976	0.9886	180.78	380	9.9380	497.50	2.0297	0.8990	0.9920	180.16
385	8.1304	502.94	2.0585	0.9053	0.9958	182.04	385	9.7969	502.47	2.0427	0.9066	0.9991	181.45
390	8.0185	507.94	2.0714	0.9130	1.0031	183.29	390	9.6601	507.49	2.0557	0.9142	1.0062	182.72
395	7.9100	512.97	2.0842	0.9207	1.0104	184.52	395	9.5275	512.54	2.0685	0.9219	1.0133	183.97
400	7.8045	518.04	2.0970	0.9284	1.0178	185.74	400	9.3988	517.62	2.0813	0.9295	1.0205	185.22
410	7.6024	528.29	2.1223	0.9438	1.0324	188.15	410	9.1524	527.90	2.1067	0.9447	1.0349	187.67
420	7.4111	538.69	2.1473	0.9590	1.0471	190.52	420	8.9196	538.32	2.1318	0.9599	1.0493	190.07
430	7.2298	549.24	2.1722	0.9742	1.0618	192.84	430	8.6991	548.89	2.1567	0.9750	1.0638	192.43
440	7.0576	559.93	2.1967	0.9893	1.0764	195.12	440	8.4899	559.60	2.1813	0.9900	1.0783	194.74
450	6.8938	570.77	2.2211	1.0043	1.0910	197.37	450	8.2912	570.45	2.2057	1.0049	1.0927	197.02
460	6.7378	581.75	2.2452	1.0192	1.1056	199.59	460	8.1020	581.45	2.2299	1.0198	1.1071	199.26
			0.35 MPa							**0.40 MPa**			
170	1591.1	71.790	0.4133	0.7922	1.1835	1120.4	170	1591.1	71.813	0.4132	0.7922	1.1835	1120.6
175	1577.9	77.709	0.4476	0.7910	1.1844	1095.1	175	1577.9	77.732	0.4475	0.7910	1.1844	1095.2
180	1564.6	83.637	0.4810	0.7913	1.1868	1069.6	180	1564.7	83.659	0.4809	0.7913	1.1867	1069.8
185	1551.3	89.580	0.5135	0.7927	1.1902	1044.3	185	1551.4	89.602	0.5135	0.7927	1.1902	1044.5
190	1538.0	95.542	0.5453	0.7950	1.1946	1019.1	190	1538.0	95.563	0.5453	0.7951	1.1945	1019.3
195	1524.5	101.52	0.5764	0.7981	1.1996	994.04	195	1524.6	101.54	0.5764	0.7981	1.1996	994.26
200	1511.0	107.53	0.6069	0.8016	1.2053	969.16	200	1511.0	107.56	0.6068	0.8016	1.2052	969.38
205	1497.3	113.58	0.6367	0.8056	1.2115	944.46	205	1497.4	113.60	0.6366	0.8056	1.2114	944.70
210	1483.6	119.65	0.6660	0.8099	1.2181	919.97	210	1483.7	119.67	0.6659	0.8099	1.2180	920.21
215	1469.8	125.76	0.6947	0.8145	1.2251	895.67	215	1469.9	125.78	0.6947	0.8145	1.2251	895.92
220	1455.8	131.90	0.7230	0.8193	1.2326	871.56	220	1455.9	131.92	0.7229	0.8193	1.2325	871.82
225	1441.7	138.09	0.7508	0.8243	1.2404	847.63	225	1441.8	138.10	0.7507	0.8244	1.2403	847.90
230	1427.4	144.31	0.7781	0.8295	1.2486	823.85	230	1427.5	144.33	0.7780	0.8295	1.2485	824.14
235	1413.0	150.57	0.8051	0.8348	1.2572	800.22	235	1413.1	150.59	0.8050	0.8348	1.2570	800.52
240	1398.4	156.88	0.8316	0.8403	1.2662	776.71	240	1398.5	156.90	0.8315	0.8403	1.2661	777.02
245	1383.5	163.24	0.8578	0.8458	1.2757	753.30	245	1383.7	163.25	0.8577	0.8458	1.2755	753.63
250	1368.5	169.64	0.8837	0.8515	1.2857	729.97	250	1368.6	169.66	0.8836	0.8515	1.2855	730.31
255	1353.2	176.09	0.9093	0.8572	1.2962	706.69	255	1353.3	176.11	0.9092	0.8572	1.2961	707.05
260	1337.6	182.60	0.9345	0.8631	1.3074	683.43	260	1337.7	182.62	0.9345	0.8631	1.3072	683.80
265	1321.7	189.17	0.9596	0.8691	1.3194	660.17	265	1321.8	189.18	0.9595	0.8690	1.3192	660.56
270	1305.4	195.80	0.9843	0.8751	1.3321	636.86	270	1305.6	195.81	0.9842	0.8751	1.3319	637.27
275	1288.7	202.49	1.0089	0.8813	1.3459	613.47	275	1288.9	202.50	1.0088	0.8813	1.3456	613.90
278.17	1277.9	206.79	1.0244	0.8854	1.3552	598.54	280	1271.9	209.27	1.0332	0.8877	1.3604	590.42
278.17	17.147	401.50	1.7244	0.7755	0.9207	146.73	282.08	1264.6	212.11	1.0433	0.8903	1.3670	580.60
280	16.982	403.18	1.7304	0.7749	0.9168	147.51	282.08	19.528	403.71	1.7225	0.7872	0.9400	146.47
285	16.553	407.74	1.7466	0.7752	0.9098	149.58	285	19.223	406.45	1.7322	0.7859	0.9330	147.75
290	16.156	412.28	1.7624	0.7778	0.9066	151.55	290	18.734	411.09	1.7483	0.7862	0.9254	149.86
295	15.785	416.81	1.7778	0.7818	0.9060	153.45	295	18.281	415.71	1.7641	0.7887	0.9218	151.88

TABLE 9. Thermodynamic properties of HFC-134a in the single-phase region — Continued

T/K	ρ/kg/m^3	h/kJ/kg	s/kJ/(kgK)	c_v/kJ/(kgK)	c_p/kJ/(kgK)	w/m/s	T/K	ρ/kg/m^3	h/kJ/kg	s/kJ/(kgK)	c_v/kJ/(kgK)	c_p/kJ/(kgK)	w/m/s
			0.35 MPa							**0.40 MPa**			
300	15.437	421.35	1.7931	0.7869	0.9072	155.28	300	17.859	420.31	1.7796	0.7926	0.9207	153.82
305	15.108	425.89	1.8081	0.7926	0.9096	157.06	305	17.462	424.92	1.7948	0.7975	0.9214	155.69
310	14.798	430.44	1.8229	0.7987	0.9129	158.79	310	17.089	429.53	1.8098	0.8031	0.9234	157.50
315	14.503	435.02	1.8375	0.8052	0.9170	160.47	315	16.737	434.16	1.8246	0.8091	0.9254	159.26
320	14.223	439.61	1.8520	0.8120	0.9215	162.11	320	16.403	438.80	1.8392	0.8154	0.9300	160.97
325	13.956	444.23	1.8664	0.8189	0.9265	163.71	325	16.085	443.46	1.8537	0.8221	0.9343	162.63
330	13.701	448.88	1.8805	0.8260	0.9319	165.28	330	15.782	448.14	1.8680	0.8289	0.9390	164.26
335	13.457	453.55	1.8946	0.8332	0.9375	166.82	335	15.494	452.85	1.8822	0.8358	0.9441	165.85
340	13.223	458.26	1.9085	0.8405	0.9434	168.33	340	15.218	457.58	1.8962	0.8429	0.9494	167.41
345	12.999	462.99	1.9223	0.8478	0.9494	169.81	345	14.953	462.34	1.9101	0.8501	0.9551	168.93
350	12.783	467.75	1.9361	0.8553	0.9557	171.26	350	14.700	467.13	1.9239	0.8573	0.9609	170.43
355	12.576	472.55	1.9497	0.8627	0.9621	172.69	355	14.456	471.95	1.9375	0.8646	0.9659	171.90
360	12.376	477.37	1.9632	0.8702	0.9686	174.10	360	14.222	476.80	1.9511	0.8720	0.9731	173.35
365	12.184	482.23	1.9766	0.8777	0.9752	175.49	365	13.997	481.69	1.9646	0.8794	0.9794	174.77
370	11.998	487.12	1.9899	0.8852	0.9818	176.86	370	13.780	486.60	1.9779	0.8868	0.9858	176.17
375	11.818	492.05	2.0031	0.8928	0.9886	178.20	375	13.570	491.54	1.9912	0.8942	0.9924	177.54
380	11.645	497.01	2.0162	0.9003	0.9954	179.53	380	13.368	496.52	2.0044	0.9017	0.9990	178.90
385	11.477	502.01	2.0293	0.9079	1.0023	180.85	385	13.172	501.53	2.0175	0.9092	1.0057	180.24
390	11.315	507.04	2.0423	0.9154	1.0093	182.14	390	12.983	506.58	2.0305	0.9167	1.0124	181.57
395	11.157	512.10	2.0552	0.9230	1.0163	183.42	395	12.800	511.66	2.0435	0.9242	1.0192	182.87
400	11.004	517.20	2.0680	0.9306	1.0233	184.69	400	12.622	516.77	2.0563	0.9316	1.0251	184.16
410	10.712	527.50	2.0934	0.9457	1.0374	187.18	410	12.283	527.10	2.0819	0.9466	1.0399	186.69
420	10.437	537.95	2.1186	0.9607	1.0516	189.62	420	11.963	537.57	2.1071	0.9616	1.0539	189.17
430	10.176	548.54	2.1435	0.9757	1.0659	192.01	430	11.661	548.18	2.1320	0.9765	1.0679	191.60
440	9.9294	559.27	2.1682	0.9907	1.0801	194.36	440	11.376	558.93	2.1568	0.9913	1.0820	193.98
450	9.6950	570.14	2.1926	1.0055	1.0944	196.67	450	11.105	569.82	2.1812	1.0062	1.0962	196.31
460	9.4720	581.16	2.2168	1.0204	1.1087	198.93	460	10.847	580.86	2.2055	1.0209	1.1103	198.61
			0.50 MPa							**0.60 MPa**			
175	1578.1	77.777	0.4474	0.7911	1.1843	1095.6	175	1578.2	77.821	0.4473	0.7911	1.1843	1096.0
180	1564.8	83.704	0.4808	0.7913	1.1867	1070.2	180	1565.0	83.748	0.4807	0.7914	1.1866	1070.6
185	1551.5	89.646	0.5134	0.7928	1.1901	1044.9	185	1551.7	89.690	0.5133	0.7928	1.1900	1045.3
190	1538.2	95.607	0.5452	0.7951	1.1944	1019.7	190	1538.3	95.650	0.5450	0.7951	1.1943	1020.1
195	1524.7	101.59	0.5763	0.7981	1.1995	994.70	195	1524.9	101.63	0.5761	0.7981	1.1994	995.13
200	1511.2	107.60	0.6067	0.8016	1.2051	969.83	200	1511.4	107.64	0.6066	0.8017	1.2050	970.28
205	1497.6	113.64	0.6365	0.8056	1.2113	945.16	205	1497.8	113.68	0.6364	0.8057	1.2111	945.63
210	1483.9	119.71	0.6658	0.8099	1.2179	920.70	210	1484.1	119.75	0.6657	0.8100	1.2177	921.18
215	1470.0	125.82	0.6945	0.8145	1.2249	896.43	215	1470.2	125.86	0.6944	0.8146	1.2247	896.93
220	1456.1	131.96	0.7228	0.8194	1.2323	872.35	220	1456.3	132.00	0.7226	0.8194	1.2321	872.87
225	1442.0	138.14	0.7506	0.8244	1.2401	848.44	225	1442.2	138.18	0.7504	0.8244	1.2399	848.99
230	1427.7	144.36	0.7779	0.8295	1.2483	824.70	230	1428.0	144.40	0.7778	0.8296	1.2480	825.27
235	1413.3	150.63	0.8048	0.8348	1.2568	801.11	235	1413.6	150.66	0.8047	0.8349	1.2566	801.70

TABLE 9. Thermodynamic properties of HFC-134a in the single-phase region — Continued

T / K	ρ / kg/m^3	h / kJ/kg	s / kJ/(kgK)	c_v / kJ/(kgK)	c_p / kJ/(kgK)	w / m/s	T / K	ρ / kg/m^3	h / kJ/kg	s / kJ/(kgK)	c_v / kJ/(kgK)	c_p / kJ/(kgK)	w / m/s
			0.50 MPa							**0.60 MPa**			
240	1398.7	156.93	0.8314	0.8403	1.2658	777.64	240	1399.0	156.97	0.8312	0.8403	1.2656	778.26
245	1383.9	163.29	0.8576	0.8458	1.2753	754.27	245	1384.2	163.32	0.8574	0.8458	1.2750	754.92
250	1368.9	169.69	0.8835	0.8515	1.2852	730.99	250	1369.2	169.72	0.8833	0.8515	1.2849	731.66
255	1353.6	176.14	0.9090	0.8572	1.2957	707.75	255	1353.9	176.17	0.9088	0.8572	1.2954	708.46
260	1338.1	182.65	0.9343	0.8631	1.3068	684.55	260	1338.4	182.68	0.9341	0.8631	1.3065	685.29
265	1322.2	189.21	0.9593	0.8690	1.3187	661.34	265	1322.5	189.24	0.9591	0.8690	1.3183	662.12
270	1306.0	195.84	0.9841	0.8751	1.3314	638.09	270	1306.3	195.86	0.9839	0.8751	1.3309	638.92
275	1289.3	202.53	1.0086	0.8813	1.3450	614.78	275	1289.8	202.55	1.0084	0.8813	1.3444	615.64
280	1272.3	209.29	1.0330	0.8876	1.3597	591.35	280	1272.7	209.31	1.0328	0.8876	1.3591	592.27
285	1254.7	216.13	1.0572	0.8941	1.3758	567.76	285	1255.2	216.14	1.0570	0.8941	1.3750	568.73
288.88	1240.7	221.50	1.0759	0.8992	1.3894	549.28	290	1237.2	223.06	1.0810	0.9007	1.3925	545.00
288.88	24.317	407.47	1.7196	0.8078	0.9761	145.76	294.72	1219.5	229.68	1.1037	0.9071	1.4108	522.34
290	24.162	408.55	1.7234	0.8068	0.9722	146.29	294.72	29.154	410.57	1.7174	0.8259	1.0101	144.88
295	23.509	413.38	1.7399	0.8049	0.9595	148.59	295	29.105	410.85	1.7184	0.8255	1.0088	145.03
300	22.908	418.16	1.7560	0.8058	0.9521	150.76	300	28.274	415.84	1.7352	0.8218	0.9914	147.50
305	22.352	422.91	1.7717	0.8085	0.9482	152.84	305	27.517	420.77	1.7515	0.8214	0.9806	149.82
310	21.834	427.64	1.7871	0.8125	0.9468	154.84	310	26.821	425.66	1.7673	0.8232	0.9741	152.03
315	21.349	432.38	1.8022	0.8173	0.9470	156.76	315	26.175	430.52	1.7829	0.8265	0.9707	154.14
320	20.893	437.12	1.8171	0.8228	0.9485	158.61	320	25.574	435.37	1.7982	0.8307	0.9693	156.16
325	20.462	441.87	1.8319	0.8286	0.9510	160.41	325	25.010	440.22	1.8132	0.8357	0.9695	158.11
330	20.053	446.63	1.8464	0.8348	0.9541	162.16	330	24.479	445.07	1.8280	0.8411	0.9708	160.00
335	19.666	451.41	1.8608	0.8413	0.9579	163.87	335	23.978	449.92	1.8426	0.8470	0.9730	161.82
340	19.297	456.21	1.8750	0.8479	0.9622	165.53	340	23.504	454.80	1.8571	0.8531	0.9759	163.60
345	18.945	461.03	1.8891	0.8547	0.9668	167.15	345	23.054	459.69	1.8713	0.8594	0.9795	165.32
350	18.609	465.88	1.9030	0.8616	0.9718	168.74	350	22.625	464.59	1.8855	0.8659	0.9834	167.00
355	18.288	470.75	1.9169	0.8686	0.9771	170.29	355	22.217	469.52	1.8994	0.8726	0.9878	168.64
350	17.979	475.65	1.9306	0.8756	0.9826	171.81	360	21.826	474.47	1.9133	0.8794	0.9925	170.25
355	17.683	480.58	1.9442	0.8828	0.9883	173.30	365	21.453	479.45	1.9270	0.8863	0.9975	171.82
370	17.399	485.53	1.9576	0.8900	0.9941	174.77	370	21.094	484.45	1.9406	0.8932	1.0028	173.35
375	17.125	490.52	1.9710	0.8972	1.0001	176.21	375	20.751	489.48	1.9541	0.9002	1.0082	174.86
380	16.861	495.53	1.9843	0.9045	1.0063	177.63	380	20.420	494.53	1.9675	0.9073	1.0139	176.34
385	16.606	500.58	1.9975	0.9118	1.0126	179.03	385	20.102	499.62	1.9808	0.9144	1.0197	177.80
390	16.361	505.65	2.0106	0.9191	1.0189	180.40	390	19.796	504.73	1.9940	0.9216	1.0256	179.23
395	16.123	510.77	2.0236	0.9265	1.0254	181.76	395	19.500	509.87	2.0071	0.9288	1.0317	180.63
400	15.894	515.91	2.0366	0.9338	1.0319	183.09	400	19.215	515.05	2.0201	0.9360	1.0379	182.02
410	15.456	526.30	2.0622	0.9485	1.0451	185.71	410	18.672	525.49	2.0459	0.9505	1.0505	184.73
420	15.045	536.82	2.0876	0.9633	1.0586	188.27	420	18.164	536.06	2.0714	0.9650	1.0634	187.36
430	14.657	547.47	2.1126	0.9780	1.0722	190.77	430	17.686	546.76	2.0966	0.9796	1.0765	189.93
440	14.291	558.26	2.1374	0.9927	1.0859	193.21	440	17.236	557.59	2.1215	0.9941	1.0898	192.44
450	13.944	569.19	2.1620	1.0074	1.0997	195.60	450	16.811	568.56	2.1461	1.0087	1.1033	194.90
450	13.616	580.26	2.1863	1.0220	1.1135	197.95	460	16.408	579.66	2.1705	1.0232	1.1168	197.30

TABLE 9. Thermodynamic properties of HFC-134a in the single-phase region — Continued

T / K	ρ / kg/m³	h / kJ/kg	s / kJ/(kgK)	c_v / kJ/(kgK)	c_p / kJ/(kgK)	w / m/s	T / K	ρ / kg/m³	h / kJ/kg	s / kJ/(kgK)	c_v / kJ/(kgK)	c_p / kJ/(kgK)	w / m/s
			0.70 MPa							**0.80 MPa**			
175	1578.3	77.866	0.4472	0.7911	1.1842	1096.4	175	1578.4	77.911	0.4471	0.7912	1.1841	1096.8
180	1565.1	83.793	0.4806	0.7914	1.1865	1071.0	180	1565.2	83.837	0.4805	0.7914	1.1864	1071.4
185	1551.8	89.733	0.5131	0.7928	1.1899	1045.7	185	1551.9	89.777	0.5130	0.7929	1.1898	1046.1
190	1538.5	95.694	0.5449	0.7951	1.1942	1020.5	190	1538.6	95.737	0.5448	0.7952	1.1941	1021.0
195	1525.0	101.67	0.5760	0.7982	1.1993	995.56	195	1525.2	101.72	0.5759	0.7982	1.1992	996.00
200	1511.5	107.68	0.6065	0.8017	1.2049	970.73	200	1511.7	107.73	0.6063	0.8017	1.2048	971.18
205	1497.9	113.72	0.6363	0.8057	1.2110	946.10	205	1498.1	113.76	0.6362	0.8057	1.2109	946.56
210	1484.2	119.79	0.6655	0.8100	1.2176	921.66	210	1484.4	119.84	0.6654	0.8100	1.2175	922.15
215	1470.4	125.90	0.6943	0.8146	1.2246	897.43	215	1470.6	125.94	0.6941	0.8146	1.2244	897.93
220	1456.5	132.04	0.7225	0.8194	1.2320	873.39	220	1456.7	132.08	0.7224	0.8194	1.2318	873.91
225	1442.4	138.22	0.7503	0.8244	1.2397	849.53	225	1442.6	138.26	0.7502	0.8244	1.2395	850.07
230	1428.2	144.44	0.7776	0.8296	1.2478	825.84	230	1428.4	144.48	0.7775	0.8296	1.2476	826.40
235	1413.8	150.70	0.8046	0.8349	1.2564	802.29	235	1414.0	150.74	0.8044	0.8349	1.2561	802.88
240	1399.2	157.00	0.8311	0.8403	1.2653	778.87	240	1399.5	157.04	0.8309	0.8403	1.2651	779.49
245	1384.5	163.35	0.8573	0.8458	1.2747	755.56	245	1384.7	163.39	0.8571	0.8458	1.2744	756.20
250	1369.5	169.75	0.8831	0.8515	1.2846	732.33	250	1369.7	169.79	0.8830	0.8515	1.2843	733.01
255	1354.2	176.20	0.9087	0.8572	1.2950	709.17	255	1354.5	176.23	0.9085	0.8572	1.2947	709.87
260	1338.7	182.70	0.9339	0.8631	1.3061	686.03	260	1339.0	182.73	0.9338	0.8631	1.3057	686.77
265	1322.9	189.26	0.9589	0.8690	1.3178	662.90	265	1323.2	189.29	0.9587	0.8690	1.3174	663.67
270	1306.7	195.88	0.9837	0.8751	1.3304	639.74	270	1307.1	195.91	0.9835	0.8751	1.3299	640.55
275	1290.2	202.57	1.0082	0.8813	1.3439	616.51	275	1290.6	202.59	1.0080	0.8812	1.3433	617.37
280	1273.2	209.33	1.0325	0.8876	1.3584	593.18	280	1273.6	209.34	1.0323	0.8875	1.3578	594.10
285	1255.7	216.16	1.0567	0.8940	1.3743	569.71	285	1256.2	216.17	1.0565	0.8940	1.3735	570.68
290	1237.7	223.07	1.0808	0.9006	1.3916	546.03	290	1238.2	223.08	1.0805	0.9006	1.3908	547.07
295	1219.0	230.08	1.1047	0.9074	1.4109	522.10	295	1219.6	230.08	1.1045	0.9073	1.4098	523.21
299.86	1200.1	236.99	1.1280	0.9142	1.4318	498.52	300	1200.2	237.19	1.1283	0.9143	1.4312	499.04
299.86	34.053	413.19	1.7156	0.8421	1.0428	143.90	304.47	1182.2	243.64	1.1497	0.9208	1.4526	477.05
300	34.024	413.33	1.7161	0.8419	1.0421	143.97	304.47	39.025	415.45	1.7140	0.8570	1.0750	142.84
305	33.007	418.49	1.7331	0.8370	1.0206	146.60	305	38.890	416.02	1.7158	0.8561	1.0717	143.14
310	32.087	423.55	1.7496	0.8357	1.0069	149.07	310	37.684	421.31	1.7330	0.8505	1.0471	145.91
315	31.246	428.57	1.7656	0.8368	0.9982	151.39	315	36.598	426.50	1.7497	0.8487	1.0310	148.49
320	30.470	433.54	1.7813	0.8395	0.9930	153.61	320	35.610	431.63	1.7658	0.8493	1.0205	150.92
325	29.749	438.50	1.7967	0.8433	0.9902	155.72	325	34.702	436.71	1.7816	0.8516	1.0138	153.23
330	29.076	443.45	1.8118	0.8479	0.9892	157.76	330	33.861	441.77	1.7970	0.8551	1.0098	155.43
335	28.444	448.40	1.8266	0.8530	0.9895	159.72	335	33.079	446.81	1.8122	0.8594	1.0077	157.54
340	27.850	453.35	1.8413	0.8585	0.9909	161.61	340	32.346	451.85	1.8271	0.8642	1.0071	159.56
345	27.288	458.31	1.8558	0.8644	0.9930	163.45	345	31.658	456.89	1.8418	0.8695	1.0077	161.52
350	26.756	463.28	1.8701	0.8705	0.9959	165.23	350	31.009	461.93	1.8563	0.8752	1.0092	163.41
355	26.250	468.27	1.8842	0.8768	0.9993	166.96	355	30.396	466.98	1.8707	0.8811	1.0115	165.24
360	25.769	473.27	1.8983	0.8832	1.0031	168.65	360	29.814	472.05	1.8848	0.8872	1.0143	167.03
365	25.310	478.30	1.9121	0.8898	1.0073	170.30	365	29.260	477.13	1.8988	0.8935	1.0177	168.76
370	24.871	483.35	1.9259	0.8965	1.0119	171.91	370	28.733	482.22	1.9127	0.8999	1.0215	170.45
375	24.451	488.42	1.9395	0.9033	1.0167	173.49	375	28.230	487.34	1.9265	0.9065	1.0256	172.10

TABLE 9. Thermodynamic properties of HFC-134a in the single-phase region — Continued

T / K	ρ / kg/m³	h / kJ/kg	s / kJ/(kgK)	c_v / kJ/(kgK)	c_p / kJ/(kgK)	w / m/s	T / K	ρ / kg/m³	h / kJ/kg	s / kJ/(kgK)	c_v / kJ/(kgK)	c_p / kJ/(kgK)	w / m/s
			0.70 MPa							**0.80 MPa**			
380	24.049	493.51	1.9530	0.9102	1.0218	175.04	380	27.749	492.48	1.9401	0.9131	1.0301	173.71
385	23.662	498.64	1.9664	0.9171	1.0271	176.55	385	27.289	497.64	1.9536	0.9199	1.0349	175.29
390	23.290	503.79	1.9797	0.9241	1.0326	178.04	390	26.846	502.83	1.9670	0.9267	1.0398	176.83
395	22.932	508.96	1.9928	0.9312	1.0382	179.50	395	26.422	508.04	1.9802	0.9336	1.0450	178.35
400	22.587	514.17	2.0059	0.9382	1.0440	180.93	400	26.013	513.28	1.9934	0.9405	1.0504	179.84
410	21.933	524.67	2.0319	0.9525	1.0560	183.73	410	25.241	523.84	2.0195	0.9544	1.0617	182.73
420	21.322	535.29	2.0575	0.9668	1.0683	186.45	420	24.521	534.52	2.0452	0.9685	1.0734	185.54
430	20.750	546.04	2.0827	0.9811	1.0810	189.10	430	23.849	545.31	2.0706	0.9827	1.0855	188.26
440	20.211	556.91	2.1077	0.9955	1.0939	191.67	440	23.218	556.23	2.0957	0.9969	1.0980	190.90
450	19.704	567.92	2.1325	1.0099	1.1069	194.19	450	22.624	567.27	2.1205	1.0112	1.1107	193.47
460	19.224	579.05	2.1570	1.0243	1.1202	196.64	460	22.064	578.44	2.1451	1.0254	1.1236	195.99
			1.00 MPa							**1.20 MPa**			
175	1578.7	78.001	0.4469	0.7912	1.1839	1097.5	175	1578.9	78.090	0.4467	0.7913	1.1838	1098.3
180	1565.5	83.926	0.4803	0.7915	1.1862	1072.2	180	1565.7	84.015	0.4800	0.7916	1.1861	1073.0
185	1552.2	89.865	0.5128	0.7929	1.1896	1046.9	185	1552.5	89.953	0.5126	0.7930	1.1895	1047.7
190	1538.9	95.824	0.5446	0.7952	1.1939	1021.8	190	1539.2	95.911	0.5444	0.7953	1.1937	1022.6
195	1525.5	101.80	0.5757	0.7982	1.1989	996.86	195	1525.8	101.89	0.5754	0.7983	1.1987	997.72
200	1512.0	107.81	0.6061	0.8018	1.2045	972.07	200	1512.3	107.90	0.6059	0.8018	1.2043	972.97
205	1498.4	113.85	0.6359	0.8058	1.2106	947.49	205	1498.8	113.93	0.6357	0.8058	1.2104	948.42
210	1484.8	119.92	0.6652	0.8101	1.2172	923.11	210	1485.1	120.00	0.6649	0.8101	1.2169	924.07
215	1471.0	126.02	0.6939	0.8147	1.2241	898.93	215	1471.3	126.10	0.6936	0.8147	1.2238	899.93
220	1457.1	132.16	0.7221	0.8195	1.2315	874.95	220	1457.5	132.24	0.7219	0.8195	1.2311	875.99
225	1443.0	138.34	0.7499	0.8245	1.2392	851.15	225	1443.4	138.41	0.7496	0.8245	1.2388	852.23
230	1428.8	144.55	0.7772	0.8296	1.2472	827.53	230	1429.3	144.63	0.7769	0.8297	1.2468	828.65
235	1414.5	150.81	0.8041	0.8349	1.2557	804.05	235	1415.0	150.88	0.8038	0.8350	1.2553	805.22
240	1400.0	157.11	0.8306	0.8403	1.2646	780.71	240	1400.5	157.18	0.8303	0.8404	1.2641	781.93
245	1385.2	163.46	0.8568	0.8459	1.2739	757.48	245	1385.8	163.53	0.8565	0.8459	1.2733	758.76
250	1370.3	169.85	0.8827	0.8515	1.2837	734.34	250	1370.9	169.92	0.8823	0.8515	1.2830	735.68
255	1355.1	176.30	0.9082	0.8572	1.2940	711.27	255	1355.7	176.36	0.9078	0.8572	1.2933	712.67
260	1339.7	182.79	0.9334	0.8631	1.3049	688.24	260	1340.3	182.85	0.9331	0.8631	1.3041	689.70
265	1323.9	189.35	0.9584	0.8690	1.3165	665.22	265	1324.6	189.40	0.9580	0.8690	1.3156	666.76
270	1307.8	195.96	0.9831	0.8750	1.3289	642.18	270	1308.5	196.01	0.9827	0.8750	1.3279	643.80
275	1291.4	202.64	1.0076	0.8812	1.3422	619.09	275	1292.1	202.68	1.0072	0.8812	1.3410	620.80
280	1274.5	209.38	1.0319	0.8875	1.3565	595.91	280	1275.3	209.42	1.0315	0.8874	1.3552	597.72
285	1257.1	216.20	1.0561	0.8939	1.3720	572.60	285	1258.0	216.24	1.0556	0.8938	1.3705	574.52
290	1239.2	223.11	1.0801	0.9005	1.3890	549.12	290	1240.2	223.13	1.0796	0.9004	1.3873	551.15
295	1220.7	230.10	1.1040	0.9072	1.4078	525.40	295	1221.8	230.11	1.1035	0.9071	1.4057	527.57
300	1201.5	237.19	1.1278	0.9142	1.4287	501.39	300	1202.7	237.19	1.1273	0.9140	1.4263	503.72
305	1181.4	244.39	1.1516	0.9213	1.4523	477.00	305	1182.8	244.38	1.1510	0.9211	1.4494	479.51
310	1160.4	251.72	1.1754	0.9288	1.4794	452.14	310	1161.9	251.69	1.1748	0.9285	1.4758	454.86

TABLE 9. Thermodynamic properties of HFC-134a in the single-phase region — Continued

T/K	ρ kg/m³	h kJ/kg	s kJ/(kgK)	c_v kJ/(kgK)	c_p kJ/(kgK)	w m/s
			1.00 MPa			
312.53	1149.3	255.49	1.1876	0.9327	1.4948	439.30
312.53	49.222	419.16	1.7112	0.8836	1.1391	140.53
315	48.366	421.94	1.7201	0.8789	1.1200	142.11
320	46.785	427.46	1.7375	0.8732	1.0916	145.10
325	45.374	432.87	1.7543	0.8712	1.0725	147.88
330	44.097	438.20	1.7705	0.8716	1.0594	150.48
335	42.929	443.47	1.7864	0.8736	1.0506	152.93
340	41.854	448.71	1.8019	0.8767	1.0448	155.26
345	40.856	453.92	1.8171	0.8806	1.0411	157.49
350	39.927	459.12	1.8321	0.8851	1.0392	159.63
355	39.056	464.32	1.8468	0.8901	1.0385	161.68
360	38.237	469.51	1.8614	0.8954	1.0390	163.67
365	37.465	474.71	1.8757	0.9011	1.0402	165.59
370	36.735	479.91	1.8899	0.9069	1.0422	167.44
375	36.042	485.13	1.9039	0.9129	1.0448	169.25
380	35.383	490.36	1.9177	0.9191	1.0478	171.01
385	34.755	495.61	1.9315	0.9255	1.0513	172.72
390	34.156	500.88	1.9450	0.9319	1.0552	174.39
395	33.583	506.16	1.9585	0.9384	1.0594	176.02
400	33.033	511.47	1.9719	0.9450	1.0639	177.62
410	32.000	522.16	1.9983	0.9585	1.0735	180.71
420	31.044	532.95	2.0242	0.9721	1.0839	183.69
430	30.155	543.84	2.0499	0.9859	1.0950	186.56
440	29.326	554.85	2.0752	0.9998	1.1065	189.35
450	28.549	565.97	2.1002	1.0137	1.1184	192.05
460	27.818	577.22	2.1249	1.0277	1.1305	194.67
			1.40 MPa			
175	1579.2	78.180	0.4465	0.7913	1.1836	1099.0
180	1566.0	84.104	0.4798	0.7916	1.1859	1073.7
185	1552.8	90.042	0.5124	0.7930	1.1893	1048.5
190	1539.5	95.999	0.5441	0.7954	1.1935	1023.5
195	1526.1	101.97	0.5752	0.7984	1.1985	998.58
200	1512.6	107.98	0.6056	0.8019	1.2041	973.86
205	1499.1	114.02	0.6354	0.8059	1.2101	949.34
210	1485.5	120.08	0.6647	0.8102	1.2166	925.03
215	1471.7	126.18	0.6934	0.8148	1.2235	900.93
220	1457.9	132.32	0.7216	0.8196	1.2308	877.02
225	1443.9	138.49	0.7493	0.8246	1.2384	853.31
230	1429.7	144.70	0.7766	0.8297	1.2464	829.77
235	1415.4	150.96	0.8035	0.8350	1.2548	806.39
240	1401.0	157.25	0.8301	0.8404	1.2636	783.15
			1.20 MPa			
315	1139.9	259.15	1.1987	0.9362	1.5065	429.65
319.46	1119.1	265.94	1.2201	0.9434	1.5388	406.54
319.46	59.814	422.04	1.7087	0.9074	1.2052	138.06
320	59.558	422.68	1.7107	0.9060	1.1993	138.45
325	57.358	428.56	1.7289	0.8964	1.1554	141.89
330	55.435	434.26	1.7463	0.8918	1.1260	145.03
335	53.723	439.83	1.7631	0.8903	1.1058	147.93
340	52.178	445.33	1.7794	0.8909	1.0916	150.64
345	50.769	450.76	1.7952	0.8930	1.0816	153.20
350	49.475	456.15	1.8107	0.8961	1.0747	155.63
355	48.277	461.51	1.8260	0.8999	1.0701	157.94
360	47.163	466.85	1.8409	0.9043	1.0672	160.15
365	46.121	472.18	1.8556	0.9091	1.0658	162.28
370	45.144	477.51	1.8701	0.9143	1.0654	164.33
375	44.223	482.84	1.8844	0.9197	1.0660	166.31
380	43.354	488.17	1.8985	0.9254	1.0674	168.22
385	42.530	493.52	1.9125	0.9313	1.0694	170.08
390	41.747	498.87	1.9263	0.9373	1.0719	171.88
395	41.003	504.24	1.9400	0.9434	1.0749	173.64
400	40.292	509.62	1.9535	0.9497	1.0783	175.35
410	38.964	520.44	1.9803	0.9626	1.0862	178.66
420	37.743	531.35	2.0065	0.9757	1.0951	181.82
430	36.614	542.35	2.0324	0.9891	1.1049	184.86
440	35.567	553.45	2.0579	1.0026	1.1154	187.79
450	34.589	564.66	2.0831	1.0163	1.1264	190.62
460	33.675	575.98	2.1080	1.0300	1.1378	193.36
			1.60 MPa			
175	1579.4	78.270	0.4462	0.7914	1.1835	1099.8
180	1566.3	84.193	0.4796	0.7917	1.1857	1074.5
185	1553.0	90.130	0.5122	0.7931	1.1891	1049.3
190	1539.8	96.086	0.5439	0.7954	1.1934	1024.3
195	1526.4	102.06	0.5750	0.7984	1.1983	999.44
200	1513.0	108.07	0.6054	0.8020	1.2038	974.75
205	1499.4	114.10	0.6352	0.8059	1.2099	950.26
210	1485.8	120.17	0.6644	0.8102	1.2164	925.99
215	1472.1	126.26	0.6931	0.8148	1.2232	901.92
220	1458.2	132.40	0.7213	0.8196	1.2305	878.05
225	1444.3	138.57	0.7491	0.8246	1.2381	854.38
230	1430.2	144.78	0.7764	0.8297	1.2460	830.88
235	1415.9	151.03	0.8033	0.8350	1.2544	807.55
240	1401.4	157.33	0.8298	0.8404	1.2631	784.36

TABLE 9. Thermodynamic properties of HFC-134a in the single-phase region — Continued

T / K	ρ / kg/m³	h / kJ/kg	s / kJ/(kgK)	c_v / kJ/(kgK)	c_p / kJ/(kgK)	w / m/s	T / K	ρ / kg/m³	h / kJ/kg	s / kJ/(kgK)	c_v / kJ/(kgK)	c_p / kJ/(kgK)	w / m/s
			1.40 MPa							**1.60 MPa**			
245	1386.3	163.60	0.8562	0.8459	1.2728	760.03	245	1386.8	163.66	0.8559	0.8459	1.2722	761.29
250	1371.4	169.98	0.8820	0.8515	1.2824	737.00	250	1372.0	170.05	0.8817	0.8515	1.2819	738.32
255	1356.3	176.42	0.9075	0.8572	1.2926	714.06	255	1356.9	176.48	0.9072	0.8572	1.2920	715.44
260	1340.9	182.91	0.9327	0.8631	1.3034	691.16	260	1341.6	182.97	0.9324	0.8631	1.3026	692.61
265	1325.3	189.46	0.9576	0.8690	1.3148	668.29	265	1325.9	189.51	0.9573	0.8690	1.3140	669.81
270	1309.3	196.06	0.9823	0.8750	1.3269	645.41	270	1310.0	196.11	0.9820	0.8750	1.3260	647.01
275	1292.9	202.73	1.0068	0.8811	1.3399	622.50	275	1293.7	202.77	1.0064	0.8811	1.3389	624.18
280	1276.2	209.46	1.0311	0.8874	1.3539	599.51	280	1277.0	209.50	1.0307	0.8873	1.3527	601.29
285	1259.0	216.27	1.0552	0.8938	1.3691	576.42	285	1259.9	216.30	1.0547	0.8937	1.3677	578.31
290	1241.2	223.16	1.0791	0.9003	1.3856	553.17	290	1242.2	223.18	1.0787	0.9002	1.3839	555.18
295	1222.9	230.13	1.1030	0.9070	1.4038	529.73	295	1224.0	230.15	1.1025	0.9068	1.4018	531.86
300	1203.9	237.20	1.1267	0.9138	1.4239	506.02	300	1205.1	237.20	1.1262	0.9137	1.4216	508.31
305	1184.2	244.37	1.1504	0.9209	1.4466	481.99	305	1185.5	244.37	1.1499	0.9207	1.4438	484.44
310	1163.5	251.67	1.1742	0.9282	1.4724	457.54	310	1165.0	251.65	1.1735	0.9280	1.4690	460.19
315	1141.7	259.10	1.1980	0.9359	1.5022	432.57	315	1143.4	259.06	1.1973	0.9356	1.4980	435.46
320	1118.5	266.70	1.2219	0.9439	1.5375	406.94	320	1120.5	266.64	1.2211	0.9435	1.5322	410.10
325	1093.8	274.49	1.2460	0.9524	1.5804	380.42	325	1096.0	274.40	1.2452	0.9519	1.5734	383.93
325.57	1090.8	275.40	1.2488	0.9534	1.5859	377.32	330	1069.6	282.39	1.2696	0.9610	1.6248	356.68
325.57	70.870	424.29	1.7062	0.9292	1.2756	135.47	331.05	1063.7	284.11	1.2748	0.9630	1.6374	350.75
330	68.277	429.81	1.7230	0.9179	1.2216	138.91	331.05	82.464	426.04	1.7035	0.9496	1.3527	132.78
335	65.748	435.81	1.7410	0.9109	1.1804	142.42	335	79.481	431.24	1.7191	0.9375	1.2892	136.20
340	63.534	441.64	1.7583	0.9078	1.1522	145.62	340	76.253	437.54	1.7378	0.9284	1.2348	140.08
345	61.562	447.35	1.7750	0.9072	1.1322	148.59	345	73.473	443.62	1.7556	0.9239	1.1979	143.58
350	59.783	452.97	1.7912	0.9083	1.1179	151.37	350	71.029	449.54	1.7726	0.9222	1.1719	146.79
355	58.161	458.53	1.8069	0.9106	1.1075	153.98	355	68.847	455.35	1.7891	0.9225	1.1531	149.78
360	56.673	464.05	1.8224	0.9138	1.1002	156.47	360	66.874	461.08	1.8051	0.9242	1.1393	152.57
365	55.296	469.54	1.8375	0.9177	1.0951	158.83	365	65.074	466.75	1.8207	0.9269	1.1293	155.21
370	54.016	475.00	1.8524	0.9220	1.0918	161.09	370	63.420	472.38	1.8361	0.9303	1.1219	157.72
375	52.821	480.46	1.8670	0.9268	1.0898	163.26	375	61.890	477.97	1.8511	0.9343	1.1168	160.10
380	51.700	485.91	1.8815	0.9319	1.0890	165.35	380	60.467	483.55	1.8658	0.9387	1.1133	162.38
385	50.645	491.35	1.8957	0.9373	1.0892	167.37	385	59.137	489.11	1.8804	0.9435	1.1112	164.58
390	49.648	496.80	1.9098	0.9428	1.0901	169.32	390	57.890	494.66	1.8947	0.9486	1.1102	166.69
395	48.705	502.25	1.9237	0.9486	1.0917	171.21	395	56.716	500.21	1.9089	0.9539	1.1101	168.72
400	47.810	507.72	1.9374	0.9545	1.0939	173.04	400	55.608	505.76	1.9228	0.9595	1.1108	170.69
410	46.146	518.68	1.9645	0.9668	1.0997	176.57	410	53.562	516.89	1.9503	0.9711	1.1142	174.46
420	44.628	529.72	1.9911	0.9794	1.1069	179.93	420	51.710	528.05	1.9772	0.9832	1.1195	178.02
430	43.233	540.83	2.0172	0.9924	1.1153	183.14	430	50.021	539.28	2.0036	0.9957	1.1264	181.40
440	41.946	552.03	2.0430	1.0055	1.1247	186.22	440	48.470	550.59	2.0296	1.0085	1.1344	184.64
450	40.750	563.32	2.0683	1.0189	1.1347	189.18	450	47.037	561.98	2.0552	1.0215	1.1434	187.75
460	39.636	574.72	2.0934	1.0324	1.1453	192.05	460	45.706	573.46	2.0804	1.0347	1.1531	190.74

TABLE 9. Thermodynamic properties of HFC-134a in the single-phase region — Continued

T/K	ρ/kg/m^3	h/kJ/kg	s/kJ/(kgK)	c_v/kJ/(kgK)	c_p/kJ/(kgK)	w/m/s	T/K	ρ/kg/m^3	h/kJ/kg	s/kJ/(kgK)	c_v/kJ/(kgK)	c_p/kJ/(kgK)	w/m/s
		1.80 MPa							**2.00 MPa**				
175	1579.7	78.360	0.4460	0.7915	1.1833	1100.5	175	1579.9	78.449	0.4458	0.7915	1.1832	1101.3
180	1566.5	84.282	0.4794	0.7917	1.1856	1075.3	180	1566.8	84.371	0.4792	0.7918	1.1854	1076.1
185	1553.3	90.218	0.5119	0.7932	1.1889	1050.1	185	1553.6	90.306	0.5117	0.7932	1.1888	1050.9
190	1540.0	96.173	0.5437	0.7955	1.1932	1025.1	190	1540.3	96.260	0.5435	0.7955	1.1930	1025.9
195	1526.7	102.15	0.5748	0.7985	1.1981	1000.3	195	1527.0	102.23	0.5745	0.7985	1.1979	1001.1
200	1513.3	108.15	0.6052	0.8020	1.2036	975.63	200	1513.6	108.24	0.6049	0.8021	1.2034	976.52
205	1499.8	114.18	0.6349	0.8060	1.2096	951.18	205	1500.1	114.27	0.6347	0.8060	1.2094	952.10
210	1486.2	120.25	0.6642	0.8103	1.2161	926.94	210	1486.5	120.33	0.6639	0.8103	1.2158	927.89
215	1472.5	126.35	0.6929	0.8149	1.2229	902.91	215	1472.8	126.43	0.6926	0.8149	1.2226	903.90
220	1458.6	132.48	0.7211	0.8197	1.2302	879.08	220	1459.0	132.56	0.7208	0.8197	1.2298	880.11
225	1444.7	138.65	0.7488	0.8246	1.2377	855.45	225	1445.1	138.73	0.7485	0.8247	1.2374	856.51
230	1430.6	144.86	0.7761	0.8298	1.2456	832.00	230	1431.0	144.93	0.7758	0.8298	1.2453	833.10
235	1416.4	151.11	0.8030	0.8351	1.2539	808.71	235	1416.8	151.18	0.8027	0.8351	1.2535	809.86
240	1401.9	157.40	0.8295	0.8404	1.2626	785.56	240	1402.4	157.47	0.8292	0.8405	1.2621	786.77
245	1387.3	163.73	0.8556	0.8459	1.2717	762.55	245	1387.8	163.80	0.8553	0.8460	1.2712	763.80
250	1372.5	170.12	0.8814	0.8516	1.2813	739.64	250	1373.1	170.18	0.8811	0.8516	1.2807	740.95
255	1357.5	176.55	0.9068	0.8573	1.2913	716.82	255	1358.1	176.61	0.9065	0.8573	1.2907	718.19
260	1342.2	183.03	0.9320	0.8631	1.3019	694.05	260	1342.8	183.09	0.9317	0.8631	1.3012	695.49
265	1326.6	189.57	0.9569	0.8689	1.3131	671.32	265	1327.3	189.62	0.9566	0.8689	1.3123	672.83
270	1310.7	196.16	0.9816	0.8749	1.3251	648.60	270	1311.4	196.21	0.9812	0.8749	1.3241	650.18
275	1294.5	202.82	1.0060	0.8811	1.3378	625.86	275	1295.3	202.87	1.0056	0.8810	1.3367	627.53
280	1277.9	209.54	1.0302	0.8873	1.3515	603.06	280	1278.7	209.58	1.0298	0.8872	1.3503	604.82
285	1260.8	216.34	1.0543	0.8936	1.3663	580.18	285	1261.7	216.37	1.0539	0.8935	1.3649	582.04
290	1243.2	223.21	1.0782	0.9001	1.3823	557.16	290	1244.2	223.24	1.0777	0.9000	1.3807	559.14
295	1225.1	230.16	1.1020	0.9067	1.3999	533.98	295	1226.2	230.18	1.1015	0.9066	1.3981	536.07
300	1206.3	237.21	1.1257	0.9135	1.4194	510.57	300	1207.5	237.22	1.1251	0.9134	1.4172	512.80
305	1186.8	244.36	1.1493	0.9205	1.4411	486.87	305	1188.1	244.36	1.1487	0.9204	1.4385	489.27
310	1166.5	251.63	1.1729	0.9278	1.4657	462.81	310	1167.9	251.61	1.1723	0.9276	1.4625	465.39
315	1145.0	259.03	1.1966	0.9353	1.4940	438.30	315	1146.7	258.99	1.1959	0.9350	1.4900	441.10
320	1122.4	266.58	1.2204	0.9432	1.5270	413.21	320	1124.3	266.52	1.2196	0.9428	1.5221	416.27
325	1098.2	274.31	1.2444	0.9514	1.5667	387.37	325	1100.4	274.22	1.2435	0.9510	1.5603	390.75
330	1072.2	282.26	1.2686	0.9603	1.6157	360.54	330	1074.7	282.14	1.2677	0.9597	1.6071	364.32
335	1043.6	290.49	1.2934	0.9701	1.6791	332.32	335	1046.7	290.31	1.2923	0.9692	1.6670	336.63
336.04	1037.3	292.25	1.2986	0.9722	1.6950	326.18	340	1015.5	298.84	1.3176	0.9800	1.7482	307.08
336.04	94.681	427.35	1.7007	0.9690	1.4393	130.00	340.63	1011.3	299.95	1.3208	0.9814	1.7606	303.17
340	90.885	432.87	1.7170	0.9548	1.3568	133.80	340.63	107.62	428.28	1.6975	0.9878	1.5389	127.16
345	86.873	439.47	1.7363	0.9441	1.2881	138.04	345	102.38	434.72	1.7164	0.9700	1.4224	131.78
350	83.474	445.79	1.7545	0.9385	1.2423	141.82	350	97.518	441.61	1.7362	0.9582	1.3391	136.34
355	80.521	451.92	1.7718	0.9360	1.2101	145.27	355	93.460	448.16	1.7548	0.9518	1.2844	140.38
360	77.909	457.91	1.7886	0.9357	1.1869	148.44	360	89.973	454.48	1.7724	0.9487	1.2463	144.03
365	75.565	463.80	1.8048	0.9369	1.1697	151.40	365	86.914	460.64	1.7894	0.9480	1.2188	147.38
370	73.441	469.61	1.8207	0.9392	1.1570	154.19	370	84.188	466.68	1.8059	0.9488	1.1984	150.49
375	71.498	475.37	1.8361	0.9422	1.1475	156.82	375	81.730	472.64	1.8219	0.9507	1.1832	153.40

TABLE 9. Thermodynamic properties of HFC-134a in the single-phase region — Continued

T/K	ρ/kg/m^3	h/kJ/kg	s/kJ/(kgK)	c_v/kJ/(kgK)	c_p/kJ/(kgK)	w/m/s	T/K	ρ/kg/m^3	h/kJ/kg	s/kJ/(kgK)	c_v/kJ/(kgK)	c_p/kJ/(kgK)	w/m/s
			1.80 MPa							**2.00 MPa**			
380	69.709	481.09	1.8513	0.9459	1.1406	159.32	380	79.494	478.52	1.8374	0.9534	1.1718	156.14
385	68.052	486.78	1.8662	0.9500	1.1356	161.70	385	77.442	484.36	1.8527	0.9569	1.1632	158.74
390	66.509	492.45	1.8808	0.9546	1.1323	163.99	390	75.548	490.16	1.8677	0.9608	1.1568	161.21
395	65.066	498.11	1.8952	0.9594	1.1302	166.18	395	73.790	495.93	1.8824	0.9651	1.1523	163.58
400	63.712	503.75	1.9094	0.9646	1.1292	168.29	400	72.150	501.68	1.8969	0.9698	1.1492	165.85
410	61.230	515.05	1.9373	0.9754	1.1297	172.31	410	69.170	513.16	1.9252	0.9799	1.1464	170.13
420	59.003	526.36	1.9645	0.9870	1.1328	176.09	420	66.521	524.62	1.9528	0.9909	1.1471	174.14
430	56.986	537.71	1.9913	0.9990	1.1380	179.66	430	64.139	536.11	1.9798	1.0024	1.1503	177.91
440	55.145	549.12	2.0175	1.0114	1.1446	183.06	440	61.979	547.64	2.0063	1.0144	1.1553	181.47
450	53.453	560.61	2.0433	1.0241	1.1524	186.31	450	60.004	559.22	2.0324	1.0268	1.1619	184.87
460	51.889	572.18	2.0687	1.0371	1.1612	189.43	460	58.188	570.88	2.0580	1.0395	1.1695	188.12
			2.50 MPa							**3.00 MPa**			
175	1580.5	78.674	0.4453	0.7917	1.1828	1103.1	175	1581.2	78.899	0.4448	0.7918	1.1824	1105.0
180	1567.4	84.593	0.4787	0.7920	1.1850	1078.0	180	1568.1	84.816	0.4781	0.7921	1.1846	1079.9
185	1554.3	90.526	0.5112	0.7934	1.1883	1052.9	185	1554.9	90.747	0.5106	0.7935	1.1879	1054.9
190	1541.0	96.478	0.5429	0.7957	1.1925	1028.0	190	1541.7	96.697	0.5424	0.7958	1.1920	1030.0
195	1527.7	102.45	0.5739	0.7987	1.1974	1003.2	195	1528.5	102.66	0.5734	0.7988	1.1969	1005.3
200	1514.4	108.45	0.6043	0.8022	1.2028	978.72	200	1515.2	108.66	0.6038	0.8023	1.2023	980.91
205	1500.9	114.48	0.6341	0.8062	1.2088	954.38	205	1501.7	114.69	0.6335	0.8063	1.2082	956.65
210	1487.4	120.54	0.6633	0.8105	1.2152	930.26	210	1488.2	120.75	0.6627	0.8106	1.2145	932.61
215	1473.7	126.63	0.6920	0.8150	1.2219	906.35	215	1474.6	126.83	0.6914	0.8152	1.2212	908.79
220	1460.0	132.76	0.7202	0.8198	1.2290	882.66	220	1460.9	132.96	0.7195	0.8199	1.2282	885.19
225	1446.1	138.92	0.7479	0.8248	1.2365	859.16	225	1447.1	139.12	0.7472	0.8249	1.2356	861.79
230	1432.1	145.12	0.7751	0.8299	1.2443	835.86	230	1433.2	145.32	0.7744	0.8300	1.2434	838.59
235	1417.9	151.37	0.8020	0.8352	1.2525	812.73	235	1419.1	151.55	0.8013	0.8353	1.2514	815.57
240	1403.6	157.65	0.8284	0.8405	1.2610	789.75	240	1404.8	157.83	0.8277	0.8406	1.2598	792.71
245	1389.1	163.98	0.8545	0.8460	1.2699	766.92	245	1390.4	164.15	0.8538	0.8461	1.2686	770.00
250	1374.4	170.35	0.8803	0.8516	1.2792	744.20	250	1375.8	170.52	0.8795	0.8517	1.2778	747.42
255	1359.5	176.77	0.9057	0.8573	1.2891	721.59	255	1361.0	176.93	0.9049	0.8573	1.2875	724.95
260	1344.4	183.24	0.9308	0.8631	1.2994	699.05	260	1345.9	183.39	0.9300	0.8631	1.2976	702.56
265	1328.9	189.77	0.9557	0.8689	1.3103	676.56	265	1330.6	189.91	0.9548	0.8689	1.3083	680.24
270	1313.2	196.35	0.9803	0.8749	1.3219	654.10	270	1315.0	196.48	0.9794	0.8748	1.3197	657.97
275	1297.2	202.99	1.0047	0.8809	1.3342	631.65	275	1299.1	203.11	1.0037	0.8809	1.3317	635.71
280	1280.8	209.69	1.0288	0.8871	1.3474	609.17	280	1282.8	209.80	1.0278	0.8870	1.3445	613.44
285	1263.9	216.46	1.0528	0.8934	1.3615	586.63	285	1266.1	216.56	1.0517	0.8933	1.3583	591.14
290	1246.7	223.31	1.0766	0.8998	1.3769	564.00	290	1249.0	223.38	1.0755	0.8996	1.3732	568.77
295	1228.8	230.23	1.1003	0.9064	1.3936	541.24	295	1231.4	230.29	1.0991	0.9061	1.3893	546.30
300	1210.4	237.25	1.1238	0.9131	1.4119	518.31	300	1213.3	237.28	1.1226	0.9128	1.4069	523.69
305	1191.4	244.36	1.1473	0.9199	1.4322	495.16	305	1194.5	244.36	1.1460	0.9196	1.4263	500.90
310	1171.5	251.57	1.1708	0.9270	1.4550	471.72	310	1175.0	251.55	1.1694	0.9266	1.4479	477.88
315	1150.7	258.91	1.1943	0.9344	1.4808	447.94	315	1154.6	258.85	1.1927	0.9338	1.4722	454.56

TABLE 9. Thermodynamic properties of HFC-134a in the single-phase region — Continued

T/K	ρ/kg/m³	h/kJ/kg	s/kJ/(kgK)	c_v/kJ/(kgK)	c_p/kJ/(kgK)	w/m/s
			2.50 MPa			
320	1128.8	266.39	1.2178	0.9420	1.5105	423.71
325	1105.7	274.03	1.2415	0.9499	1.5455	398.92
330	1080.9	281.85	1.2654	0.9584	1.5876	373.39
335	1054.0	289.92	1.2897	0.9674	1.6400	346.89
340	1024.5	298.28	1.3145	0.9773	1.7083	319.00
345	991.37	307.05	1.3401	0.9888	1.8036	289.00
350	952.48	316.41	1.3670	1.0032	1.9531	255.42
350.72	946.14	317.84	1.3711	1.0057	1.9829	250.07
350.72	144.08	429.00	1.6880	1.0336	1.8832	119.73
355	134.91	436.49	1.7092	1.0085	1.6473	125.61
360	126.89	444.31	1.7311	0.9917	1.4977	131.24
365	120.55	451.56	1.7511	0.9823	1.4072	136.04
370	115.31	458.44	1.7698	0.9773	1.3470	140.29
375	110.83	465.06	1.7876	0.9750	1.3046	144.12
380	106.92	471.50	1.8047	0.9746	1.2736	147.63
385	103.45	477.81	1.8212	0.9756	1.2503	150.89
390	100.34	484.01	1.8372	0.9776	1.2326	153.94
395	97.517	490.14	1.8528	0.9803	1.2189	156.80
400	94.935	496.21	1.8681	0.9836	1.2085	159.52
410	90.360	508.22	1.8977	0.9916	1.1945	164.56
420	86.400	520.12	1.9264	1.0009	1.1871	169.19
430	82.915	531.98	1.9543	1.0111	1.1842	173.48
440	79.810	543.82	1.9815	1.0221	1.1846	177.49
450	77.012	555.68	2.0082	1.0336	1.1873	181.28
460	74.471	567.57	2.0343	1.0454	1.1920	184.87
			3.50 MPa			
175	1581.8	79.124	0.4443	0.7920	1.1821	1106.8
180	1568.7	85.039	0.4776	0.7923	1.1842	1081.8
185	1555.6	90.968	0.5101	0.7937	1.1875	1056.9
190	1542.4	96.916	0.5418	0.7960	1.1916	1032.1
195	1529.2	102.88	0.5728	0.7990	1.1964	1007.5
200	1515.9	108.88	0.6032	0.8025	1.2017	983.09
205	1502.6	114.90	0.6329	0.8064	1.2076	958.90
210	1489.1	120.95	0.6621	0.8107	1.2139	934.94
215	1475.6	127.04	0.6907	0.8153	1.2205	911.21
220	1461.9	133.16	0.7189	0.8201	1.2275	887.70
225	1448.1	139.31	0.7465	0.8250	1.2348	864.40
230	1434.2	145.51	0.7738	0.8301	1.2424	841.30
235	1420.2	151.74	0.8006	0.8354	1.2504	818.39
240	1406.0	158.01	0.8270	0.8407	1.2587	795.65
245	1391.7	164.33	0.8530	0.8462	1.2674	773.06

T/K	ρ/kg/m³	h/kJ/kg	s/kJ/(kgK)	c_v/kJ/(kgK)	c_p/kJ/(kgK)	w/m/s
			3.00 MPa			
320	1133.2	266.27	1.2161	0.9412	1.5000	430.88
325	1110.7	273.85	1.2396	0.9490	1.5322	406.74
330	1086.6	281.61	1.2633	0.9571	1.5704	382.01
335	1060.8	289.57	1.2872	0.9658	1.6169	356.51
340	1032.8	297.80	1.3116	0.9752	1.6756	329.96
345	1001.6	306.36	1.3366	0.9856	1.7537	301.90
350	966.21	315.39	1.3626	0.9979	1.8662	271.48
355	923.81	325.14	1.3903	1.0140	2.0524	236.94
359.35	876.21	334.70	1.4170	1.0360	2.3876	200.05
359.35	189.34	427.33	1.6748	1.0812	2.5274	111.90
360	186.15	428.92	1.6792	1.0738	2.3968	113.25
365	168.26	439.35	1.7080	1.0364	1.8670	121.69
370	156.44	448.06	1.7317	1.0172	1.6425	128.11
375	147.53	455.93	1.7528	1.0065	1.5163	133.47
380	140.36	463.30	1.7723	1.0006	1.4355	138.13
385	134.37	470.33	1.7907	0.9976	1.3797	142.31
390	129.22	477.12	1.8083	0.9967	1.3393	146.11
395	124.71	483.74	1.8251	0.9972	1.3090	149.61
400	120.69	490.23	1.8414	0.9987	1.2859	152.87
410	113.81	502.91	1.8728	1.0040	1.2542	158.80
420	108.05	515.35	1.9027	1.0114	1.2349	164.14
430	103.12	527.64	1.9317	1.0201	1.2236	169.01
440	98.811	539.84	1.9597	1.0299	1.2178	173.51
450	94.993	552.01	1.9871	1.0404	1.2158	177.71
460	91.570	564.17	2.0138	1.0515	1.2167	181.66
			4.00 MPa			
175	1582.4	79.349	0.4437	0.7921	1.1817	1108.7
180	1569.4	85.262	0.4771	0.7924	1.1838	1083.7
185	1556.3	91.189	0.5095	0.7938	1.1870	1058.8
190	1543.1	97.134	0.5412	0.7961	1.1911	1034.1
195	1530.0	103.10	0.5722	0.7991	1.1959	1009.5
200	1516.7	109.09	0.6026	0.8026	1.2012	985.26
205	1503.4	115.11	0.6323	0.8066	1.2070	961.15
210	1490.0	121.16	0.6615	0.8109	1.2132	937.27
215	1476.5	127.24	0.6901	0.8154	1.2198	913.62
220	1462.8	133.36	0.7182	0.8202	1.2267	890.20
225	1449.1	139.51	0.7459	0.8251	1.2340	866.99
230	1435.3	145.70	0.7731	0.8302	1.2415	843.99
235	1421.3	151.93	0.7999	0.8354	1.2494	821.19
240	1407.2	158.20	0.8263	0.8408	1.2576	798.56
245	1392.9	164.51	0.8523	0.8462	1.2662	776.09

TABLE 9. Thermodynamic properties of HFC-134a in the single-phase region — Continued

T/K	ρ kg/m³	h kJ/kg	s kJ/(kgK)	c_v kJ/(kgK)	c_p kJ/(kgK)	w m/s	T/K	ρ kg/m³	h kJ/kg	s kJ/(kgK)	c_v kJ/(kgK)	c_p kJ/(kgK)	w m/s
			3.50 MPa							**4.00 MPa**			
250	1377.1	170.69	0.8787	0.8517	1.2765	750.61	250	1378.4	170.86	0.8779	0.8518	1.2751	753.77
255	1362.4	177.09	0.9041	0.8574	1.2860	728.28	255	1363.8	177.26	0.9033	0.8574	1.2845	731.57
260	1347.4	183.55	0.9292	0.8631	1.2959	706.04	260	1348.9	183.70	0.9283	0.8631	1.2943	709.48
265	1332.2	190.05	0.9539	0.8689	1.3064	683.88	265	1333.8	190.20	0.9531	0.8689	1.3046	687.48
270	1316.7	196.61	0.9785	0.8748	1.3175	661.78	270	1318.4	196.75	0.9776	0.8748	1.3155	665.55
275	1300.9	203.23	1.0027	0.8808	1.3293	639.71	275	1302.7	203.36	1.0018	0.8808	1.3270	643.66
280	1284.8	209.91	1.0268	0.8869	1.3418	617.65	280	1286.8	210.02	1.0258	0.8868	1.3392	621.80
285	1268.3	216.65	1.0507	0.8931	1.3552	595.58	285	1270.4	216.75	1.0496	0.8930	1.3522	599.94
290	1251.4	223.46	1.0744	0.8995	1.3696	573.46	290	1253.7	223.55	1.0733	0.8993	1.3662	578.06
295	1234.0	230.35	1.0979	0.9059	1.3852	551.26	295	1236.5	230.42	1.0968	0.9057	1.3813	556.12
300	1216.1	237.32	1.1213	0.9125	1.4021	528.95	300	1218.8	237.36	1.1201	0.9122	1.3976	534.11
305	1197.6	244.37	1.1447	0.9192	1.4207	506.50	305	1200.5	244.39	1.1434	0.9189	1.4154	511.98
310	1178.3	251.53	1.1679	0.9261	1.4412	483.86	310	1181.6	251.52	1.1665	0.9257	1.4350	489.70
315	1158.3	258.79	1.1912	0.9332	1.4642	460.99	315	1162.0	258.75	1.1897	0.9327	1.4568	467.23
320	1137.4	266.18	1.2144	0.9405	1.4902	437.81	320	1141.5	266.09	1.2128	0.9399	1.4812	444.52
325	1115.4	273.70	1.2378	0.9481	1.5201	414.26	325	1120.0	273.57	1.2360	0.9474	1.5090	421.50
330	1092.1	281.39	1.2612	0.9561	1.5550	390.24	330	1097.3	281.19	1.2593	0.9551	1.5411	398.11
335	1067.2	289.26	1.2849	0.9644	1.5967	365.61	335	1073.3	288.99	1.2827	0.9632	1.5789	374.24
340	1040.4	297.37	1.3089	0.9733	1.6480	340.17	340	1047.4	296.99	1.3064	0.9718	1.6244	349.76
345	1010.9	305.77	1.3335	0.9831	1.7138	313.62	345	1019.4	305.25	1.3305	0.9809	1.6811	324.44
350	978.08	314.55	1.3587	0.9940	1.8032	285.45	350	988.60	313.83	1.3552	0.9910	1.7547	297.97
355	940.10	323.87	1.3852	1.0073	1.9361	254.71	355	953.80	322.85	1.3808	1.0026	1.8566	269.80
360	893.69	334.07	1.4137	1.0254	2.1686	219.41	360	913.11	332.49	1.4078	1.0169	2.0126	238.94
365	828.82	346.11	1.4469	1.0577	2.7721	174.01	365	862.29	343.18	1.4373	1.0370	2.3000	203.34
366.87	791.62	351.87	1.4626	1.0821	3.4836	150.35	370	787.42	356.29	1.4729	1.0747	3.1454	157.31
366.87	252.01	422.22	1.6544	1.1368	4.2922	103.53	373.49	632.86	375.56	1.5247	1.1854	26.325	97.697
370	223.39	432.44	1.6821	1.0889	2.6737	111.78	373.49	390.23	405.37	1.6045	1.2261	37.631	93.112
375	199.47	443.83	1.7127	1.0532	2.0098	120.57	375	309.97	421.21	1.6469	1.1550	5.5638	101.80
380	184.26	453.14	1.7374	1.0351	1.7428	127.25	380	251.91	438.79	1.6935	1.0887	2.6008	114.10
385	173.03	461.45	1.7591	1.0249	1.5957	132.81	385	225.87	450.16	1.7232	1.0616	2.0370	122.12
390	164.11	469.18	1.7791	1.0192	1.5023	137.65	390	208.71	459.64	1.7477	1.0471	1.7837	128.50
395	156.73	476.53	1.7978	1.0164	1.4381	141.97	395	195.91	468.17	1.7694	1.0388	1.6380	133.92
400	150.43	483.59	1.8156	1.0154	1.3915	145.91	400	185.71	476.11	1.7894	1.0343	1.5433	138.70
410	140.11	497.17	1.8491	1.0173	1.3300	152.90	410	170.04	490.91	1.8259	1.0315	1.4288	146.93
420	131.84	510.27	1.8807	1.0223	1.2928	159.04	420	158.21	504.85	1.8595	1.0337	1.3640	153.96
430	124.98	523.08	1.9108	1.0294	1.2698	164.55	430	148.77	518.27	1.8911	1.0389	1.3242	160.15
440	119.13	535.70	1.9398	1.0379	1.2557	169.57	440	140.94	531.38	1.9212	1.0460	1.2991	165.71
450	114.04	548.21	1.9679	1.0474	1.2476	174.21	450	134.27	544.28	1.9502	1.0544	1.2833	170.80
460	109.55	560.67	1.9953	1.0576	1.2439	178.53	460	128.49	557.07	1.9783	1.0638	1.2739	175.50

TABLE 9. Thermodynamic properties of HFC-134a in the single-phase region — Continued

T/K	ρ kg/m³	h kJ/kg	s kJ/(kgK)	c_v kJ/(kgK)	c_p kJ/(kgK)	w m/s	T/K	ρ kg/m³	h kJ/kg	s kJ/(kgK)	c_v kJ/(kgK)	c_p kJ/(kgK)	w m/s
			5.00 MPa							**6.00 MPa**			
175	1583.6	79.799	0.4427	0.7925	1.1810	1112.3	175	1584.8	80.250	0.4417	0.7928	1.1803	1115.9
180	1570.6	85.709	0.4760	0.7927	1.1831	1087.5	180	1571.9	86.156	0.4750	0.7931	1.1823	1091.2
185	1557.6	91.632	0.5085	0.7942	1.1862	1062.7	185	1558.9	92.075	0.5074	0.7945	1.1854	1066.6
190	1544.5	97.573	0.5401	0.7964	1.1902	1038.1	190	1545.9	98.012	0.5391	0.7968	1.1893	1042.1
195	1531.4	103.53	0.5711	0.7994	1.1949	1013.7	195	1532.9	103.97	0.5700	0.7997	1.1939	1017.8
200	1518.2	109.52	0.6014	0.8029	1.2001	989.55	200	1519.8	109.95	0.6003	0.8032	1.1991	993.79
205	1505.0	115.53	0.6311	0.8069	1.2059	965.59	205	1506.6	115.96	0.6300	0.8072	1.2047	969.98
210	1491.7	121.58	0.6603	0.8111	1.2120	941.87	210	1493.3	122.00	0.6591	0.8114	1.2108	946.41
215	1478.2	127.65	0.6889	0.8157	1.2184	918.38	215	1480.0	128.07	0.6876	0.8159	1.2171	923.09
220	1464.7	133.76	0.7170	0.8204	1.2252	895.14	220	1466.6	134.17	0.7157	0.8207	1.2238	900.01
225	1451.1	139.91	0.7446	0.8254	1.2323	872.12	225	1453.1	140.31	0.7433	0.8256	1.2308	877.17
230	1437.4	146.09	0.7717	0.8304	1.2397	849.31	230	1439.4	146.48	0.7704	0.8307	1.2380	854.55
235	1423.5	152.31	0.7985	0.8356	1.2475	826.71	235	1425.7	152.69	0.7971	0.8359	1.2456	832.15
240	1409.5	158.56	0.8248	0.8410	1.2555	804.30	240	1411.8	158.93	0.8234	0.8412	1.2534	809.95
245	1395.4	164.86	0.8508	0.8464	1.2638	782.06	245	1397.8	165.22	0.8494	0.8465	1.2616	787.93
250	1381.1	171.20	0.8764	0.8519	1.2725	759.99	250	1383.6	171.55	0.8749	0.8520	1.2700	766.09
255	1366.6	177.59	0.9017	0.8575	1.2816	738.05	255	1369.3	177.92	0.9002	0.8576	1.2789	744.41
260	1351.9	184.02	0.9267	0.8632	1.2911	716.25	260	1354.7	184.34	0.9251	0.8632	1.2881	722.87
265	1336.9	190.50	0.9514	0.8689	1.3011	694.55	265	1340.0	190.81	0.9497	0.8690	1.2977	701.45
270	1321.8	197.03	0.9758	0.8748	1.3115	672.94	270	1325.0	197.32	0.9741	0.8748	1.3078	680.15
275	1306.3	203.62	1.0000	0.8807	1.3225	651.40	275	1309.8	203.88	0.9982	0.8807	1.3184	658.94
280	1290.6	210.26	1.0239	0.8867	1.3342	629.92	280	1294.3	210.50	1.0220	0.8866	1.3295	637.81
285	1274.6	216.96	1.0476	0.8928	1.3466	608.47	285	1278.6	217.18	1.0457	0.8927	1.3413	616.74
290	1258.1	223.73	1.0712	0.8990	1.3598	587.03	290	1262.4	223.92	1.0691	0.8988	1.3538	595.72
295	1241.3	230.56	1.0945	0.9053	1.3739	565.59	295	1246.0	230.72	1.0923	0.9050	1.3672	574.72
300	1224.0	237.47	1.1177	0.9118	1.3891	544.11	300	1229.1	237.59	1.1154	0.9114	1.3814	553.73
305	1206.3	244.45	1.1408	0.9183	1.4056	522.57	305	1211.7	244.54	1.1384	0.9178	1.3968	532.72
310	1187.9	251.53	1.1638	0.9250	1.4236	500.95	310	1193.9	251.56	1.1612	0.9244	1.4133	511.69
315	1168.9	258.69	1.1868	0.9318	1.4433	479.21	315	1175.5	258.67	1.1840	0.9311	1.4313	490.60
320	1149.2	265.96	1.2097	0.9388	1.4651	457.33	320	1156.4	265.88	1.2067	0.9379	1.4511	469.44
325	1128.6	273.35	1.2326	0.9460	1.4895	435.26	325	1136.7	273.19	1.2294	0.9449	1.4728	448.18
330	1107.1	280.87	1.2555	0.9535	1.5172	412.96	330	1116.0	280.61	1.2520	0.9521	1.4970	426.80
335	1084.4	288.53	1.2786	0.9612	1.5488	390.38	335	1094.5	288.16	1.2747	0.9595	1.5242	405.25
340	1060.3	296.36	1.3018	0.9692	1.5858	367.43	340	1071.8	295.86	1.2975	0.9671	1.5552	383.51
345	1034.5	304.40	1.3252	0.9776	1.6297	344.02	345	1047.8	303.72	1.3205	0.9750	1.5909	361.53
350	1006.7	312.68	1.3491	0.9865	1.6835	320.00	350	1022.2	311.78	1.3437	0.9833	1.6328	339.24
355	976.37	321.26	1.3734	0.9962	1.7516	295.18	355	994.81	320.07	1.3672	0.9920	1.6831	316.57
360	942.46	330.23	1.3985	1.0071	1.8419	269.24	360	964.98	328.63	1.3911	1.0013	1.7449	293.41
365	903.68	339.74	1.4247	1.0197	1.9704	241.70	365	932.15	337.54	1.4157	1.0114	1.8236	269.61
370	857.42	350.06	1.4528	1.0357	2.1738	211.76	370	895.34	346.91	1.4412	1.0228	1.9282	244.98
375	797.97	361.77	1.4843	1.0582	2.5623	178.12	375	853.01	356.90	1.4680	1.0359	2.0756	219.34
380	707.99	376.73	1.5239	1.0968	3.6466	138.88	380	802.55	367.79	1.4969	1.0520	2.3000	192.53
385	526.36	402.59	1.5914	1.1591	6.5852	106.37	385	739.25	380.14	1.5292	1.0725	2.6718	164.91

TABLE 9. Thermodynamic properties of HFC-134a in the single-phase region — Continued

T/K	ρ kg/m³	h kJ/kg	s kJ/(kgK)	c_v kJ/(kgK)	c_p kJ/(kgK)	w m/s	T/K	ρ kg/m³	h kJ/kg	s kJ/(kgK)	c_v kJ/(kgK)	c_p kJ/(kgK)	w m/s
			5.00 MPa							**6.00 MPa**			
390	377.18	429.39	1.6606	1.1305	3.9290	110.04	390	655.55	394.91	1.5673	1.0982	3.2729	139.14
395	318.11	445.28	1.7011	1.0985	2.6553	117.81	395	551.84	412.68	1.6125	1.1196	3.7256	123.06
400	285.05	457.15	1.7310	1.0802	2.1579	124.51	400	458.74	430.63	1.6577	1.1188	3.3383	119.99
410	245.61	476.32	1.7783	1.0630	1.7427	135.45	410	354.00	458.21	1.7259	1.0949	2.3028	127.67
420	221.02	492.74	1.8179	1.0578	1.5629	144.32	420	302.04	478.75	1.7754	1.0818	1.8656	137.00
430	203.38	507.84	1.8535	1.0584	1.4650	151.89	430	269.64	496.26	1.8166	1.0775	1.6582	145.35
440	189.75	522.17	1.8864	1.0623	1.4057	158.53	440	246.66	512.21	1.8533	1.0781	1.5421	152.75
450	178.72	536.02	1.9175	1.0684	1.3677	164.50	450	229.10	527.25	1.8871	1.0818	1.4706	159.37
460	169.50	549.57	1.9473	1.0759	1.3428	169.93	460	215.04	541.71	1.9188	1.0875	1.4240	165.38
			7.00 MPa							**8.00 MPa**			
175	1586.0	80.702	0.4406	0.7931	1.1796	1119.5	175	1587.2	81.154	0.4396	0.7934	1.1790	1123.0
180	1573.1	86.604	0.4739	0.7934	1.1816	1094.9	180	1574.4	87.053	0.4729	0.7937	1.1809	1098.5
185	1560.2	92.520	0.5063	0.7948	1.1846	1070.4	185	1561.5	92.965	0.5053	0.7951	1.1838	1074.1
190	1547.3	98.452	0.5380	0.7971	1.1885	1046.0	190	1548.6	98.893	0.5369	0.7974	1.1876	1049.9
195	1534.3	104.40	0.5689	0.8000	1.1930	1021.9	195	1535.7	104.84	0.5678	0.8003	1.1921	1025.9
200	1521.3	110.38	0.5992	0.8035	1.1981	997.99	200	1522.7	110.81	0.5980	0.8038	1.1971	1002.1
205	1508.2	116.38	0.6288	0.8074	1.2037	974.32	205	1509.7	116.81	0.6277	0.8077	1.2026	978.61
210	1495.0	122.42	0.6579	0.8117	1.2096	950.90	210	1496.6	122.84	0.6567	0.8120	1.2084	955.34
215	1481.7	128.48	0.6864	0.8162	1.2158	927.74	215	1483.5	128.90	0.6852	0.8165	1.2146	932.32
220	1468.4	134.58	0.7145	0.8209	1.2224	904.82	220	1470.2	134.99	0.7132	0.8212	1.2211	909.57
225	1455.0	140.71	0.7420	0.8258	1.2293	882.15	225	1456.9	141.11	0.7407	0.8261	1.2278	887.07
230	1441.5	146.87	0.7691	0.8309	1.2364	859.71	230	1443.5	147.26	0.7678	0.8311	1.2348	864.80
235	1427.8	153.07	0.7958	0.8361	1.2438	837.50	235	1429.9	153.46	0.7944	0.8363	1.2420	842.78
240	1414.1	159.31	0.8220	0.8413	1.2514	815.50	240	1416.3	159.69	0.8207	0.8416	1.2495	820.97
245	1400.2	165.59	0.8479	0.8467	1.2594	793.70	245	1402.5	165.95	0.8465	0.8469	1.2573	799.37
250	1386.1	171.90	0.8734	0.8522	1.2677	772.09	250	1388.6	172.26	0.8720	0.8523	1.2654	777.97
255	1371.9	178.26	0.8986	0.8577	1.2763	750.64	255	1374.6	178.61	0.8971	0.8579	1.2738	756.76
260	1357.6	184.67	0.9235	0.8633	1.2852	729.36	260	1360.3	185.00	0.9219	0.8635	1.2824	735.71
265	1343.0	191.12	0.9481	0.8690	1.2945	708.21	265	1345.9	191.43	0.9465	0.8691	1.2915	714.83
270	1328.2	197.61	0.9724	0.8748	1.3042	687.20	270	1331.4	197.91	0.9707	0.8749	1.3009	694.09
275	1313.2	204.16	0.9964	0.8806	1.3144	666.30	275	1316.6	204.44	0.9947	0.8807	1.3107	673.48
280	1298.0	210.76	1.0202	0.8866	1.3251	645.50	280	1301.5	211.02	1.0184	0.8865	1.3210	652.99
285	1282.5	217.41	1.0437	0.8926	1.3364	624.78	285	1286.2	217.65	1.0418	0.8925	1.3318	632.60
290	1266.6	224.12	1.0671	0.8986	1.3483	604.14	290	1270.7	224.34	1.0651	0.8985	1.3432	612.31
295	1250.5	230.90	1.0902	0.9048	1.3609	583.55	295	1254.8	231.09	1.0882	0.9046	1.3552	592.11
300	1233.9	237.74	1.1132	0.9111	1.3744	563.00	300	1238.6	237.90	1.1110	0.9108	1.3679	571.97
305	1217.0	244.64	1.1360	0.9174	1.3887	542.49	305	1222.0	244.77	1.1338	0.9171	1.3813	551.90
310	1199.6	251.63	1.1588	0.9239	1.4041	521.98	310	1205.1	251.71	1.1563	0.9235	1.3957	531.87
315	1181.7	258.69	1.1813	0.9305	1.4207	501.47	315	1187.6	258.73	1.1788	0.9299	1.4111	511.88
320	1163.3	265.83	1.2039	0.9372	1.4386	480.95	320	1169.7	265.82	1.2011	0.9365	1.4276	491.92
325	1144.2	273.08	1.2263	0.9440	1.4583	460.39	325	1151.3	273.01	1.2234	0.9432	1.4454	471.98

TABLE 9. Thermodynamic properties of HFC-134a in the single-phase region — Continued

T/K	ρ kg/m³	h kJ/kg	s kJ/(kgK)	c_v kJ/(kgK)	c_p kJ/(kgK)	w m/s	T/K	ρ kg/m³	h kJ/kg	s kJ/(kgK)	c_v kJ/(kgK)	c_p kJ/(kgK)	w m/s
			7.00 MPa							**8.00 MPa**			
330	1124.4	280.42	1.2487	0.9510	1.4798	439.78	330	1132.2	280.28	1.2456	0.9500	1.4648	452.05
335	1103.8	287.88	1.2712	0.9581	1.5036	419.11	335	1112.4	287.66	1.2678	0.9570	1.4860	432.13
340	1082.2	295.46	1.2936	0.9655	1.5302	398.36	340	1091.8	295.15	1.2900	0.9641	1.5093	412.20
345	1059.6	303.19	1.3162	0.9730	1.5602	377.50	345	1070.4	302.75	1.3122	0.9714	1.5350	392.26
350	1035.8	311.07	1.3389	0.9808	1.5943	356.52	350	1047.9	310.50	1.3345	0.9788	1.5637	372.32
355	1010.5	319.14	1.3618	0.9889	1.6338	335.39	355	1024.3	318.40	1.3569	0.9865	1.5961	352.35
360	983.54	327.42	1.3849	0.9973	1.6801	314.06	360	999.45	326.47	1.3795	0.9944	1.6328	332.37
365	954.44	335.96	1.4085	1.0062	1.7354	292.52	365	972.99	334.74	1.4023	1.0026	1.6749	312.38
370	922.80	344.80	1.4325	1.0157	1.8030	270.72	370	944.72	343.23	1.4254	1.0111	1.7238	292.39
375	887.95	354.01	1.4573	1.0260	1.8876	248.65	375	914.32	351.99	1.4489	1.0200	1.7812	272.44
380	849.03	363.71	1.4830	1.0373	1.9963	226.36	380	881.39	361.06	1.4729	1.0294	1.8493	252.59
385	804.82	374.03	1.5100	1.0499	2.1396	204.03	385	845.45	370.50	1.4976	1.0394	1.9307	232.99
390	753.72	385.19	1.5387	1.0641	2.3290	182.21	390	805.95	380.39	1.5232	1.0500	2.0278	213.88
395	694.22	397.40	1.5699	1.0795	2.5628	162.21	395	762.38	390.81	1.5497	1.0611	2.1404	195.71
400	626.75	410.79	1.6035	1.0942	2.7806	146.32	400	714.52	401.81	1.5774	1.0725	2.2616	179.21
410	493.97	438.89	1.6729	1.1061	2.6996	133.10	410	609.72	425.44	1.6357	1.0924	2.4324	155.02
420	403.92	463.43	1.7321	1.0992	2.2163	135.79	420	511.20	449.50	1.6937	1.1013	2.3311	145.45
430	348.97	483.81	1.7801	1.0933	1.8903	142.46	430	436.95	471.54	1.7456	1.1018	2.0734	145.87
440	312.32	501.70	1.8212	1.0919	1.7027	149.50	440	384.99	491.13	1.7906	1.1016	1.8560	150.28
450	285.70	518.11	1.8581	1.0938	1.5886	156.18	450	347.58	508.89	1.8305	1.1031	1.7077	155.83
460	265.18	533.60	1.8921	1.0980	1.5150	162.39	460	319.31	525.44	1.8669	1.1067	1.6084	161.56
			10.00 MPa							**12.00 MPa**			
175	1589.5	82.060	0.4376	0.7941	1.1777	1130.1	175	1591.8	82.968	0.4356	0.7948	1.1764	1136.9
180	1576.8	87.952	0.4708	0.7944	1.1795	1105.8	180	1579.2	88.854	0.4688	0.7950	1.1781	1112.9
185	1564.1	93.857	0.5032	0.7958	1.1823	1081.6	185	1566.6	94.751	0.5011	0.7964	1.1809	1088.9
190	1551.3	99.778	0.5347	0.7980	1.1860	1057.6	190	1554.0	100.66	0.5326	0.7987	1.1845	1065.1
195	1538.5	105.71	0.5656	0.8010	1.1904	1033.8	195	1541.3	106.59	0.5635	0.8016	1.1887	1041.6
200	1525.7	111.68	0.5958	0.8045	1.1953	1010.3	200	1528.6	112.55	0.5936	0.8051	1.1935	1018.3
205	1512.8	117.67	0.6254	0.8084	1.2006	987.06	205	1515.8	118.53	0.6231	0.8090	1.1986	995.32
210	1499.8	123.68	0.6544	0.8126	1.2062	964.06	210	1503.0	124.54	0.6521	0.8132	1.2042	972.59
215	1486.8	129.73	0.6828	0.8171	1.2122	941.34	215	1490.2	130.57	0.6805	0.8176	1.2100	950.14
220	1473.8	135.81	0.7108	0.8218	1.2185	918.89	220	1477.2	136.64	0.7084	0.8223	1.2160	927.98
225	1460.6	141.92	0.7382	0.8266	1.2250	896.70	225	1464.3	142.73	0.7358	0.8272	1.2224	906.10
230	1447.4	148.06	0.7652	0.8316	1.2317	874.78	230	1451.2	148.86	0.7627	0.8321	1.2289	884.48
235	1434.0	154.23	0.7918	0.8368	1.2387	853.10	235	1438.1	155.02	0.7892	0.8372	1.2356	863.13
240	1420.6	160.45	0.8180	0.8420	1.2459	831.66	240	1424.8	161.22	0.8153	0.8424	1.2426	842.03
245	1407.1	166.70	0.8437	0.8473	1.2534	810.45	245	1411.5	167.45	0.8410	0.8477	1.2498	821.18
250	1393.4	172.98	0.8691	0.8527	1.2611	789.45	250	1398.1	173.72	0.8663	0.8531	1.2571	800.56
255	1379.6	179.31	0.8942	0.8582	1.2691	768.67	255	1384.6	180.02	0.8913	0.8585	1.2648	780.17
260	1365.7	185.67	0.9189	0.8637	1.2773	748.07	260	1370.9	186.37	0.9159	0.8640	1.2726	759.99
265	1351.6	192.08	0.9433	0.8693	1.2858	727.66	265	1357.1	192.75	0.9403	0.8696	1.2807	740.01

TABLE 9. Thermodynamic properties of HFC-134a in the single-phase region — Continued

T/K	ρ/kg/m³	h/kJ/kg	s/kJ/(kgK)	c_v/kJ/(kgK)	c_p/kJ/(kgK)	w/m/s	T/K	ρ/kg/m³	h/kJ/kg	s/kJ/(kgK)	c_v/kJ/(kgK)	c_p/kJ/(kgK)	w/m/s
			10.00 MPa							**12.00 MPa**			
270	1337.4	198.53	0.9674	0.8750	1.2947	707.43	270	1343.2	199.17	0.9643	0.8752	1.2891	720.23
275	1323.0	205.03	0.9913	0.8807	1.3039	687.35	275	1329.1	205.64	0.9880	0.8809	1.2977	700.64
280	1308.3	211.57	1.0149	0.8865	1.3135	667.43	280	1314.8	212.15	1.0115	0.8866	1.3067	681.22
285	1293.5	218.16	1.0382	0.8924	1.3234	647.65	285	1300.4	218.71	1.0347	0.8924	1.3160	661.98
290	1278.4	224.81	1.0613	0.8983	1.3339	628.00	290	1285.8	225.31	1.0577	0.8983	1.3256	642.89
295	1263.1	231.50	1.0842	0.9043	1.3448	608.48	295	1270.9	231.96	1.0804	0.9042	1.3357	623.97
300	1247.5	238.26	1.1069	0.9104	1.3562	589.07	300	1255.8	238.67	1.1029	0.9102	1.3461	605.20
305	1231.6	245.07	1.1294	0.9165	1.3683	569.78	305	1240.5	245.43	1.1253	0.9162	1.3571	586.57
310	1215.3	251.94	1.1518	0.9228	1.3810	550.59	310	1224.9	252.24	1.1474	0.9223	1.3685	568.09
315	1198.7	258.88	1.1740	0.9291	1.3944	531.50	315	1209.0	259.11	1.1694	0.9285	1.3805	549.75
320	1181.7	265.89	1.1960	0.9355	1.4087	512.50	320	1192.7	266.05	1.1913	0.9348	1.3931	531.56
325	1164.3	272.97	1.2180	0.9420	1.4239	493.60	325	1176.2	273.05	1.2130	0.9411	1.4063	513.51
330	1146.4	280.13	1.2399	0.9485	1.4400	474.80	330	1159.2	280.11	1.2345	0.9475	1.4202	495.61
335	1128.0	287.37	1.2616	0.9552	1.4574	456.09	335	1141.9	287.25	1.2560	0.9539	1.4349	477.86
340	1109.0	294.70	1.2834	0.9620	1.4760	437.48	340	1124.1	294.46	1.2774	0.9605	1.4504	460.27
345	1089.4	302.13	1.3051	0.9689	1.4960	418.98	345	1105.8	301.76	1.2987	0.9671	1.4669	442.85
350	1069.0	309.67	1.3267	0.9759	1.5177	400.59	350	1087.1	309.13	1.3199	0.9738	1.4843	425.61
355	1047.9	317.32	1.3484	0.9830	1.5413	382.34	355	1067.7	316.60	1.3411	0.9806	1.5028	408.57
360	1026.0	325.09	1.3702	0.9902	1.5670	364.24	360	1047.8	324.16	1.3622	0.9875	1.5225	391.76
365	1003.0	332.99	1.3920	0.9976	1.5950	346.31	365	1027.2	331.83	1.3834	0.9944	1.5434	375.20
370	979.11	341.04	1.4139	1.0052	1.6258	328.60	370	1006.0	339.60	1.4045	1.0015	1.5657	358.91
375	953.96	349.25	1.4359	1.0129	1.6596	311.14	375	983.98	347.49	1.4257	1.0086	1.5892	342.95
380	927.52	357.64	1.4581	1.0207	1.6967	294.00	380	961.17	355.50	1.4469	1.0158	1.6142	327.35
385	899.67	356.23	1.4806	1.0288	1.7373	277.25	385	937.52	363.63	1.4682	1.0231	1.6405	312.16
390	870.28	375.02	1.5033	1.0370	1.7816	261.01	390	913.00	371.90	1.4895	1.0304	1.6680	297.46
395	839.26	384.05	1.5263	1.0453	1.8290	245.42	395	887.58	380.32	1.5110	1.0378	1.6965	283.33
400	806.57	393.32	1.5496	1.0537	1.8786	230.68	400	861.28	388.87	1.5325	1.0452	1.7255	269.83
410	736.54	412.59	1.5972	1.0704	1.9748	204.66	410	806.18	406.41	1.5758	1.0600	1.7822	245.18
420	662.77	432.70	1.6457	1.0855	2.0382	184.94	420	748.53	424.49	1.6194	1.0743	1.8302	224.35
430	590.89	453.13	1.6937	1.0972	2.0326	172.69	430	690.08	442.95	1.6628	1.0875	1.8583	208.05
440	527.11	473.12	1.7397	1.1053	1.9573	167.19	440	633.33	461.56	1.7056	1.0992	1.8577	196.55
450	474.40	492.17	1.7825	1.1113	1.8513	166.41	450	580.83	480.01	1.7470	1.1092	1.8279	189.50
460	432.14	510.17	1.8220	1.1167	1.7502	168.34	460	534.24	498.05	1.7867	1.1179	1.7784	186.10
			14.00 MPa							**16.00 MPa**			
180	1581.6	89.758	0.4668	0.7957	1.1769	1119.8	180	1583.9	90.663	0.4648	0.7964	1.1756	1126.7
185	1569.1	95.648	0.4991	0.7971	1.1795	1096.1	185	1571.5	96.548	0.4970	0.7978	1.1782	1103.1
190	1556.6	101.55	0.5306	0.7994	1.1830	1072.5	190	1559.1	102.44	0.5285	0.8000	1.1816	1079.8
195	1544.0	107.48	0.5613	0.8023	1.1871	1049.2	195	1546.7	108.36	0.5592	0.8030	1.1856	1056.7
200	1531.4	113.42	0.5915	0.8057	1.1918	1026.1	200	1534.2	114.30	0.5893	0.8064	1.1901	1033.8
205	1518.8	119.39	0.6209	0.8095	1.1968	1003.4	205	1521.7	120.26	0.6188	0.8102	1.1951	1011.3
210	1506.1	125.39	0.6498	0.8138	1.2022	980.94	210	1509.2	126.25	0.6476	0.8144	1.2003	989.11

TABLE 9. Thermodynamic properties of HFC-134a in the single-phase region — Continued

T/K	ρ kg/m³	h kJ/kg	s kJ/(kgK)	c_v kJ/(kgK)	c_p kJ/(kgK)	w m/s	T/K	ρ kg/m³	h kJ/kg	s kJ/(kgK)	c_v kJ/(kgK)	c_p kJ/(kgK)	w m/s
			14.00 MPa							**16.00 MPa**			
215	1493.4	131.42	0.6782	0.8182	1.2078	958.75	215	1496.6	132.27	0.6759	0.8189	1.2058	967.18
220	1480.6	137.47	0.7060	0.8229	1.2138	936.86	220	1484.0	138.31	0.7037	0.8235	1.2116	945.55
225	1467.8	143.56	0.7334	0.8277	1.2199	915.26	225	1471.3	144.38	0.7310	0.8283	1.2175	924.21
230	1454.9	149.67	0.7603	0.8327	1.2262	893.94	230	1458.6	150.49	0.7578	0.8332	1.2237	903.17
235	1442.0	155.82	0.7867	0.8378	1.2327	872.90	235	1445.8	156.62	0.7842	0.8383	1.2300	882.42
240	1428.9	162.00	0.8127	0.8429	1.2395	852.12	240	1432.9	162.79	0.8102	0.8434	1.2365	861.94
245	1415.8	168.21	0.8384	0.8482	1.2464	831.60	245	1420.0	168.99	0.8358	0.8487	1.2432	841.74
250	1402.6	174.46	0.8636	0.8535	1.2535	811.33	250	1407.0	175.22	0.8609	0.8540	1.2501	821.79
255	1389.3	180.75	0.8885	0.8589	1.2608	791.30	255	1393.9	181.49	0.8858	0.8593	1.2571	802.10
260	1375.9	187.07	0.9131	0.8644	1.2683	771.50	260	1380.8	187.79	0.9103	0.8648	1.2643	782.65
265	1362.4	193.43	0.9373	0.8699	1.2760	751.93	265	1367.5	194.13	0.9344	0.8703	1.2716	763.44
270	1348.8	199.83	0.9612	0.8755	1.2839	732.56	270	1354.1	200.51	0.9582	0.8758	1.2792	744.45
275	1335.0	206.27	0.9849	0.8811	1.2921	713.40	275	1340.6	206.93	0.9818	0.8814	1.2870	725.69
280	1321.1	212.75	1.0082	0.8868	1.3006	694.44	280	1327.0	213.38	1.0051	0.8870	1.2950	707.15
285	1307.0	219.28	1.0313	0.8925	1.3093	675.68	285	1313.3	219.88	1.0280	0.8927	1.3032	688.81
290	1292.7	225.85	1.0542	0.8983	1.3183	657.10	290	1299.4	226.41	1.0508	0.8985	1.3117	670.68
295	1278.3	232.46	1.0768	0.9042	1.3276	638.70	295	1285.3	232.99	1.0733	0.9042	1.3204	652.76
300	1263.7	239.13	1.0992	0.9101	1.3373	620.48	300	1271.1	239.62	1.0956	0.9101	1.3295	635.03
305	1248.8	245.84	1.1214	0.9160	1.3473	602.44	305	1256.7	246.29	1.1176	0.9160	1.3388	617.50
310	1233.8	252.60	1.1433	0.9221	1.3577	584.57	310	1242.1	253.01	1.1395	0.9219	1.3484	600.17
315	1218.4	259.42	1.1652	0.9281	1.3686	566.88	315	1227.3	259.77	1.1611	0.9279	1.3583	583.03
320	1202.9	266.29	1.1868	0.9343	1.3799	549.36	320	1212.3	266.59	1.1826	0.9339	1.3685	566.10
325	1187.0	273.22	1.2083	0.9404	1.3916	532.02	325	1197.1	273.46	1.2039	0.9400	1.3792	549.36
330	1170.9	280.20	1.2296	0.9467	1.4039	514.86	330	1181.7	280.38	1.2250	0.9462	1.3902	532.83
335	1154.4	287.26	1.2508	0.9530	1.4167	497.89	335	1165.9	287.36	1.2460	0.9524	1.4016	516.52
340	1137.6	294.37	1.2719	0.9594	1.4301	481.12	340	1149.9	294.40	1.2669	0.9586	1.4134	500.42
345	1120.5	301.56	1.2929	0.9658	1.4441	464.55	345	1133.7	301.50	1.2876	0.9649	1.4256	484.56
350	1102.9	308.81	1.3138	0.9723	1.4587	448.21	350	1117.1	308.66	1.3082	0.9712	1.4382	468.93
355	1084.9	316.15	1.3346	0.9789	1.4740	432.10	355	1100.2	315.88	1.3287	0.9776	1.4513	453.57
360	1066.5	323.56	1.3553	0.9855	1.4899	416.25	360	1082.9	323.17	1.3491	0.9841	1.4648	438.47
365	1047.6	331.05	1.3760	0.9922	1.5066	400.68	365	1065.3	330.53	1.3694	0.9906	1.4788	423.67
370	1028.2	338.62	1.3966	0.9989	1.5240	385.42	370	1047.4	337.96	1.3896	0.9971	1.4931	409.19
375	1008.4	346.29	1.4172	1.0057	1.5421	370.49	375	1029.1	345.46	1.4097	1.0036	1.5079	395.03
380	987.97	354.05	1.4377	1.0125	1.5609	355.93	380	1010.4	353.04	1.4298	1.0102	1.5230	381.25
385	966.99	361.90	1.4582	1.0194	1.5802	341.78	385	991.31	360.69	1.4498	1.0169	1.5383	367.85
390	945.45	369.85	1.4788	1.0263	1.6001	328.08	390	971.83	368.43	1.4698	1.0235	1.5539	354.88
395	923.35	377.90	1.4993	1.0332	1.6202	314.88	395	951.97	376.23	1.4897	1.0302	1.5695	342.36
400	900.70	386.05	1.5198	1.0402	1.6404	302.23	400	931.73	384.12	1.5095	1.0369	1.5851	330.33
410	853.86	402.66	1.5608	1.0540	1.6798	278.81	410	890.24	400.12	1.5490	1.0502	1.6153	307.89
420	805.38	419.64	1.6017	1.0676	1.7149	258.26	420	847.65	416.42	1.5883	1.0633	1.6429	287.81
430	756.07	436.93	1.6424	1.0808	1.7415	240.97	430	804.43	432.97	1.6272	1.0762	1.6657	270.34
440	707.07	454.42	1.6826	1.0932	1.7555	227.16	440	761.21	449.71	1.6657	1.0887	1.6817	255.63
450	659.73	471.99	1.7221	1.1047	1.7544	216.81	450	718.77	466.57	1.7036	1.1007	1.6893	243.70

TABLE 9. Thermodynamic properties of HFC-134a in the single-phase region — Continued

T/K	ρ kg/m³	h kJ/kg	s kJ/(kgK)	c_v kJ/(kgK)	c_p kJ/(kgK)	w m/s	T/K	ρ kg/m³	h kJ/kg	s kJ/(kgK)	c_v kJ/(kgK)	c_p kJ/(kgK)	w m/s
			14.00 MPa							**16.00 MPa**			
460	615.30	489.46	1.7605	1.1153	1.7387	209.68	460	677.90	483.47	1.7407	1.122	1.6880	234.45
			20.00 MPa							**25.00 MPa**			
180	1588.5	92.481	0.4609	0.7978	1.1733	1140.1	180	1594.1	94.764	0.4561	0.7996	1.1707	1156.2
185	1576.3	98.354	0.4931	0.7992	1.1758	1116.9	185	1582.1	100.62	0.4882	0.8009	1.1729	1133.5
190	1564.1	104.24	0.5245	0.8014	1.1790	1093.9	190	1570.1	106.49	0.5195	0.8031	1.1760	1111.0
195	1551.9	110.14	0.5551	0.8043	1.1828	1071.2	195	1558.2	112.38	0.5501	0.8060	1.1796	1088.7
200	1539.6	116.07	0.5851	0.8077	1.1871	1048.8	200	1546.2	118.29	0.5800	0.8094	1.1837	1066.8
205	1527.4	122.01	0.6145	0.8116	1.1918	1026.7	205	1534.2	124.22	0.6093	0.8132	1.1882	1045.2
210	1515.1	127.98	0.6433	0.8157	1.1968	1004.9	210	1522.2	130.17	0.6380	0.8174	1.1929	1023.9
215	1502.8	133.98	0.6715	0.8201	1.2021	983.51	215	1510.2	136.15	0.6661	0.8217	1.1979	1003.0
220	1490.4	140.01	0.6992	0.8247	1.2076	962.36	220	1498.1	142.15	0.6937	0.8263	1.2031	982.44
225	1478.0	146.06	0.7264	0.8295	1.2133	941.52	225	1486.1	148.18	0.7208	0.8310	1.2085	962.16
230	1465.6	152.14	0.7531	0.8344	1.2191	921.00	230	1474.0	154.24	0.7475	0.8359	1.2140	942.21
235	1453.2	158.25	0.7794	0.8394	1.2251	900.77	235	1461.9	160.32	0.7736	0.8409	1.2196	922.57
240	1440.6	164.39	0.8053	0.8445	1.2312	880.85	240	1449.8	166.43	0.7994	0.8459	1.2254	903.25
245	1428.1	170.56	0.8307	0.8497	1.2375	861.21	245	1437.6	172.57	0.8247	0.8511	1.2313	884.23
250	1415.5	176.77	0.8558	0.8549	1.2439	841.85	250	1425.4	178.75	0.8496	0.8563	1.2372	865.52
255	1402.8	183.00	0.8805	0.8603	1.2504	822.76	255	1413.2	184.95	0.8742	0.8615	1.2433	847.09
260	1390.0	189.27	0.9048	0.8656	1.2571	803.95	260	1400.9	191.18	0.8984	0.8668	1.2495	828.95
265	1377.2	195.57	0.9288	0.8711	1.2639	785.39	265	1388.6	197.44	0.9223	0.8722	1.2558	811.08
270	1364.3	201.91	0.9525	0.8765	1.2709	767.08	270	1376.2	203.74	0.9458	0.8776	1.2622	793.49
275	1351.3	208.28	0.9759	0.8820	1.2780	749.02	275	1363.7	210.07	0.9690	0.8830	1.2687	776.17
280	1338.3	214.69	0.9990	0.8876	1.2853	731.20	280	1351.2	216.43	0.9919	0.8885	1.2753	759.11
285	1325.1	221.14	1.0218	0.8932	1.2928	713.62	285	1338.7	222.82	1.0146	0.8941	1.2820	742.30
290	1311.8	227.62	1.0444	0.8989	1.3004	696.27	290	1326.0	229.25	1.0369	0.8996	1.2888	725.75
295	1298.4	234.14	1.0667	0.9046	1.3082	679.15	295	1313.3	235.71	1.0590	0.9052	1.2958	709.45
300	1284.9	240.70	1.0887	0.9103	1.3162	662.26	300	1300.5	242.20	1.0808	0.9109	1.3029	693.40
305	1271.3	247.30	1.1106	0.9161	1.3243	645.59	305	1287.7	248.74	1.1024	0.9166	1.3101	677.60
310	1257.5	253.95	1.1322	0.9219	1.3327	629.15	310	1274.7	255.31	1.1238	0.9223	1.3174	662.05
315	1243.6	260.63	1.1536	0.9277	1.3413	612.94	315	1261.7	261.91	1.1449	0.9280	1.3248	646.74
320	1229.6	267.36	1.1747	0.9336	1.3501	596.96	320	1248.6	268.55	1.1659	0.9338	1.3324	631.68
325	1215.3	274.13	1.1957	0.9396	1.3591	581.21	325	1235.4	275.24	1.1866	0.9396	1.3401	616.87
330	1201.0	280.95	1.2166	0.9456	1.3683	565.69	330	1222.0	281.96	1.2071	0.9455	1.3479	602.31
335	1186.4	287.82	1.2372	0.9516	1.3777	550.42	335	1208.6	288.72	1.2274	0.9513	1.3559	588.00
340	1171.7	294.73	1.2577	0.9577	1.3874	535.39	340	1195.1	295.52	1.2476	0.9573	1.3639	573.95
345	1156.8	301.69	1.2780	0.9638	1.3973	520.61	345	1181.4	302.36	1.2676	0.9632	1.3721	560.17
350	1141.7	308.70	1.2982	0.9699	1.4074	506.09	350	1167.7	309.24	1.2874	0.9692	1.3803	546.65
355	1126.4	315.77	1.3182	0.9761	1.4177	491.85	355	1153.8	316.16	1.3070	0.9752	1.3887	533.41
360	1110.9	322.88	1.3381	0.9823	1.4282	477.89	360	1139.8	323.12	1.3265	0.9812	1.3971	520.45
365	1095.2	330.05	1.3579	0.9885	1.4389	464.23	365	1125.7	330.13	1.3458	0.9873	1.4057	507.77
370	1079.3	337.27	1.3776	0.9948	1.4497	450.88	370	1111.5	337.18	1.3650	0.9933	1.4142	495.40

TABLE 9. Thermodynamic properties of HFC-134a in the single-phase region — Continued

T/K	ρ kg/m³	h kJ/kg	s kJ/(kgK)	c_v kJ/(kgK)	c_p kJ/(kgK)	w m/s
			20.00 MPa			
375	1063.2	344.55	1.3971	1.0011	1.4607	437.85
380	1046.8	351.88	1.4165	1.0074	1.4717	425.16
385	1030.3	359.26	1.4358	1.0137	1.4828	412.83
390	1013.5	366.71	1.4550	1.0201	1.4940	400.87
395	996.61	374.20	1.4741	1.0264	1.5050	389.31
400	979.46	381.76	1.4931	1.0328	1.5160	378.15
410	944.64	397.03	1.5308	1.0455	1.5372	357.14
420	909.27	412.50	1.5681	1.0582	1.5570	337.98
430	873.59	428.16	1.6050	1.0707	1.5747	320.76
440	837.87	443.98	1.6413	1.0831	1.5894	305.55
450	802.44	459.94	1.6772	1.0953	1.6006	292.38
460	767.68	475.98	1.7125	1.1072	1.6079	281.20
			30.00 MPa			
180	1599.5	97.057	0.4514	0.8014	1.1683	1171.8
185	1587.7	102.90	0.4835	0.8027	1.1704	1149.4
190	1576.0	108.76	0.5147	0.8049	1.1732	1127.4
195	1564.2	114.63	0.5453	0.8078	1.1767	1105.6
200	1552.5	120.53	0.5751	0.8112	1.1806	1084.1
205	1540.7	126.44	0.6043	0.8149	1.1849	1062.9
210	1529.0	132.38	0.6329	0.8190	1.1894	1042.1
215	1517.3	138.34	0.6610	0.8234	1.1942	1021.7
220	1505.5	144.32	0.6885	0.8279	1.1992	1001.6
225	1493.8	150.33	0.7155	0.8326	1.2043	981.81
230	1482.0	156.36	0.7420	0.8374	1.2096	962.37
235	1470.2	162.42	0.7681	0.8424	1.2149	943.26
240	1458.4	168.51	0.7937	0.8474	1.2204	924.47
245	1446.6	174.63	0.8189	0.8525	1.2259	906.00
250	1434.8	180.77	0.8438	0.8577	1.2315	887.84
255	1422.9	186.94	0.8682	0.8629	1.2372	869.98
260	1411.0	193.15	0.8923	0.8681	1.2430	852.42
265	1399.1	199.38	0.9160	0.8734	1.2489	835.15
270	1387.2	205.63	0.9394	0.8788	1.2548	818.17
275	1375.2	211.92	0.9625	0.8842	1.2609	801.47
280	1363.2	218.24	0.9853	0.8896	1.2670	785.04
285	1351.2	224.59	1.0077	0.8951	1.2732	768.88
290	1339.1	230.98	1.0299	0.9006	1.2794	752.99
295	1326.9	237.39	1.0519	0.9061	1.2858	737.36
300	1314.8	243.83	1.0735	0.9117	1.2922	721.99
305	1302.5	250.31	1.0949	0.9173	1.2987	706.89
310	1290.2	256.82	1.1161	0.9229	1.3053	692.03
315	1277.9	263.37	1.1371	0.9286	1.3120	677.44
			25.00 MPa			
375	1097.1	344.27	1.3840	0.9994	1.4228	483.32
380	1082.7	351.41	1.4029	1.0055	1.4314	471.56
385	1068.1	358.59	1.4217	1.0117	1.4400	460.12
390	1053.5	365.81	1.4403	1.0178	1.4486	449.02
395	1038.7	373.07	1.4588	1.0240	1.4570	438.25
400	1023.9	380.38	1.4772	1.0301	1.4654	427.83
410	994.00	395.12	1.5136	1.0425	1.4818	408.08
420	963.85	410.01	1.5495	1.0548	1.4973	389.82
430	933.58	425.06	1.5849	1.0671	1.5116	373.10
440	903.34	440.24	1.6198	1.0793	1.5245	357.95
450	873.30	455.55	1.6542	1.0915	1.5358	344.38
460	843.62	470.95	1.6881	1.1035	1.5452	332.35
			35.00 MPa			
185	1593.2	105.19	0.4789	0.8045	1.1681	1164.9
190	1581.6	111.04	0.5101	0.8067	1.1708	1143.2
195	1570.1	116.90	0.5405	0.8096	1.1741	1121.8
200	1558.6	122.78	0.5703	0.8129	1.1779	1100.7
205	1547.1	128.68	0.5994	0.8167	1.1820	1080.0
210	1535.6	134.60	0.6280	0.8207	1.1863	1059.6
215	1524.1	140.54	0.6559	0.8251	1.1909	1039.6
220	1512.6	146.51	0.6834	0.8296	1.1957	1019.9
225	1501.1	152.50	0.7103	0.8342	1.2006	1000.6
230	1489.6	158.52	0.7367	0.8390	1.2056	981.61
235	1478.1	164.56	0.7627	0.8439	1.2107	962.97
240	1466.6	170.63	0.7883	0.8489	1.2159	944.65
245	1455.1	176.72	0.8134	0.8540	1.2212	926.67
250	1443.6	182.84	0.8381	0.8591	1.2266	909.00
255	1432.1	188.98	0.8625	0.8643	1.2320	891.64
260	1420.6	195.16	0.8864	0.8695	1.2375	874.59
265	1409.1	201.36	0.9101	0.8748	1.2430	857.84
270	1397.5	207.59	0.9333	0.8801	1.2486	841.38
275	1386.0	213.85	0.9563	0.8854	1.2543	825.21
280	1374.4	220.13	0.9790	0.8908	1.2600	809.32
285	1362.8	226.45	1.0013	0.8962	1.2658	793.71
290	1351.2	232.79	1.0234	0.9017	1.2716	778.38
295	1339.5	239.16	1.0452	0.9072	1.2775	763.31
300	1327.8	245.57	1.0667	0.9127	1.2835	748.51
305	1316.1	252.00	1.0880	0.9182	1.2895	733.98
310	1304.4	258.46	1.1090	0.9238	1.2956	719.71
315	1292.6	264.95	1.1298	0.9294	1.3017	705.70
320	1280.8	271.48	1.1503	0.9350	1.3079	691.95

TABLE 9. Thermodynamic properties of HFC-134a in the single-phase region — Continued

T/K	ρ/kg/m³	h/kJ/kg	s/kJ/(kgK)	c_v/kJ/(kgK)	c_p/kJ/(kgK)	w/m/s
			30.00 MPa			
320	1265.5	269.94	1.1578	0.9343	1.3188	663.10
325	1253.0	276.55	1.1783	0.9400	1.3256	649.02
330	1240.5	283.20	1.1986	0.9458	1.3325	635.20
335	1228.0	289.88	1.2187	0.9516	1.3395	621.64
340	1215.3	296.59	1.2386	0.9574	1.3465	608.33
345	1202.6	303.35	1.2583	0.9632	1.3537	595.29
350	1189.8	310.13	1.2778	0.9691	1.3608	582.52
355	1177.0	316.95	1.2971	0.9750	1.3680	570.01
360	1164.1	323.81	1.3163	0.9809	1.3753	557.78
365	1151.1	330.71	1.3354	0.9869	1.3826	545.82
370	1138.1	337.64	1.3542	0.9928	1.3899	534.15
375	1125.0	344.61	1.3729	0.9988	1.3972	522.76
380	1111.9	351.61	1.3915	1.0048	1.4045	511.66
385	1098.7	358.65	1.4099	1.0108	1.4117	500.86
390	1085.4	365.73	1.4281	1.0168	1.4190	490.36
395	1072.1	372.84	1.4463	1.0229	1.4261	480.16
400	1058.8	379.99	1.4643	1.0289	1.4332	470.27
410	1032.0	394.39	1.4998	1.0410	1.4471	451.45
420	1005.2	408.93	1.5348	1.0532	1.4604	433.90
430	978.35	423.60	1.5694	1.0653	1.4731	417.67
440	951.58	438.39	1.6034	1.0774	1.4849	402.75
450	925.00	453.30	1.6369	1.0895	1.4957	389.13
			40.00 MPa			
185	1598.4	107.49	0.4744	0.8063	1.1659	1179.8
190	1587.1	113.33	0.5055	0.8085	1.1685	1158.5
195	1575.7	119.18	0.5359	0.8113	1.1717	1137.4
200	1564.4	125.05	0.5656	0.8147	1.1754	1116.7
205	1553.2	130.93	0.5947	0.8184	1.1793	1096.4
210	1541.9	136.84	0.6232	0.8225	1.1835	1076.4
215	1530.6	142.77	0.6511	0.8267	1.1880	1056.8
220	1519.4	148.72	0.6784	0.8312	1.1926	1037.5
225	1508.1	154.70	0.7053	0.8359	1.1973	1018.6
230	1496.9	160.69	0.7316	0.8406	1.2021	1000.0
235	1485.7	166.72	0.7576	0.8455	1.2071	981.82
240	1474.5	172.77	0.7830	0.8505	1.2121	963.93
245	1463.3	178.84	0.8081	0.8555	1.2171	946.38
250	1452.1	184.94	0.8327	0.8606	1.2222	929.15
255	1440.9	191.06	0.8570	0.8657	1.2274	912.23
260	1429.7	197.21	0.8808	0.8709	1.2326	895.63
265	1418.5	203.39	0.9044	0.8761	1.2379	879.34
270	1407.3	209.59	0.9276	0.8814	1.2432	863.34
			35.00 MPa			
325	1269.0	278.03	1.1706	0.9407	1.3141	678.46
330	1257.1	284.62	1.1907	0.9464	1.3204	665.23
335	1245.2	291.24	1.2106	0.9521	1.3268	652.25
340	1233.3	297.89	1.2304	0.9579	1.3331	639.54
345	1221.3	304.57	1.2499	0.9636	1.3396	627.08
350	1209.3	311.28	1.2692	0.9694	1.3460	614.89
355	1197.3	318.03	1.2883	0.9752	1.3525	602.96
360	1185.2	324.81	1.3073	0.9811	1.3590	591.29
365	1173.1	331.62	1.3261	0.9869	1.3655	579.89
370	1161.0	338.47	1.3447	0.9928	1.3720	568.75
375	1148.8	345.34	1.3632	0.9987	1.3785	557.89
380	1136.6	352.25	1.3815	1.0046	1.3850	547.30
385	1124.4	359.19	1.3996	1.0106	1.3915	536.98
390	1112.2	366.17	1.4176	1.0165	1.3979	526.94
395	1099.9	373.17	1.4355	1.0225	1.4043	517.18
400	1087.7	380.21	1.4532	1.0285	1.4107	507.70
410	1063.1	394.38	1.4881	1.0404	1.4231	489.60
420	1038.6	408.67	1.5226	1.0524	1.4352	472.64
430	1014.2	423.08	1.5565	1.0645	1.4469	456.83
440	989.87	437.61	1.5899	1.0765	1.4580	442.17
450	965.71	452.24	1.6228	1.0885	1.4685	428.65
460	941.80	466.98	1.6552	1.1005	1.4783	416.26
			50.00 MPa			
185	1608.5	112.12	0.4657	0.8099	1.1622	1208.2
190	1597.5	117.94	0.4967	0.8121	1.1646	1187.6
195	1586.6	123.77	0.5270	0.8149	1.1676	1167.2
200	1575.7	129.61	0.5566	0.8182	1.1710	1147.2
205	1564.8	135.48	0.5856	0.8219	1.1748	1127.6
210	1553.9	141.36	0.6139	0.8259	1.1787	1108.3
215	1543.0	147.27	0.6417	0.8301	1.1829	1089.3
220	1532.2	153.19	0.6690	0.8346	1.1873	1070.8
225	1521.4	159.14	0.6957	0.8392	1.1917	1052.6
230	1510.7	165.11	0.7219	0.8439	1.1962	1034.7
235	1499.9	171.10	0.7477	0.8487	1.2009	1017.3
240	1489.2	177.12	0.7730	0.8536	1.2055	1000.1
245	1478.5	183.16	0.7979	0.8586	1.2103	983.35
250	1467.8	189.22	0.8224	0.8636	1.2151	966.87
255	1457.1	195.31	0.8466	0.8687	1.2199	950.72
260	1446.5	201.42	0.8703	0.8738	1.2247	934.88
265	1435.9	207.56	0.8937	0.8790	1.2296	919.35
270	1425.2	213.72	0.9167	0.8842	1.2345	904.12

TABLE 9. Thermodynamic properties of HFC-134a in the single-phase region — Continued

T/K	ρ/kg/m³	h/kJ/kg	s/kJ/(kgK)	c_v/kJ/(kgK)	c_p/kJ/(kgK)	w/m/s
			40.00 MPa			
275	1396.1	215.82	0.9504	0.8867	1.2486	847.63
280	1384.9	222.08	0.9730	0.8921	1.2540	832.21
285	1373.6	228.36	0.9952	0.8974	1.2595	817.08
290	1362.4	234.67	1.0172	0.9028	1.2650	802.22
295	1351.2	241.01	1.0388	0.9083	1.2706	787.63
300	1339.9	247.38	1.0602	0.9138	1.2762	773.32
305	1328.7	253.78	1.0814	0.9193	1.2818	759.27
310	1317.4	260.20	1.1023	0.9248	1.2875	745.49
315	1306.1	266.65	1.1229	0.9304	1.2932	731.97
320	1294.8	273.13	1.1433	0.9359	1.2990	718.71
325	1283.5	279.64	1.1635	0.9416	1.3048	705.71
330	1272.2	286.18	1.1835	0.9472	1.3107	692.96
335	1260.8	292.75	1.2032	0.9529	1.3165	680.47
340	1249.5	299.35	1.2228	0.9586	1.3224	668.24
345	1238.1	305.97	1.2421	0.9643	1.3284	656.26
350	1226.7	312.63	1.2613	0.9700	1.3343	644.54
355	1215.3	319.32	1.2803	0.9758	1.3403	633.07
360	1203.9	326.03	1.2991	0.9815	1.3463	621.86
365	1192.5	332.78	1.3177	0.9874	1.3523	610.90
370	1181.1	339.56	1.3361	0.9932	1.3583	600.20
375	1169.7	346.36	1.3544	0.9990	1.3643	589.76
380	1158.2	353.20	1.3725	1.0049	1.3702	579.57
385	1146.8	360.07	1.3904	1.0108	1.3762	569.64
390	1135.3	366.96	1.4082	1.0166	1.3821	559.97
395	1123.9	373.89	1.4259	1.0225	1.3880	550.56
400	1112.4	380.84	1.4434	1.0285	1.3939	541.41
410	1089.6	394.84	1.4779	1.0403	1.4055	523.90
420	1066.8	408.95	1.5120	1.0522	1.4168	507.42
430	1044.2	423.18	1.5454	1.0642	1.4278	491.99
440	1021.6	437.51	1.5784	1.0761	1.4385	477.59
450	999.34	451.95	1.6108	1.0881	1.4487	464.21
460	977.22	466.48	1.6428	1.1001	1.4585	451.83
			60.00 MPa			
185	1618.1	116.78	0.4574	0.8136	1.1591	1235.1
190	1607.4	122.58	0.4883	0.8157	1.1614	1215.0
195	1596.8	128.39	0.5185	0.8184	1.1642	1195.3
200	1586.2	134.22	0.5480	0.8217	1.1674	1175.9
205	1575.7	140.07	0.5769	0.8254	1.1710	1156.8
210	1565.2	145.93	0.6052	0.8293	1.1748	1138.2
215	1554.7	151.82	0.6328	0.8335	1.1788	1119.8
220	1544.2	157.72	0.6600	0.8379	1.1829	1101.9

T/K	ρ/kg/m³	h/kJ/kg	s/kJ/(kgK)	c_v/kJ/(kgK)	c_p/kJ/(kgK)	w/m/s
			50.00 MPa			
275	1414.6	219.90	0.9394	0.8894	1.2395	889.19
280	1404.0	226.11	0.9618	0.8947	1.2445	874.55
285	1393.5	232.35	0.9839	0.9000	1.2495	860.20
290	1382.9	238.61	1.0056	0.9053	1.2545	846.13
295	1372.4	244.89	1.0271	0.9107	1.2596	832.33
300	1361.8	251.21	1.0483	0.9161	1.2647	818.80
305	1351.3	257.54	1.0693	0.9215	1.2698	805.54
310	1340.8	263.90	1.0900	0.9270	1.2750	792.54
315	1330.3	270.29	1.1104	0.9325	1.2802	779.80
320	1319.8	276.71	1.1306	0.9380	1.2854	767.32
325	1309.3	283.15	1.1506	0.9435	1.2906	755.09
330	1298.8	289.61	1.1703	0.9491	1.2959	743.11
335	1288.4	296.11	1.1899	0.9547	1.3012	731.38
340	1277.9	302.63	1.2092	0.9603	1.3065	719.90
345	1267.5	309.17	1.2283	0.9659	1.3118	708.66
350	1257.0	315.74	1.2472	0.9716	1.3171	697.67
355	1246.6	322.34	1.2659	0.9773	1.3225	686.91
360	1236.2	328.97	1.2845	0.9830	1.3278	676.40
365	1225.8	335.62	1.3028	0.9887	1.3332	666.12
370	1215.5	342.30	1.3210	0.9945	1.3385	656.08
375	1205.1	349.01	1.3390	1.0002	1.3439	646.27
380	1194.8	355.74	1.3568	1.0060	1.3493	636.70
385	1184.4	362.50	1.3745	1.0118	1.3546	627.37
390	1174.2	369.29	1.3920	1.0176	1.3600	618.26
395	1163.9	376.10	1.4094	1.0234	1.3653	609.39
400	1153.6	382.94	1.4266	1.0293	1.3706	600.74
410	1133.2	396.70	1.4606	1.0410	1.3811	584.14
420	1112.9	410.56	1.4940	1.0528	1.3916	568.44
430	1092.8	424.53	1.5268	1.0646	1.4018	553.64
440	1072.8	438.60	1.5592	1.0765	1.4119	539.71
450	1053.0	452.77	1.5910	1.0883	1.4218	526.64
460	1033.5	467.04	1.6224	1.1003	1.4315	514.41
			70.00 MPa			
185	1627.2	121.46	0.4493	0.8171	1.1565	1260.6
190	1616.8	127.25	0.4802	0.8192	1.1586	1241.1
195	1606.5	133.05	0.5103	0.8219	1.1613	1221.9
200	1596.2	138.86	0.5398	0.8252	1.1644	1203.0
205	1586.0	144.69	0.5686	0.8288	1.1678	1184.5
210	1575.8	150.54	0.5968	0.8327	1.1715	1166.4
215	1565.6	156.41	0.6244	0.8368	1.1754	1148.6
220	1555.5	162.29	0.6515	0.8412	1.1793	1131.2

TABLE 9. Thermodynamic properties of HFC-134a in the single-phase region — Continued

T/K	ρ kg/m³	h kJ/kg	s kJ/(kgK)	c_v kJ/(kgK)	c_p kJ/(kgK)	w m/s	T/K	ρ kg/m³	h kJ/kg	s kJ/(kgK)	c_v kJ/(kgK)	c_p kJ/(kgK)	w m/s
			60.00 MPa							**70.00 MPa**			
225	1533.8	163.55	0.6866	0.8424	1.1872	1084.3	225	1545.4	168.20	0.6780	0.8457	1.1834	1114.2
230	1523.4	169.59	0.7128	0.8471	1.1915	1067.1	230	1535.4	174.13	0.7041	0.8503	1.1876	1097.5
235	1513.1	175.56	0.7384	0.8519	1.1959	1050.2	235	1525.4	180.08	0.7296	0.8550	1.1918	1081.2
240	1502.8	181.55	0.7637	0.8567	1.2003	1033.7	240	1515.5	186.05	0.7548	0.8598	1.1961	1065.2
245	1492.5	187.56	0.7885	0.8616	1.2048	1017.5	245	1505.6	192.04	0.7795	0.8647	1.2004	1049.5
250	1482.3	193.60	0.8128	0.8666	1.2094	1001.7	250	1495.7	198.05	0.8038	0.8696	1.2048	1034.2
255	1472.0	199.66	0.8368	0.8716	1.2139	986.21	255	1485.8	204.09	0.8277	0.8746	1.2092	1019.2
260	1461.9	205.74	0.8605	0.8767	1.2185	971.01	260	1476.0	210.14	0.8512	0.8796	1.2136	1004.6
265	1451.7	211.84	0.8837	0.8818	1.2232	956.11	265	1466.3	216.22	0.8744	0.8847	1.2180	990.25
270	1441.6	217.97	0.9066	0.8870	1.2278	941.51	270	1456.6	222.33	0.8972	0.8898	1.2225	976.18
275	1431.5	224.12	0.9292	0.8922	1.2325	927.21	275	1446.9	228.45	0.9197	0.8949	1.2269	962.41
280	1421.4	230.30	0.9514	0.8974	1.2372	913.20	280	1437.2	234.59	0.9418	0.9001	1.2314	948.92
285	1411.3	236.50	0.9734	0.9026	1.2419	899.47	285	1427.6	240.76	0.9636	0.9053	1.2359	935.71
290	1401.3	242.72	0.9950	0.9079	1.2466	886.03	290	1418.0	246.95	0.9852	0.9105	1.2405	922.78
295	1391.3	248.96	1.0164	0.9132	1.2514	872.85	295	1408.5	253.17	1.0064	0.9158	1.2450	910.11
300	1381.3	255.23	1.0374	0.9186	1.2562	859.94	300	1398.9	259.41	1.0274	0.9211	1.2496	897.71
305	1371.4	261.52	1.0582	0.9240	1.2610	847.29	305	1389.5	265.66	1.0481	0.9264	1.2542	885.56
310	1361.4	267.84	1.0788	0.9294	1.2658	834.90	310	1380.0	271.95	1.0685	0.9318	1.2588	873.67
315	1351.5	274.18	1.0991	0.9348	1.2706	822.77	315	1370.6	278.25	1.0887	0.9372	1.2634	862.02
320	1341.7	280.55	1.1191	0.9403	1.2755	810.89	320	1361.2	284.58	1.1086	0.9426	1.2680	850.62
325	1331.8	286.94	1.1389	0.9457	1.2804	799.25	325	1351.9	290.93	1.1283	0.9480	1.2727	839.46
330	1322.0	293.35	1.1585	0.9512	1.2853	787.86	330	1342.6	297.31	1.1478	0.9535	1.2774	828.53
335	1312.2	299.79	1.1779	0.9568	1.2902	776.70	335	1333.3	303.71	1.1670	0.9589	1.2821	817.83
340	1302.4	306.25	1.1971	0.9623	1.2952	765.79	340	1324.1	310.13	1.1861	0.9645	1.2868	807.36
345	1292.7	312.74	1.2160	0.9679	1.3001	755.10	345	1314.9	316.58	1.2049	0.9700	1.2915	797.12
350	1283.0	319.26	1.2347	0.9735	1.3051	744.65	350	1305.7	323.05	1.2235	0.9755	1.2962	787.10
355	1273.3	325.79	1.2533	0.9791	1.3101	734.43	355	1296.6	329.54	1.2419	0.9811	1.3010	777.29
360	1263.6	332.36	1.2716	0.9848	1.3151	724.43	360	1287.5	336.06	1.2601	0.9867	1.3058	767.70
365	1253.9	338.95	1.2898	0.9904	1.3201	714.66	365	1278.4	342.60	1.2782	0.9924	1.3106	758.33
370	1244.3	345.56	1.3078	0.9961	1.3251	705.11	370	1269.4	349.16	1.2961	0.9980	1.3153	749.16
375	1234.8	352.20	1.3256	1.0018	1.3301	695.78	375	1260.4	355.75	1.3137	1.0037	1.3202	740.20
380	1225.2	358.86	1.3433	1.0076	1.3351	686.66	380	1251.4	362.36	1.3313	1.0093	1.3250	731.44
385	1215.7	365.55	1.3608	1.0133	1.3401	677.76	385	1242.5	369.00	1.3486	1.0150	1.3298	722.89
390	1206.2	372.26	1.3781	1.0191	1.3451	669.08	390	1233.6	375.66	1.3658	1.0208	1.3346	714.53
395	1196.7	379.00	1.3953	1.0249	1.3502	660.60	395	1224.8	382.35	1.3828	1.0265	1.3394	706.37
400	1187.3	385.76	1.4123	1.0306	1.3552	652.34	400	1216.0	389.06	1.3997	1.0323	1.3443	698.40
410	1168.6	399.37	1.4459	1.0423	1.3652	636.42	410	1198.6	402.55	1.4330	1.0438	1.3539	683.04
420	1150.0	413.07	1.4789	1.0540	1.3751	621.32	420	1181.3	416.14	1.4658	1.0554	1.3636	668.42
430	1131.6	426.87	1.5114	1.0657	1.3850	607.02	430	1164.1	429.82	1.4980	1.0671	1.3733	654.53
440	1113.4	440.77	1.5433	1.0775	1.3948	593.49	440	1147.2	443.60	1.5297	1.0788	1.3829	641.35
450	1095.4	454.77	1.5748	1.0893	1.4045	580.72	450	1130.5	457.48	1.5608	1.0905	1.3925	628.86
460	1077.6	468.86	1.6057	1.1011	1.4141	568.70	460	1113.9	471.45	1.5916	1.1023	1.4020	617.03